



# Characterization of Flat-Plate Heat Pipe Functionality for Fuel Cell Application

*Phillip J. Smith*  
*Glenn Research Center, Cleveland, Ohio*

*Anthony J. Colozza*  
*Vantage Partners, LLC, Brook Park, Ohio*

## NASA STI Program . . . in Profile

Since its founding, NASA has been dedicated to the advancement of aeronautics and space science. The NASA Scientific and Technical Information (STI) Program plays a key part in helping NASA maintain this important role.

The NASA STI Program operates under the auspices of the Agency Chief Information Officer. It collects, organizes, provides for archiving, and disseminates NASA's STI. The NASA STI Program provides access to the NASA Technical Report Server—Registered (NTRS Reg) and NASA Technical Report Server—Public (NTRS) thus providing one of the largest collections of aeronautical and space science STI in the world. Results are published in both non-NASA channels and by NASA in the NASA STI Report Series, which includes the following report types:

- **TECHNICAL PUBLICATION.** Reports of completed research or a major significant phase of research that present the results of NASA programs and include extensive data or theoretical analysis. Includes compilations of significant scientific and technical data and information deemed to be of continuing reference value. NASA counter-part of peer-reviewed formal professional papers, but has less stringent limitations on manuscript length and extent of graphic presentations.
- **TECHNICAL MEMORANDUM.** Scientific and technical findings that are preliminary or of specialized interest, e.g., “quick-release” reports, working papers, and bibliographies that contain minimal annotation. Does not contain extensive analysis.
- **CONTRACTOR REPORT.** Scientific and technical findings by NASA-sponsored contractors and grantees.
- **CONFERENCE PUBLICATION.** Collected papers from scientific and technical conferences, symposia, seminars, or other meetings sponsored or co-sponsored by NASA.
- **SPECIAL PUBLICATION.** Scientific, technical, or historical information from NASA programs, projects, and missions, often concerned with subjects having substantial public interest.
- **TECHNICAL TRANSLATION.** English-language translations of foreign scientific and technical material pertinent to NASA's mission.

For more information about the NASA STI program, see the following:

- Access the NASA STI program home page at <http://www.sti.nasa.gov>
- E-mail your question to [help@sti.nasa.gov](mailto:help@sti.nasa.gov)
- Fax your question to the NASA STI Information Desk at 757-864-6500
- Telephone the NASA STI Information Desk at 757-864-9658
- Write to:  
NASA STI Program  
Mail Stop 148  
NASA Langley Research Center  
Hampton, VA 23681-2199



# Characterization of Flat-Plate Heat Pipe Functionality for Fuel Cell Application

*Phillip J. Smith*  
*Glenn Research Center, Cleveland, Ohio*

*Anthony J. Colozza*  
*Vantage Partners, LLC, Brook Park, Ohio*

National Aeronautics and  
Space Administration

Glenn Research Center  
Cleveland, Ohio 44135

Trade names and trademarks are used in this report for identification only. Their usage does not constitute an official endorsement, either expressed or implied, by the National Aeronautics and Space Administration.

*Level of Review:* This material has been technically reviewed by technical management.

Available from

NASA STI Program  
Mail Stop 148  
NASA Langley Research Center  
Hampton, VA 23681-2199

National Technical Information Service  
5285 Port Royal Road  
Springfield, VA 22161  
703-605-6000

This report is available in electronic form at <http://www.sti.nasa.gov/> and <http://ntrs.nasa.gov/>



# Characterization of Flat-Plate Heat Pipe Functionality for Fuel Cell Application

Phillip J. Smith  
National Aeronautics and Space Administration  
Glenn Research Center  
Cleveland, Ohio 44135

Anthony J. Colozza  
Vantage Partners, LLC  
Brook Park, Ohio 44142

## Summary

For many exothermic systems such as proton exchange membrane (PEM) fuel cells, cooling is necessary to maintain consistent and uniform operating temperatures, which are generally in the range of 60 to 80 °C. A potential solution is a heat pipe (HP) employing the principle of conduction in combination with a phase change. The purpose of this study was to fully characterize the operation of an HP with unique geometry designed for fuel cell heat removal at operating temperatures up to 100 °C and to assess the suitability of the resulting performance for cooling system integration. Test variables consist of cold sink thermal-contact conductance coefficient improving material usage, heat rejection temperature, contact pressure and area, HP orientation, operational hours, and variability between units.

The test results showed that HP performance improves through increased condenser and heat sink contact pressure, thermal contact coating usage, greater condenser area utilization, and colder heat sink temperature. Higher initial HP temperature and greater age or operational time reduce HP capabilities. Placing the condenser lower than the evaporator is the only HP orientation that affects evaporator plate temperature. Condensing fluid in the lower section reduces heat transfer capacity as that orientation requires liquid water to transport by wicking against gravity.

## Nomenclature

HP	heat pipe
PEM	proton exchange membrane
TC	thermocouple
TOT	total operational time
V	valve

## Symbols

$A$	cross-sectional area of heat pipe condenser section
$A_c$	heat transfer area
$A_s$	exterior surface area of insulation wrapping
$F$	pound-force
$h_{eff}$	effective heat transfer coefficient
$h_f$	heat transfer coefficient for gases in free convection
$I$	current
$k$	thermal conductivity of polyester insulation

$n$	total number of thermocouples on plate
$P$	power
$Q$	thermal power
$Q_l$	heat loss rate
$t$	insulation thickness
$T_a$	ambient air temperature
$T_{avg}$	average heat pipe evaporator temperature
$T_i$	individual thermocouple temperature
$T_p$	press platen cold sink temperature in direct contact with heat pipe condenser surface
$T_s$	average insulation exterior surface temperature
$V$	voltage
$\Theta$	degrees of vise handle rotation clockwise from initial contact and 0.0 lb of force

## 1.0 Background and Purpose

To operate chemical process units, sufficient heat transfer is an essential factor in maintaining equipment performance. The transfer of thermal energy in these unit operations may occur by conduction, radiation, or convection. Convective heat transfer is simple to control, but adds complexity when circulating a cooling fluid through a device such as a fuel cell. In a solid component, utilizing only conduction does not allow for precise control of system temperature since solid materials typically exhibit near constant thermal conductivity. With a given heat transfer area and heat flow quantity, a temperature gradient is established within the material for heat flow to occur. Depending on the material conductivity, this gradient can be significant. To minimize thermal gradients, it is desirable to combine the uniform temperature control capability of convection with a high effective thermal conductivity.

For exothermic systems such as fuel cells, cooling is necessary to maintain consistent and uniform operating temperatures, which are generally in the range of 60 to 80 °C. A potential solution is a heat pipe (HP) employing a phase change that produces a very high effective conductivity with no temperature gradient and without the complexity of circulating a fluid through the fuel cell stack. Within an HP at a designed pressure, fluid vaporization occurs at a particular temperature, absorbing a significant quantity of heat energy. HPs present an innovative potential cooling method for a fuel cell, although this application is not well evaluated.

Typical HPs are thoroughly understood devices that are commonly used in electronics and aerospace applications. Fuel cell geometry and heat removal requirements necessitate a somewhat nonconventional flat-plate HP geometry. With this type of HP, the goal is to have heat entering from anywhere on its surface and transferred to a cooled edge where it is removed to an external coolant source. HP geometry and heat removal can be tested experimentally to verify effective operation and determine operational limits. Data from this type of testing could then be used to validate analytical models of flat-plate HP operation for a fuel cell application.

The purpose of this study was to fully characterize the operation of an HP designed for fuel cell heat removal at operating temperatures up to 100 °C and to assess the suitability of the resulting performance for cooling system integration. Test variables consist of cold sink thermal-contact conductance coefficient improving material usage, heat rejection temperature, contact pressure and area, HP orientation, operational hours, and variability between units.

## 2.0 Theory

An HP is a device that transfers heat energy through the phase change of a working fluid. The HP absorbs energy in the form of heat from an external source. The heat is conducted through the HP wall to

the internal working fluid. Heat produced by the external source causes the temperature of the source and HP to increase. Once the temperature of the HP internal fluid reaches its boiling point, the internal fluid will begin to vaporize. This portion of the HP where vaporization takes place is termed “the evaporator section.” The phase change of the internal fluid absorbs the heat generated by the external source and holds the temperature of the HP and source at this boiling point temperature. This is akin to how a pot of boiling water will remain at 100 °C even as heat from the stove is continually added.

As the internal fluid vaporizes, it is transported to the condenser section of the HP, which is held at a temperature below the boiling point of the internal fluid by an external cooling source. Once at the cool condenser section, the fluid will undergo a phase change back to a liquid releasing heat, which is removed by the cooling source. The cooling source can be a secondary cooling loop or a radiator that rejects heat to the surroundings to maintain temperature.

Once the fluid is back in a liquid state, it is returned to the evaporator section of the HP by either an internal wicking structure that utilizes capillary forces to transport the fluid or by the force of gravity. The method used for fluid transportation within the HP will depend on the application, amount of heat being moved, and the orientation of the HP during operation.

Figure 1 shows a diagram of the basic HP operational mechanism. Heat is input into a section called the evaporator and causes the working fluid to evaporate. The vapor travels to the condenser section where heat is transferred to a heat sink. As this occurs, the working fluid undergoes a phase change back to a liquid and returns to the evaporator.

Once a working fluid is selected, internal pressure remains as the primary design factor affecting the operating temperature. By utilizing water as the working fluid, flat-plate HPs may be made to operate over a temperature range of 273 to 643 K by adjusting the internal pressure within the HP (Bejan and Kraus, 2003). A single HP, however, functions over a much narrower temperature span.

Generally, HPs for use in fuel cell applications are constructed as flat plates as presented in Figure 2. This enables the HP to remove heat over the full area of a cell where the reactions take place within a fuel cell. This geometry also allows for a constant cross-sectional area for the entire working fluid flow path so that there is no restriction in that channel.

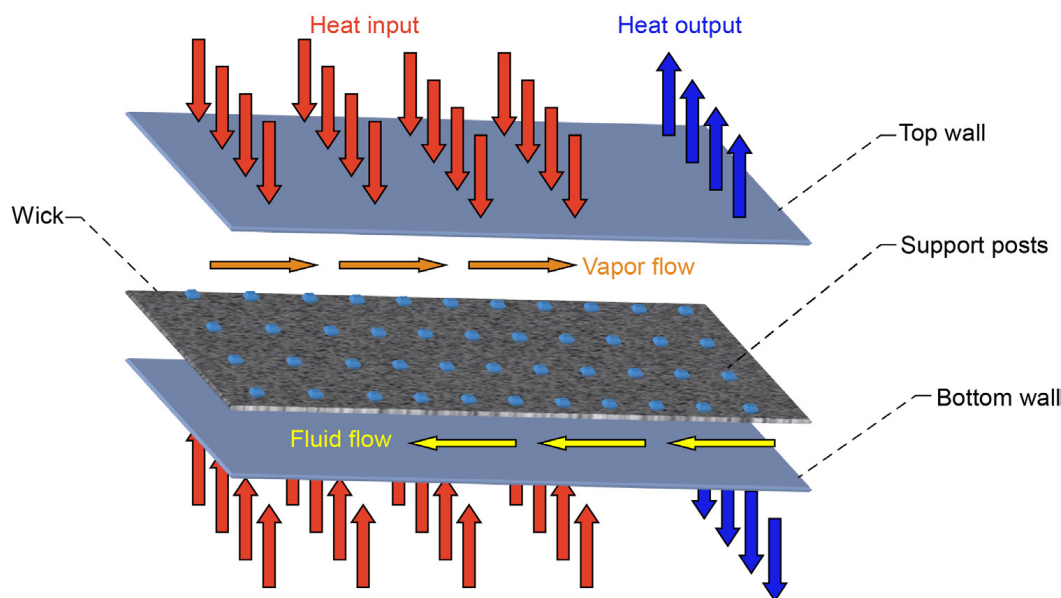


Figure 1.—Flat-plate heat pipe operation (Colozza et al., 2014).

Fuel cell stacks consist of many single fuel cells joined together in series and are designed as plates with an active area that has channels for transporting reactant gases and the water byproduct from cell to cell. A fuel cell may be constructed with a circular active area to reduce overall stack mass, minimize pressure variation across the sealing surface, and maximize the total active area relative to the entire cross-sectional area of a stack. In such a case, the flat-plate HP will need to be designed to match the shape of the cells in order to provide consistent pressure across the active area and effective sealing between the cells. In Figure 3, an example is shown for an HP developed to fit within such a stack assembly.



Figure 2.—Silver-coated flat-plate Ti heat pipe (Colozza et al., 2014).

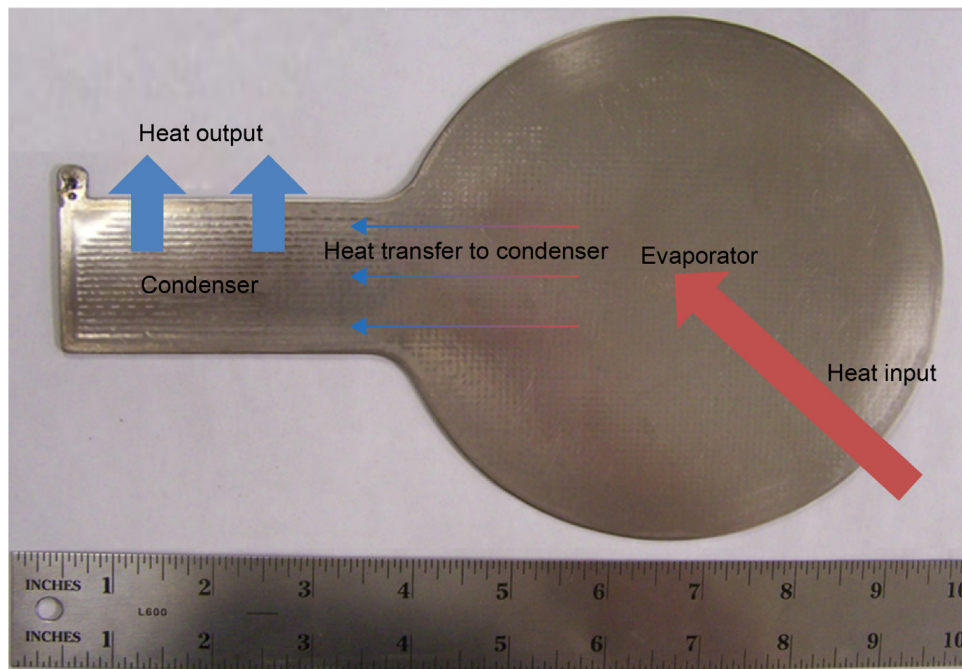


Figure 3.—Ti heat pipe for fuel cell application.

The condenser section is narrow relative to the evaporator plate sized to match the fuel cell. In assessing the applicability of flat-plate HPs to provide a simple, passive means of cooling a fuel cell stack, it is critical to evaluate the performance of such an HP relative to the heat management needs within a fuel cell.

### 3.0 Test Setup, Material, Equipment, and Procedures

The experimental test system diagram is presented in Figure 4 and pictures are shown in Figure 5 and Figure 6. For testing the HPs in a horizontal orientation, a hydraulic press manufactured by Carver, Inc., is used. The press provides a pressure gauge for monitoring the compressive force or pressure between the platens as well as digital displays for monitoring the platen temperature. The applied force from the press is controlled manually through the press handle. A NesLab Coolflow CFT-33 refrigerated recirculating chiller (Thermo Electron Corporation) maintains the water at a specified temperature between 0 °C and room temperature. Chilled water exits the chiller through a three-way valve (V1), which directs fluid to drain out of the system or towards the CARVER® press platens. A second valve (V2) is used to vent air out of the system in order to allow for coolant to flow unrestricted through the platens. This valve is located before the fluid inlet to the platens. Once the air is vented, this valve is closed during operation of the test. Water flows to the platens in parallel from the chiller. This minimizes the coolant differential temperature between the platens. After leaving the platens, water is recombined to one stream that is sent to a three-way valve (V3) that directs water out of the system or to the chiller inlet.

The operational performance testing utilized eight Thermacore water-filled Ti HPs (Thermacore, Inc.) of similar specifications. Throughout the report, these units are denoted as HP 1, HP 2, HP A, HP B, HP C, HP D, HP E, and HP F. Photographs of two-dimensioned HPs appear in Figure 7 and Figure 8. The evaporator section of the HPs is circular and has a diameter slightly greater than 14 cm, whereas the condenser section is rectangular with dimensions of 4.1 by 9.1 cm. The HPs are designed to begin operation at a temperature of approximately 60 °C.

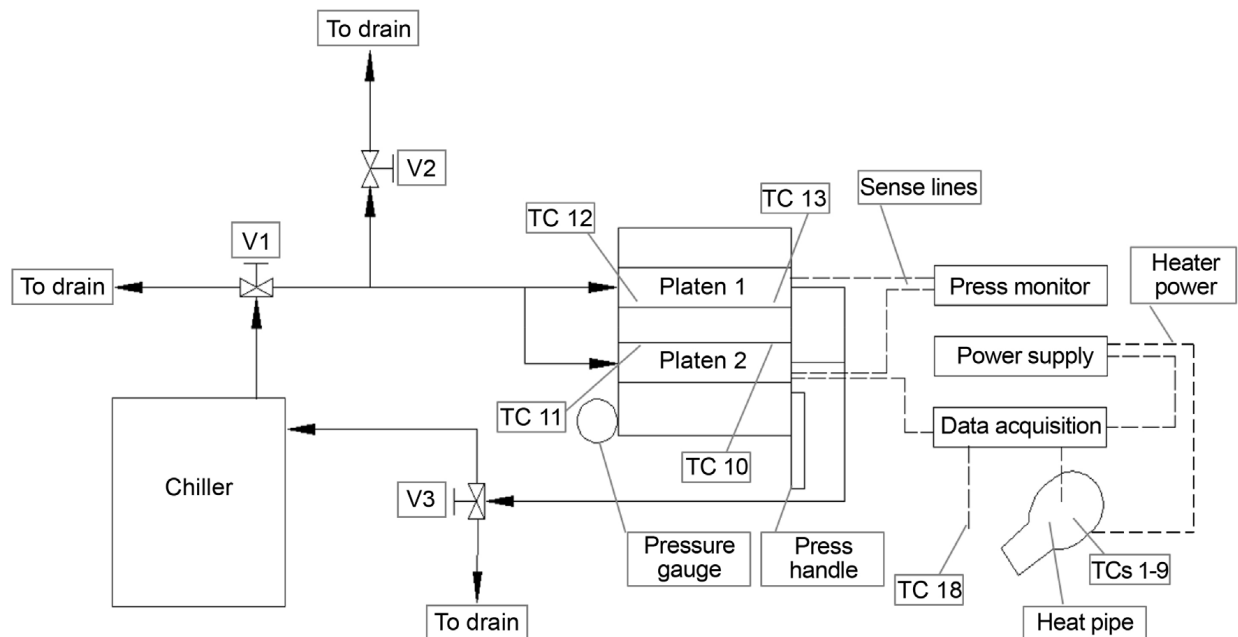


Figure 4.—Experimental test system. TC, thermocouple; V, valve.





Figure 5.—Horizontal heat pipe test setup.

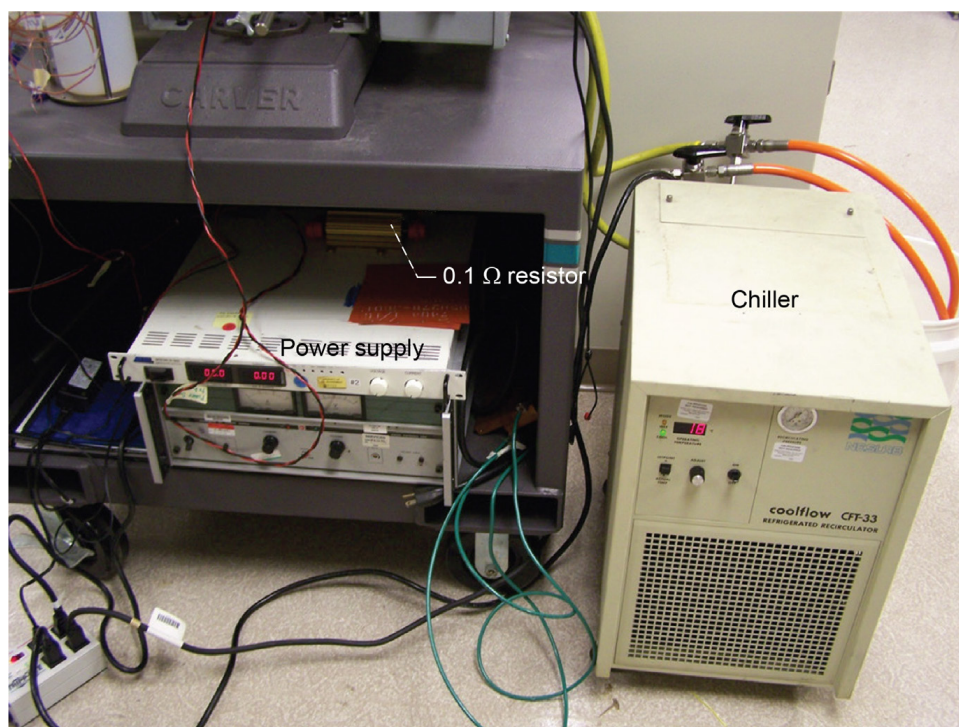


Figure 6.—Power supply and chiller employed for testing.

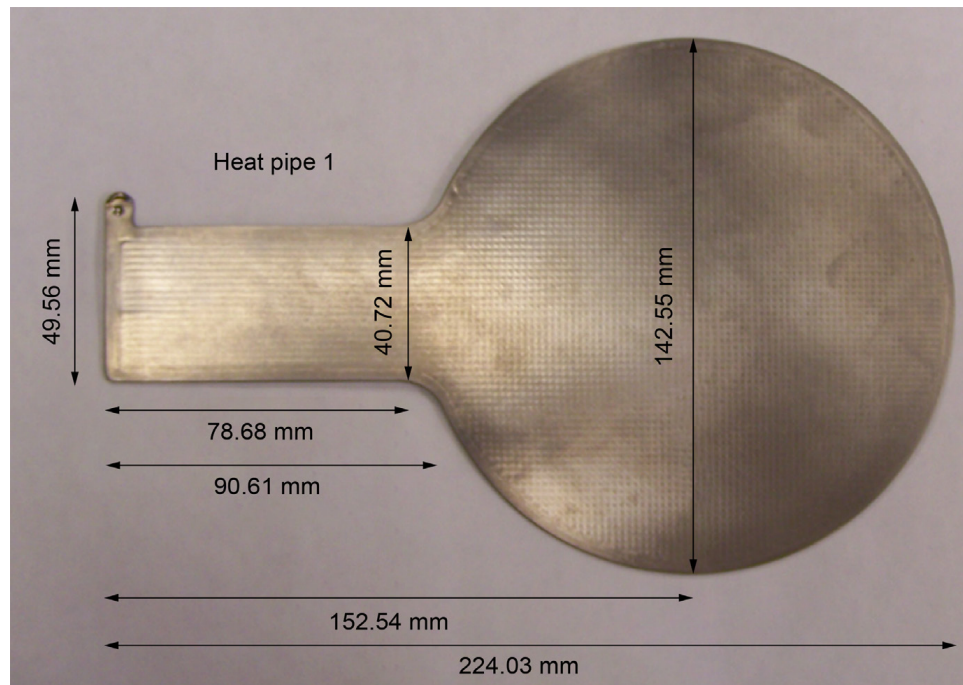


Figure 7.—Dimensions of heat pipe 1.

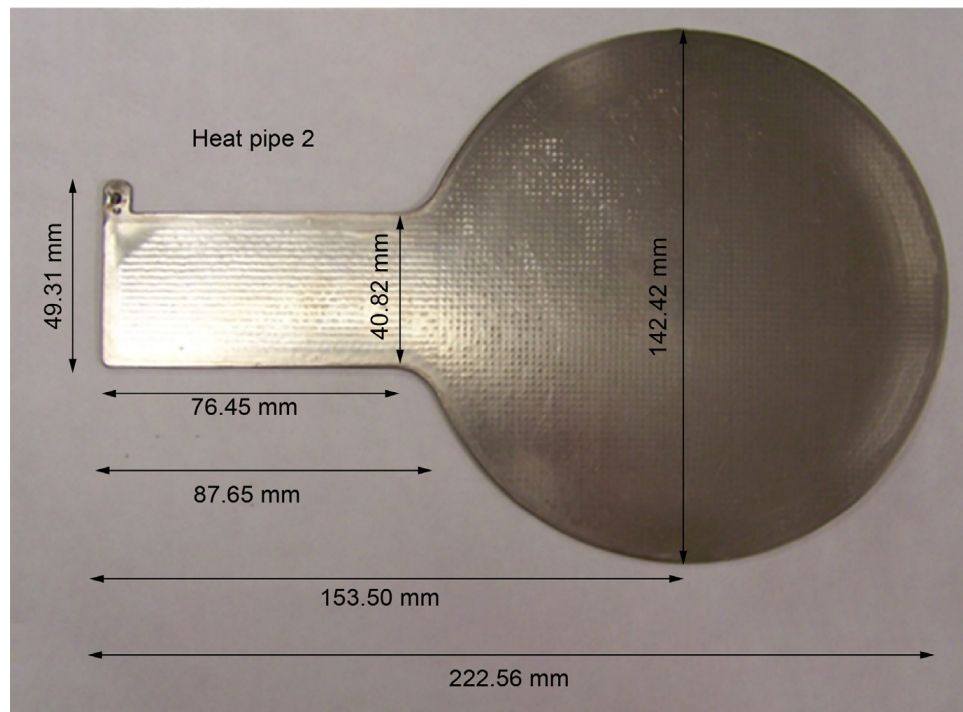


Figure 8.—Dimensions of heat pipe 2.



On one side of each HP evaporator section, a 3- by 3-in<sup>2</sup> Si heating pad is attached to the flat surface, as shown in Figure 9. The heaters each had a measured internal resistance of 154.6  $\Omega$ . Power was sent to the heater from a manually controlled direct current power supply.

To record the operating temperature of the evaporator, each HP was instrumented with nine type K thermocouples (TCs) numbered 1 to 9, as shown in Figure 10 and Figure 11. The TCs are evenly spaced over the evaporator section and adhered to the surface of the HP with Kapton tape.

As shown in Figure 12, four type K TCs (10 to 13) are mounted on the press platens to record temperature during the testing. A single type K thermocouple (TC 18), mounted away from the balance of the testing equipment as presented in Figure 13, monitors the ambient temperature. All TC outputs are recorded by a GL800 data logger (GRAPHTEC Corporation).

To minimize experimental error due to heat loss to the surroundings, the evaporator is wrapped with five layers, approximately 4-cm total thickness, of polyester fiber insulation on all sides while leaving the condenser uncovered as shown in Figure 14, Figure 15, and Figure 16. The TC and heater wires are passed through a narrow gap in the insulation to minimize any heat loss. The evaporator insulation is sealed along the interface with the condenser and evaporator sections of the HP with Kapton tape.

In Figure 17 and Figure 18, two type K TCs (19 and 20), measuring surface temperature, are added to the exterior of the insulation on the evaporator section. The insulation surface temperature provides a means of estimating any heat loss from the HP through the insulation.

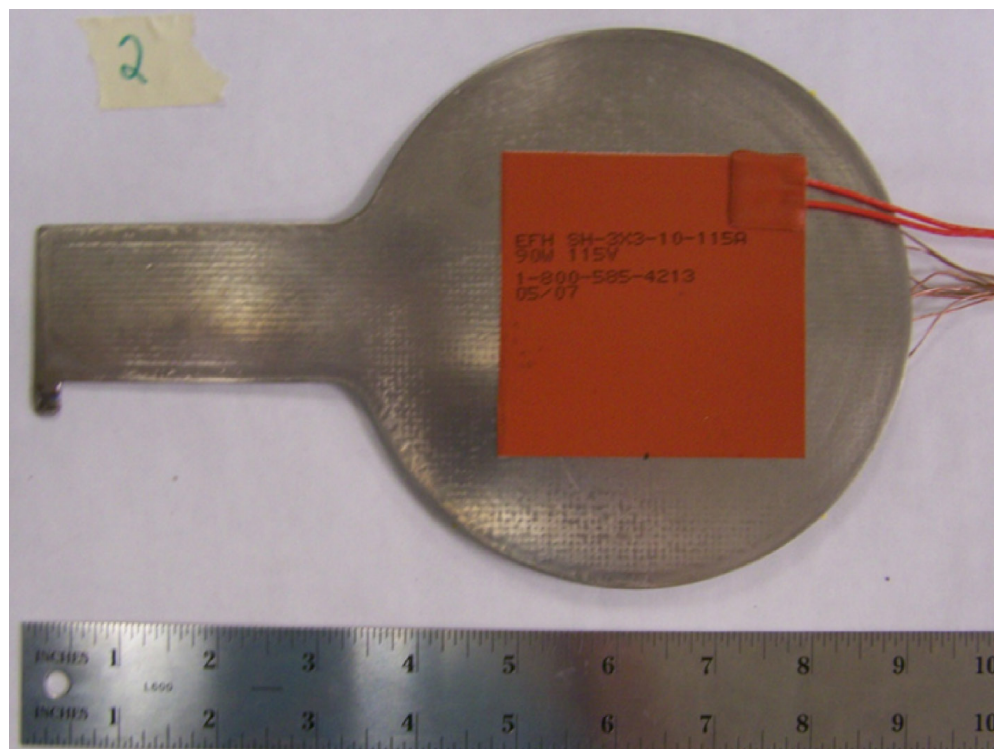


Figure 9.—Location of pad heater on heat pipe 2 evaporator.



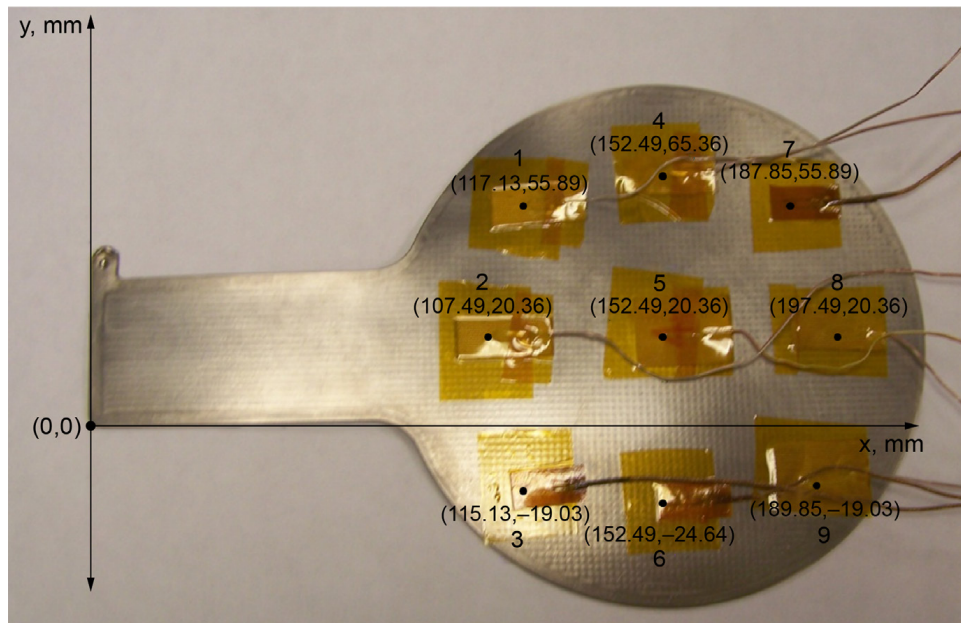


Figure 10.—Thermocouple placement on the evaporator section of heat pipe 1.

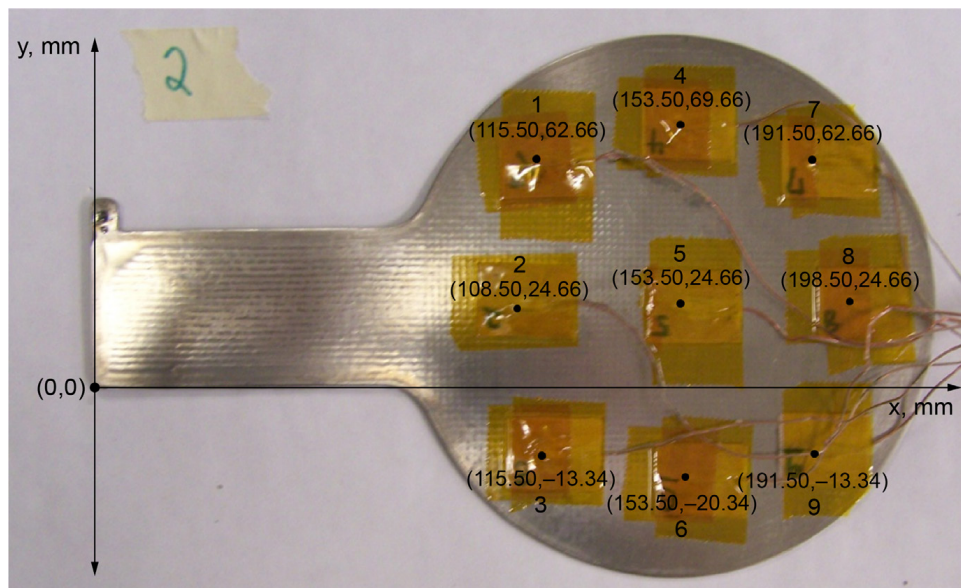


Figure 11.—Thermocouple placement on the evaporator section of heat pipe 2.

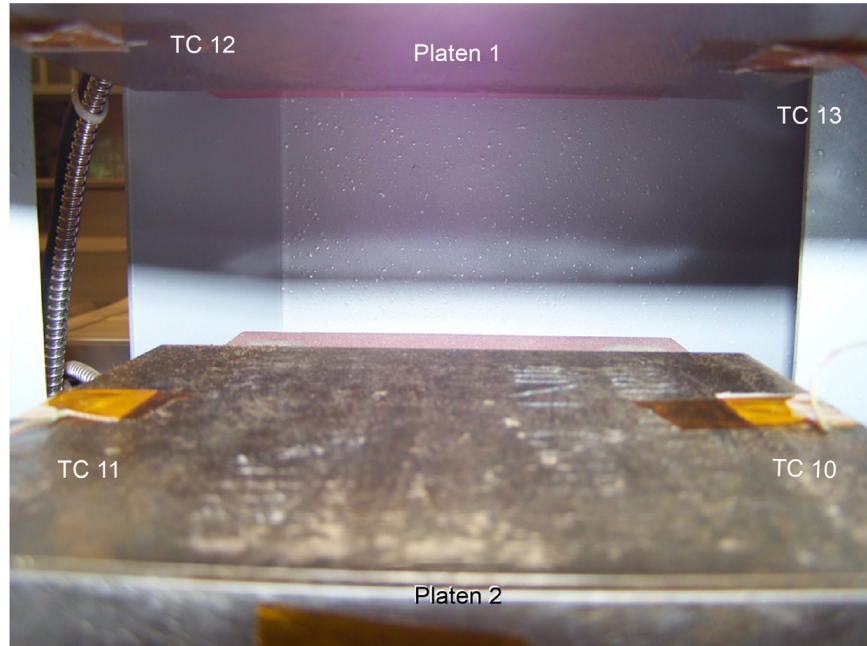


Figure 12.—Placement of thermocouples (TCs) 10 to 13 on press platens.

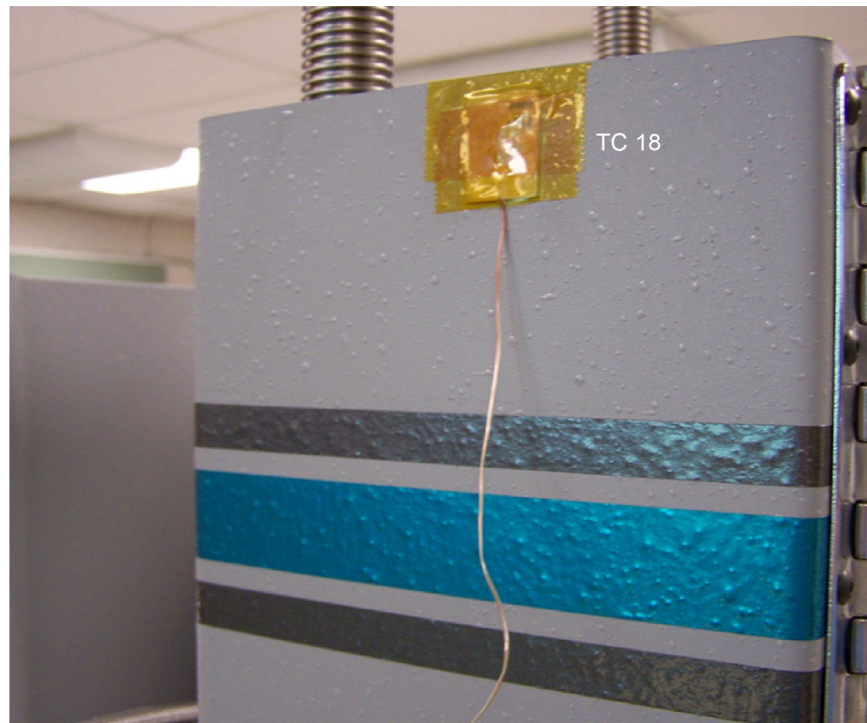


Figure 13.—Side of press unit mounting location of ambient temperature monitoring thermocouple (TC) 18.



Figure 14.—Side view of insulation surrounding heat pipe 2 evaporator.

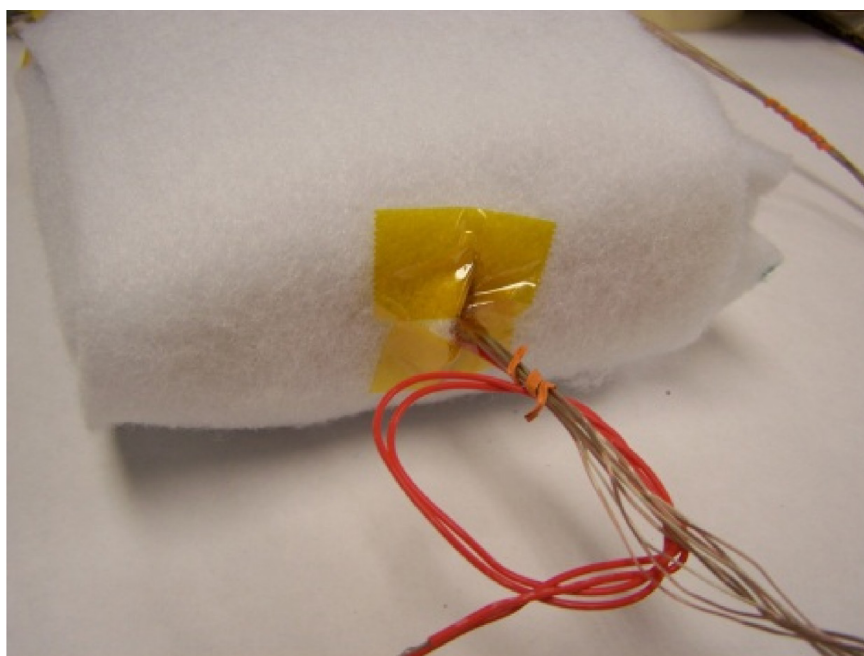


Figure 15.—Wiring exit from insulation.



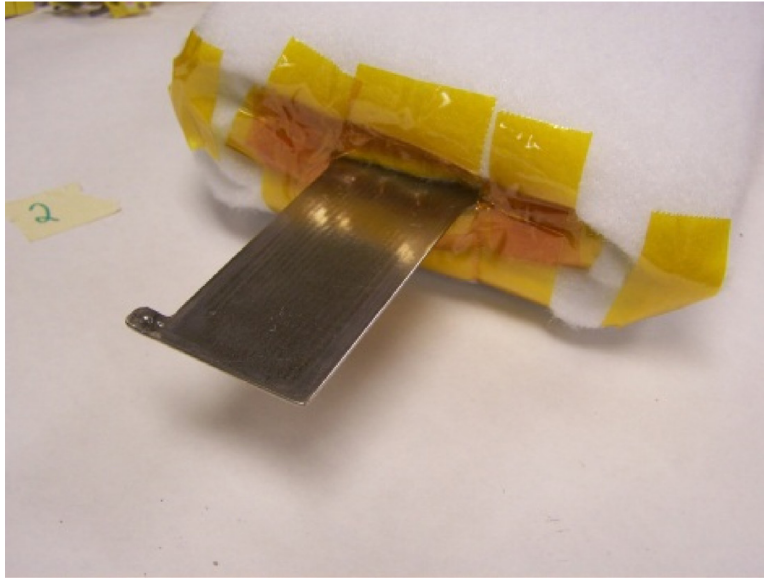


Figure 16.—Condenser protruding from insulated region.

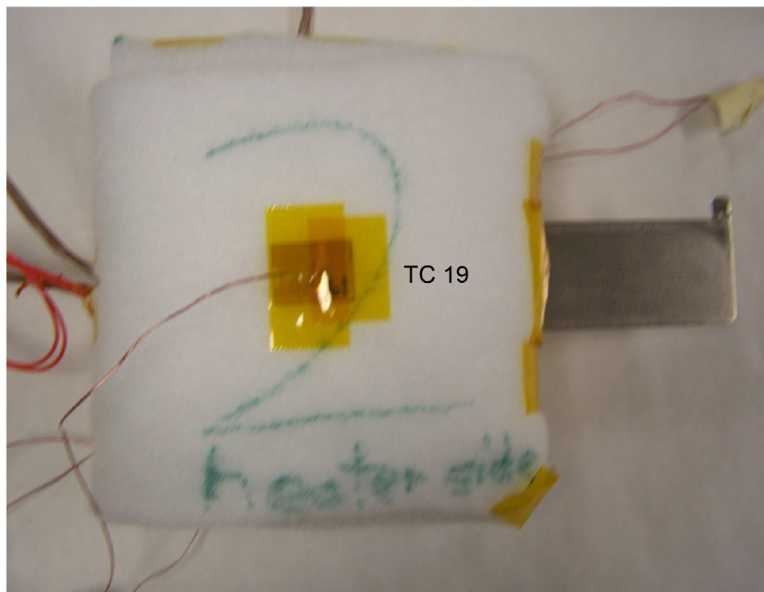


Figure 17.—Thermocouple (TC) 19 on outside of insulation.

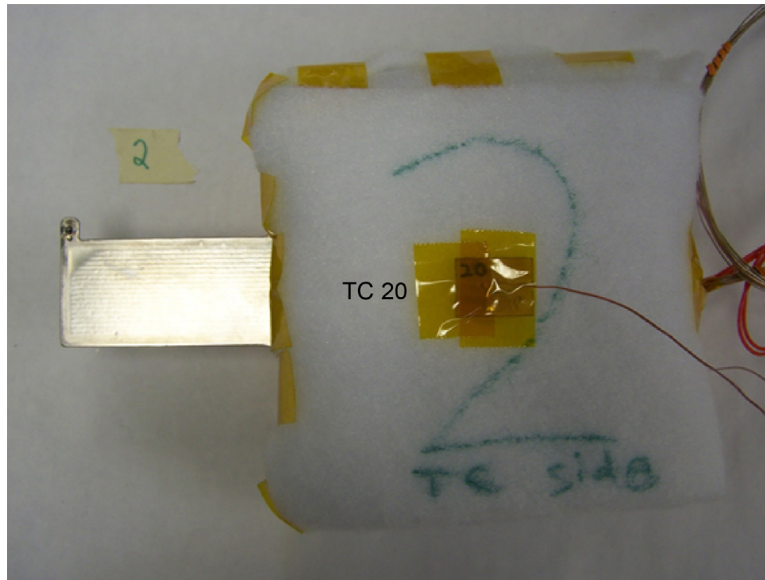


Figure 18.—Thermocouple (TC) 20 on outside of insulation.

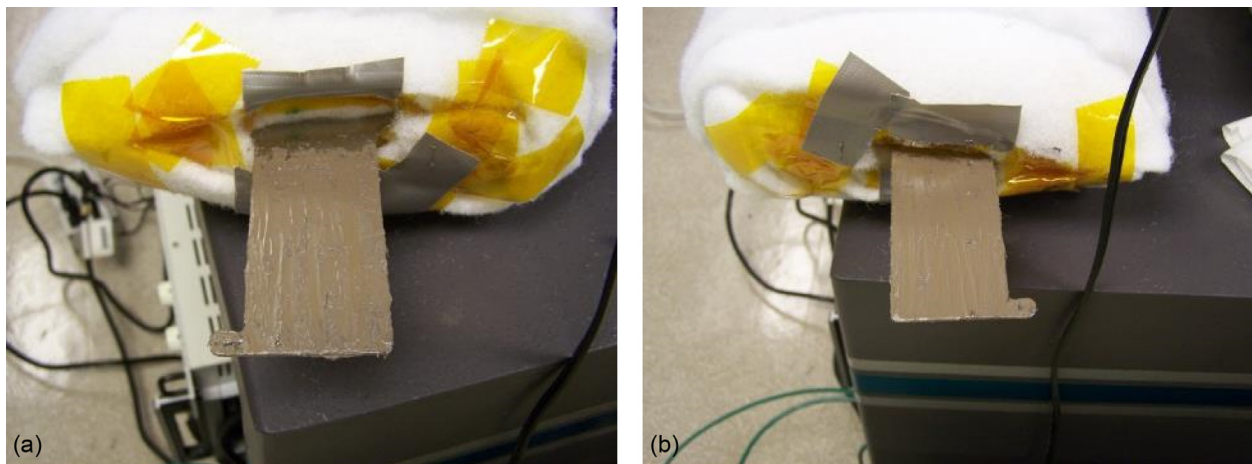


Figure 19.—Application of silver paste to condenser exterior. (a) Side one. (b) Side two.

To ensure good thermal contact between the condenser section of the cold plates and the press platens, prior to HP installation in the press, Arctic Silver® 5 thermal compound (Arctic Silver, Inc.) is uniformly spread on both sides of the condenser surface as presented in Figure 19. Once in the press, the thermal compound is compressed, filling in any surface imperfections and thickness variations to provide full thermal contact between the condenser section and platens.

During testing, the condenser section is held between the cooled platens to remove heat at a consistent heat sink temperature. For the condenser area testing, the total area held within the cooled platens or press was varied. This is exemplified in Figure 20 where only a small portion of the condenser is held within the platens.

Between test runs, the HPs are sealed within a plastic bag and stored as shown in Figure 21. This is done to keep the thermal compound from drying out between the tests.

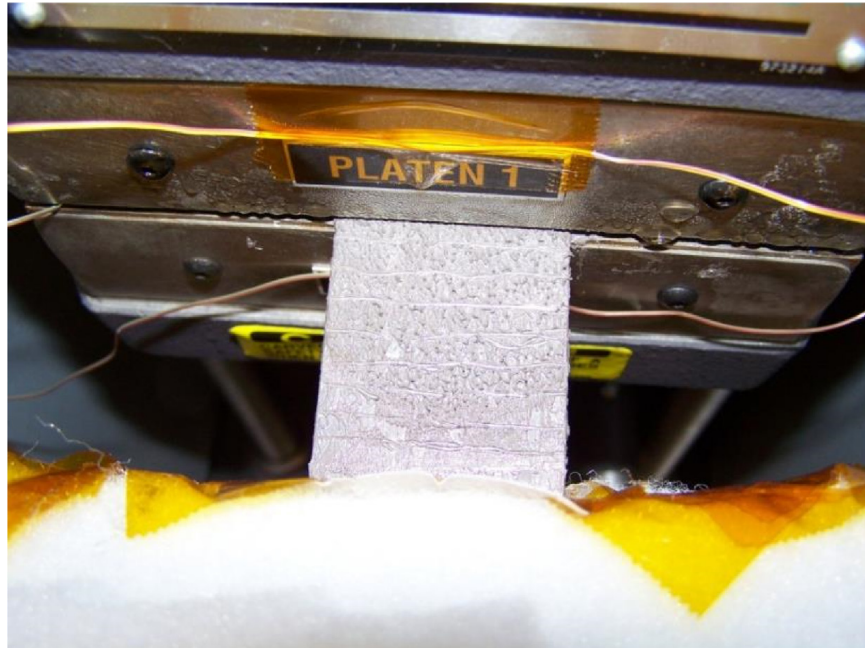


Figure 20.—Heat pipe condenser during functional area test.



Figure 21.—Storage of heat pipe between test runs.

Prior to initiating a test, all electrical connections, the presence of a flash drive for data recording, and the water level in the chiller are verified. The HP condenser is placed in the press at the desired depth and orientation, then the chiller, power supply, and data logger are powered on. The tests are run by setting the chiller to the desired water temperature, ranging from 8 to 20 °C, and the press to a specified clamping force between 60 and 100 lb. Temperature and voltage sensor channels are verified to function while waiting for the platens to cool to a steady-state temperature.



The desired power level is set on the power supply by turning the current knob to full, then adjusting the voltage dial so that nominally 15 W is supplied to the heating pad. Once a steady-state evaporator temperature is determined, the power supplied is increased in 10 W increments until providing a maximum of 75 W. The steady-state temperature profile is established at each interval by maintaining constant power input for a predetermined amount of time, up to 20 minutes per step.

If at any time the temperature reaches 100 °C on the HP evaporator plate, the test is immediately shut down by turning off the power supply. Otherwise, once steady state is attained at the 75-W step, the supply is powered off by moving voltage and current knobs counterclockwise until 0 A appeared on the display. Data recording is continued until the HP surface temperature decreases below 40 °C.

In order to test the HPs in orientations other than horizontal, a vise is used in conjunction with two copper cold plates. The vise compressive force is calibrated by using a scale and a protractor for the turning bar as shown in Figure 22 to Figure 24. The relation for clamping force versus handle angle is provided in Appendix C.

To perform the tests, the copper cold plates are positioned between the vise jaws. The HP condenser section is then placed between the copper cold plates. The cold plates are cooled by water flow from the chiller. There are six type T TCs used to measure the temperature of each cold plate. These TCs are fit into the cold plates with one near each corner and two toward the center of the plate. All instrumentation on the HPs is the same as the tests performed with the press.

In total, four different HP orientations are tested with the cold plates:

- HP oriented vertically with the condenser and evaporator on the same plane (shown in Figure 25)
- HP oriented with the condenser above the evaporator (shown in Figure 26)
- HP oriented with the condenser below the evaporator (shown in Figure 27)
- HP oriented horizontally with the copper cold plates

A test is run in each orientation with 8 °C coolant water and approximately 100 lb of force on the condenser. All other operational procedures remain identical to the horizontal test.

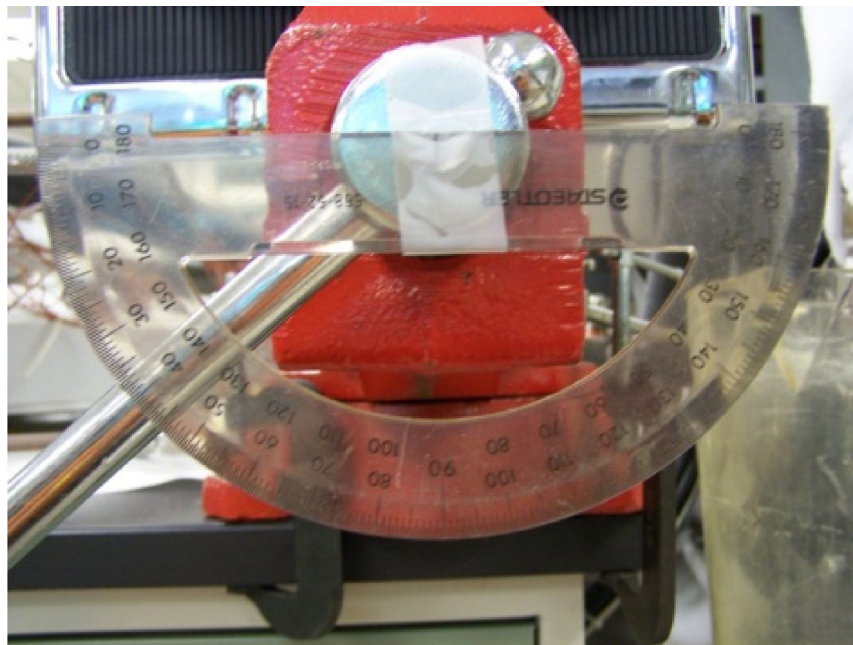


Figure 22.—Calibration of vise force: 0.0 lb at 218°.

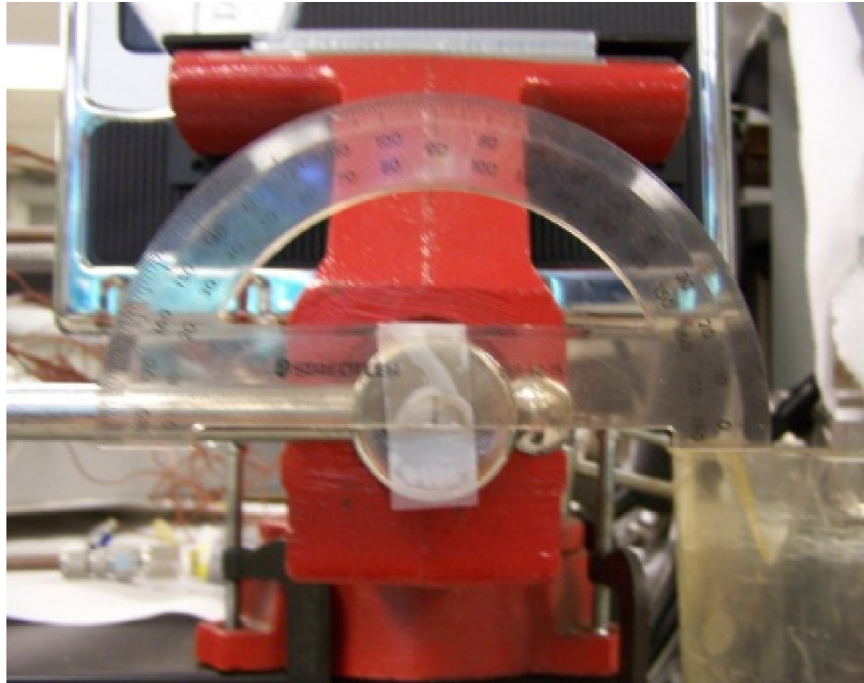


Figure 23.—Calibration of vise force: 11.4 lb at 180°.

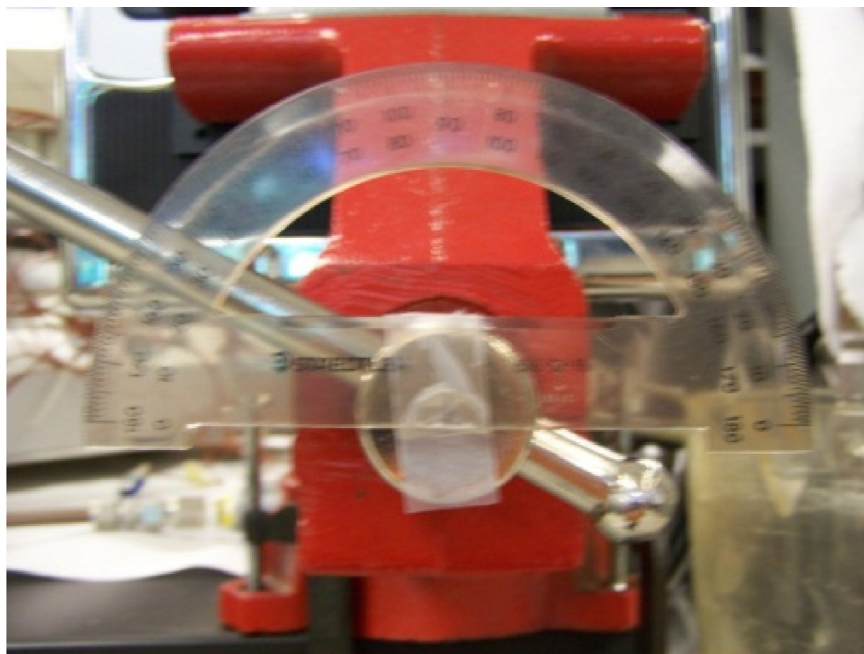


Figure 24.—Calibration of vise force: 27.0 lb at 150°.



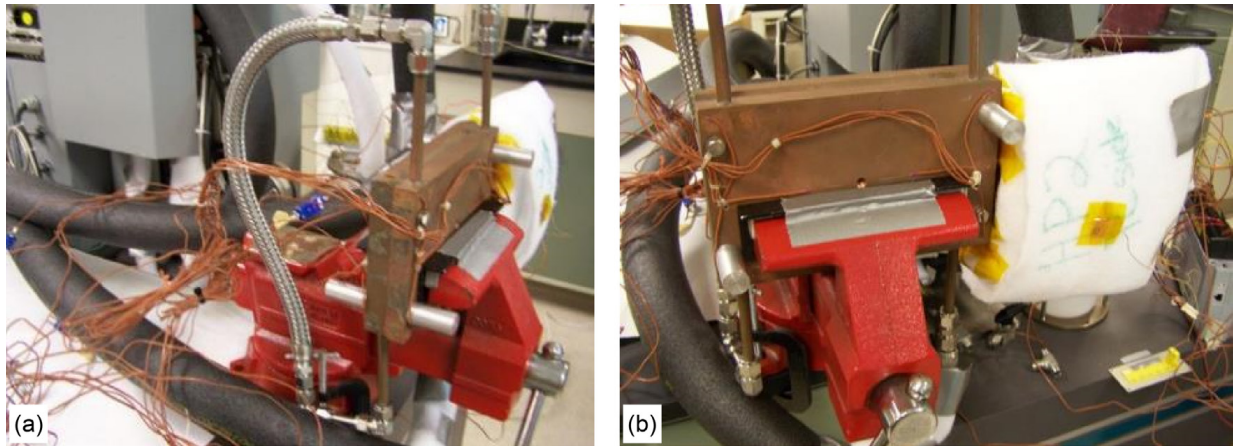


Figure 25.—Condenser out to side test setup. (a) Left side view. (b) Straight on view.

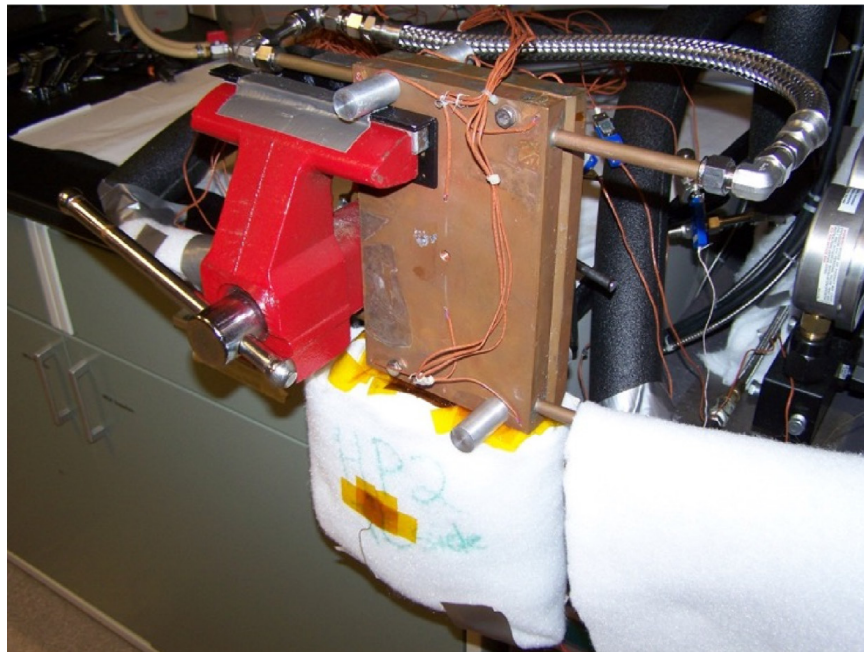


Figure 26.—Condenser on top test setup. HP, heat pipe.

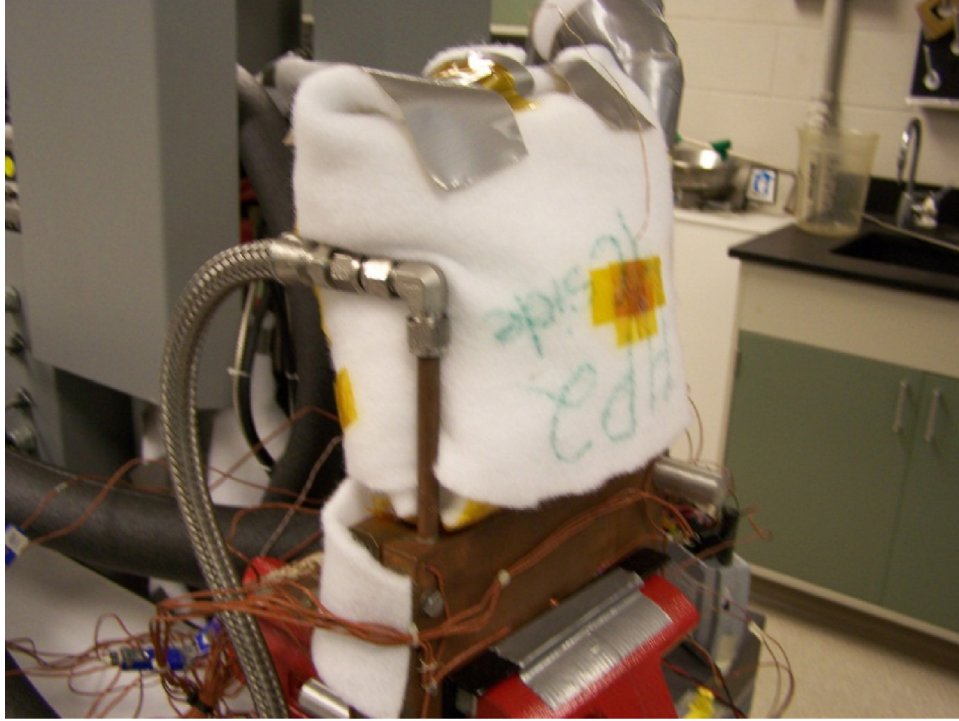


Figure 27.—Condenser on bottom test setup. HP, heat pipe.

## 4.0 Data Analysis

The power,  $P$ , supplied to the HP was calculated from Equation (1),

$$P = IV \quad (1)$$

where  $I$  represents current and  $V$  is the voltage. Resistive line losses were assumed to be negligible in comparison to the resistance of the heating pad. The average HP evaporator surface temperature,  $T_{\text{avg}}$ , is determined from Equation (2),

$$T_{\text{avg}} = \frac{\sum_i^n (T_i + T_{i+1} + \dots + T_n)}{n} \quad (2)$$

where  $T_i$  is the temperature measured by an individual TC and  $n$  is the total number of TCs on the plate. In this document, average HP evaporator surface temperature is frequently shortened to average HP temperature.

To characterize HP heat transfer effectiveness, it is possible to calculate an effective heat transfer coefficient,  $h_{\text{eff}}$ , from Equation (3) (Mills, 1994),

$$h_{\text{eff}} = \frac{Q}{A(T_{\text{avg}} - T_p)} \quad (3)$$

where  $Q$  is the thermal power,  $A$  is cross-sectional area of the HP condenser section, and  $T_p$  is the press platen cold sink temperature in direct contact with the HP condenser surface.

Similar equation formats were used to quantify heat lost through the insulation rather than transferred to the condenser section. This estimation was performed in two distinct ways. In the first, thermal power transferred through the insulation was assessed by considering convection at the insulation exterior surface into the surrounding ambient air. As given by Equation (4) (Mills, 1994), heat loss rate,  $Q_1$ , is

$$Q_1 = h_f A_s (T_s - T_a) \quad (4)$$

where  $h_f$  is the heat transfer coefficient for gases in free convection,  $A_s$  is the exterior surface area of the insulation wrapping,  $T_s$  is the average insulation exterior surface temperature, and  $T_a$  is the ambient air temperature. The free-convection heat transfer coefficient was assumed to be 10 W/m<sup>2</sup>K. The insulation exterior surface area is approximately 0.14 m<sup>2</sup>.

Additionally, thermal power loss was calculated by supposing conduction through the polyester insulation. As given by Equation (5) (Mills, 1994),

$$Q_1 = \frac{k}{t} A_c (T_{\text{avg}} - T_s) \quad (5)$$

where  $k$  is the thermal conductivity of the polyester insulation,  $t$  is the insulation thickness, and  $A_c$  is the heat transfer area. Polyester fiber thermal conductivity was conservatively assumed to equal 0.05 W/(m•K) (Tilioua et al., 2012) and the insulation thickness was generally 0.05 m. The heat transfer area is estimated as halfway between the surface area of the HP evaporator section and the insulation exterior. The calculated value was 0.09 m<sup>2</sup>.

## 5.0 Results and Discussion

To fully evaluate the operation of the eight HPs, a number of tests were performed. The first two HPs used in the testing are labeled HPs 1 and 2. The subsequent six HPs are labeled HP A, HP B, HP C, HP D, HP E, and HP F. The preliminary tests of the first two HPs consisted of verifying proper operation. Both HPs were initially tested on the press in a horizontal orientation without any thermal compound on the condenser section. The full condenser area was placed within the press platens to maximize the condenser area and heat transfer to the chilled water. The chiller was set to 8 °C and the compressive force of the press was set to 445 N, equivalent to 100 lb.

Initial testing indicated that HP 1 was not functional. The slow asymptotic approaches to equilibrium evaporator surface temperatures seen in Figure 28 characterize conduction through the Ti more so than phase change heat transfer. The temperature increases of greater than 30 °C between power levels demonstrate nonfunctionality of the internal evaporation and condensation process as well. With input heater power increases in 10-W intervals, the evaporator temperature is expected to rise less than 10 °C per step.

HP 1 performance is poor in comparison to HP 2 results. For HP 2, the temperature increase per step in heater power was minimal, as presented in Figure 29. Additionally, the time to reach equilibrium after an increase in heater power was relatively short, on the order of minutes, compared to much longer times needed to reach equilibrium for HP 1. These characteristics are indicative of a functioning HP.

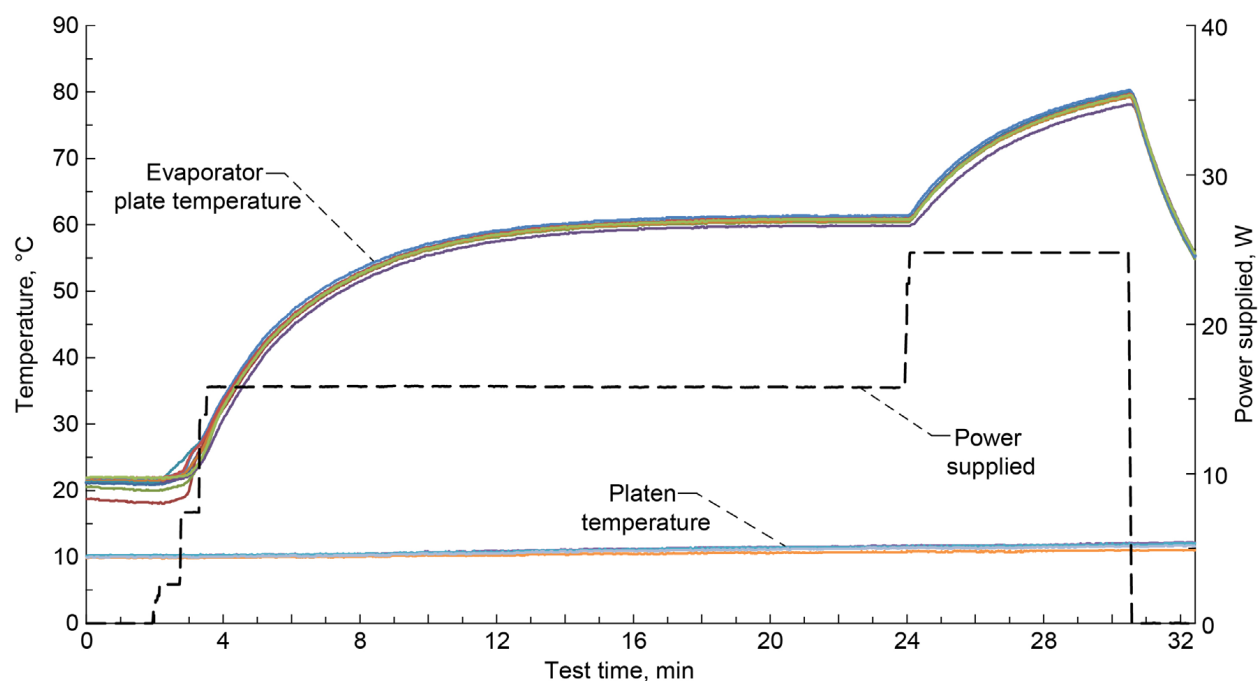


Figure 28.—Heat pipe 1 evaporator surface temperatures, press platen temperature, and heating power supplied over test duration on August 8, 2012, without Arctic Silver<sup>®</sup> paste, with full condenser, 100-lb force, 8 °C chiller setpoint, and horizontal operation.

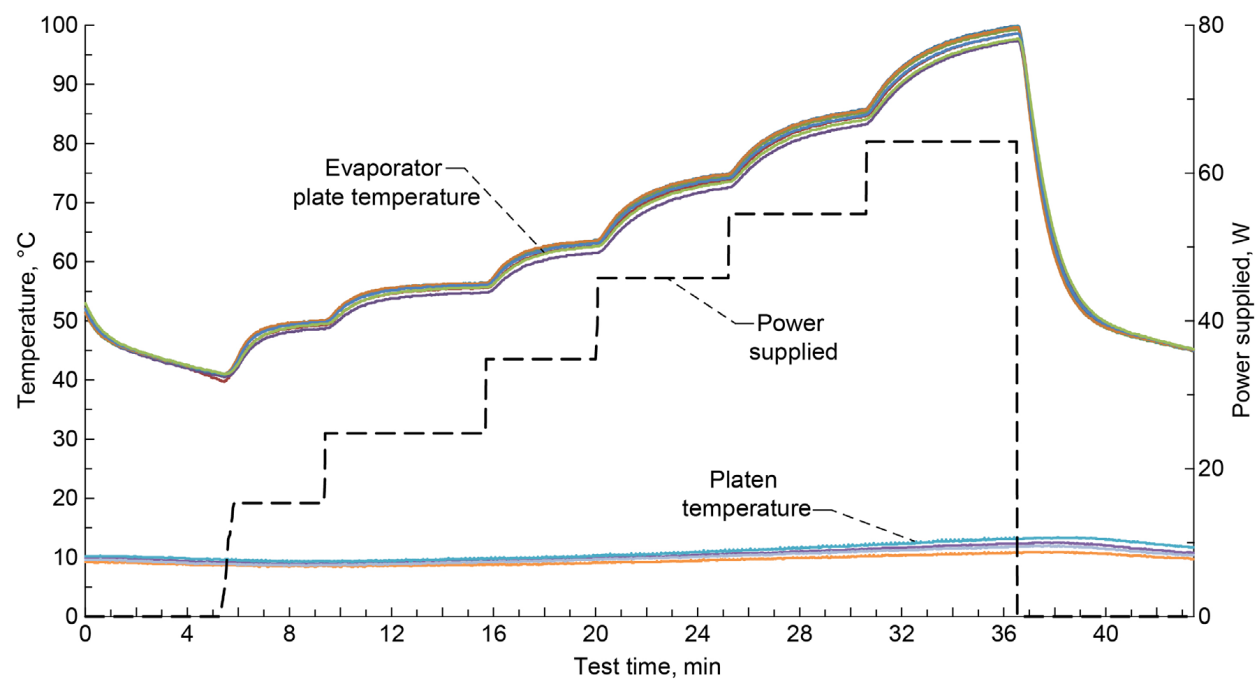


Figure 29.—Heat pipe 2 temperature increase per step in heater power on August 9, 2012, without Arctic Silver<sup>®</sup> paste, with full condenser, 100-lb platen force, 8 °C chiller setpoint, and horizontal operation.

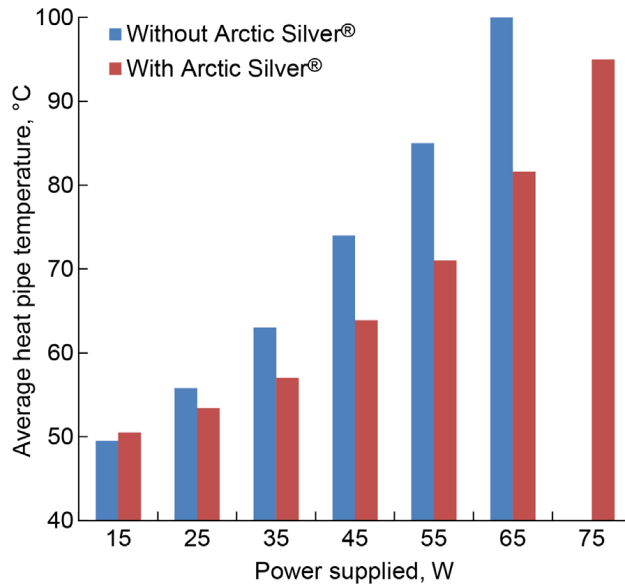


Figure 30.—Steady-state heat pipe 2 surface temperature, with and without the use of an Arctic Silver® thermal compound paste as a function of heater power on August 9 and 13, 2012, with and without full condenser, with 100-lb platen force, 8 °C chiller setpoint, and horizontal operation.

## 5.1 Thermal Paste Usage

The initial tests for HPs 1 and 2 did not include a thermal compound to enhance the heat transfer between the condenser section and the press platens. Improved heat transfer between the condenser and platens should increase the performance of the HP. To evaluate this, tests were conducted with a thermal compound applied to the condenser section of HP 2, as discussed previously and shown in Figure 19.

Figure 30 displays the results of these tests compared to those without the thermal compound. In this figure, the steady-state average evaporator plate temperature for HP 2 is given at each operational power level. With the Arctic Silver® paste ensuring complete contact from HP condenser to cold platens, the HP operates at lower temperatures for all but the lowest studied thermal power supplied level and ultimately transfers more heat while remaining below the imposed 100 °C temperature limit. The test data used to generate Figure 30 is given in Figure 29 and Figure A.2 and Figure A.3 in Appendix A.

Figure 30 shows a clear advantage in lower operating temperature with the use of a thermal compound to decrease the contact resistance between the condenser and the platens. This effect is negligible at low heater power levels of 15 W or less and increases significantly as the heater power is increased.

## 5.2 Condenser Heat Sink Temperature

Colder press platen temperatures should allow the HP evaporator section to operate at lower temperatures for a given heat load. In Figure 31 and Figure 32, the average evaporator surface temperature is shown for cold sink temperatures ranging from 8 to 20 °C. With 80 lb of platen force on the condenser over the range of platen temperatures tested, evaporator temperature was minimally affected by the platen temperature. At lower heater power levels, below 55 W, the average HP operating temperature decreased slightly with increased platen temperature. However, at power levels higher than 55 W, this trend reversed and, for a given power level, the average HP temperature was slightly lower at



lower platen temperatures. Variation over the course of the test was slight and likely within the experimental error of the temperature measurements being taken. These results indicate that the 80 lb of platen force on the condenser enabled satisfactory heat transfer to the platens. Heat transfer enhancement, which would be expected with a reduction in the platen temperature, was within the average HP temperature measurement error and therefore could not be fully resolved.

To reduce the heat transfer from the condenser section to the platens, the compressive pressure of the platens on the condenser was reduced to 60 lb. The results for this case are shown in Figure 32. The coldest platen temperature provided the lowest average evaporator surface temperature at all levels of heating power supplied. The test runs at each platen temperature were performed consecutively and, as a result, some error may have been introduced into the measurements if sufficient time was not allowed for all components to completely cool down to room temperature prior to initiating another test run at a higher platen temperature. Therefore, the results are somewhat varied at the beginning of the test runs for the platen temperature setpoints above 8 °C. At lower power levels early in the tests, 12 and 16 °C platen temperatures resulted in higher evaporator temperatures than the 20 °C trial. Beyond test times of 45 min, evaporator temperature was highest with the 20 °C platens and lowest with the 8 °C platens. In addition, due to the relatively close average HP temperatures for the cases with platen temperatures above 8 °C, the inherent measurement error could account for the demonstrated variation.

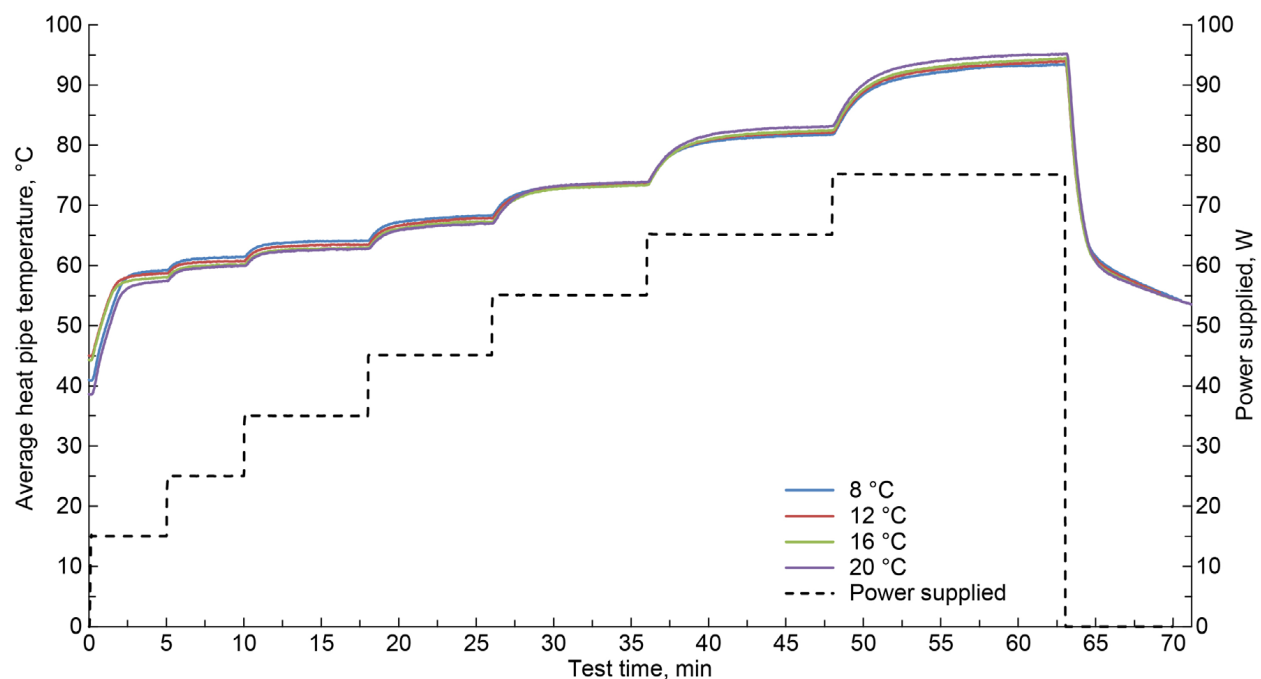


Figure 31.—Effect of varying platen cold plate temperatures and chiller setpoint on average heat pipe 2 evaporator surface temperature as heating power supplied increased in steps over time on August 15, 2012, with Arctic Silver® paste, full condenser, 80-lb platen force, multiple chiller setpoints, and horizontal operation.

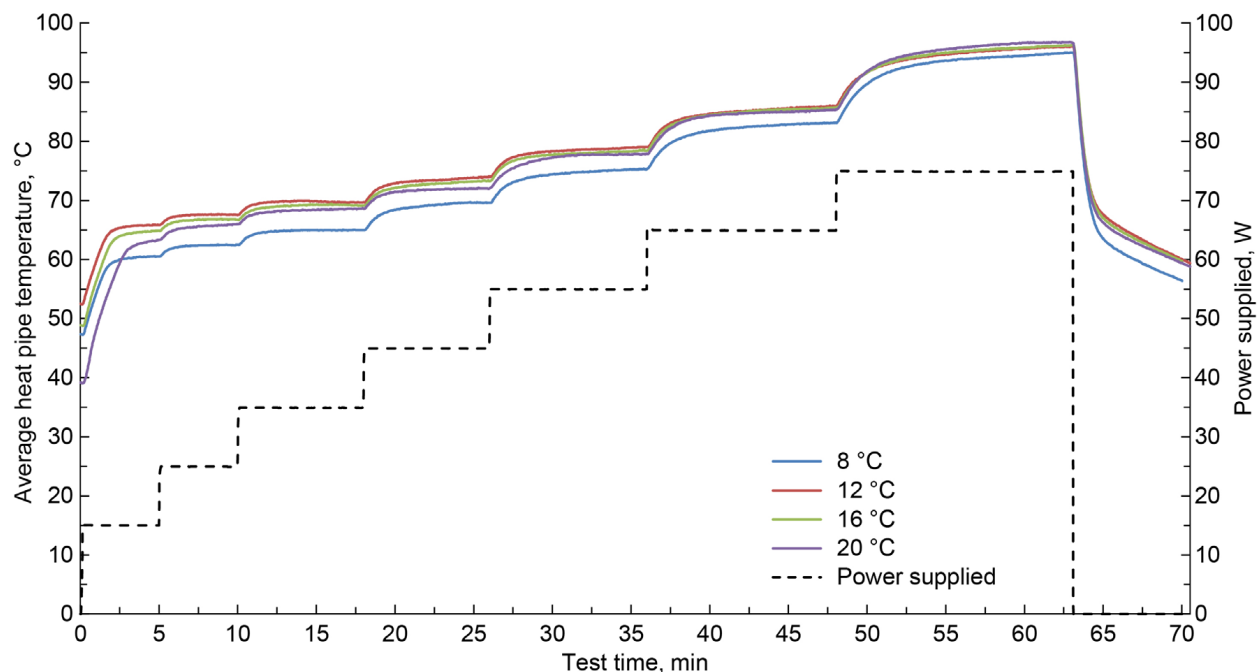


Figure 32.—Effect of varying platen cold plate temperatures and chiller setpoint on average heat pipe 2 evaporator surface temperature as heating power supplied increased in steps over time from August 15 to 16, 2012, with Arctic Silver® paste, full condenser, 60-lb platen force, multiple chiller setpoints, and horizontal operation.

The individual TC data, for each combination of platen pressure (100, 80, and 60 lb) and platen temperature (8, 12, 16, and 20 °C), are given in Figure A.3 to Figure A.15.

### 5.3 Condenser Section Contact Force

To further evaluate the effect of platen force on the operation of the HP, three different force levels were applied to the condenser section so that it could be determined if heat transfer improved with increased contact force. For these trials, a 71-mm condenser length was placed between the platens that resulted in 29 cm<sup>2</sup> (4.5 in<sup>2</sup>) of heat transfer area. The 60, 80, and 100 lb of force over the condenser area provides pressures of 13, 18, and 22 psi, respectively. In Figure 33, it is shown that greater contact force results in lower average evaporator surface temperatures for nearly all power levels. This test was conducted with HP 2 by using Arctic Silver® 5 thermal compound to enhance the heat transfer from the condenser to the platens. The platen temperature was set at 8 °C and the HP was used with the press in a horizontal orientation.

With the chiller set to maintain 16 °C instead of 8 °C, Figure 34 again shows that greater condenser section contact pressures correspond to lower average HP temperatures. It is possible that the performance gap would lessen if the temperatures were more similar near the beginning of all test runs, though it appears that steady-state conditions were obtained. As with the previous test, Arctic Silver® 5 thermal compound was used on the condenser to enhance the heat transfer, and the HP was oriented horizontally. The individual HP temperature raw data, used to generate the curves in Figure 33 and Figure 34, are given in Figure A.3, Figure A.6, Figure A.8, Figure A.10, Figure A.12, and Figure A.14 in Appendix A.

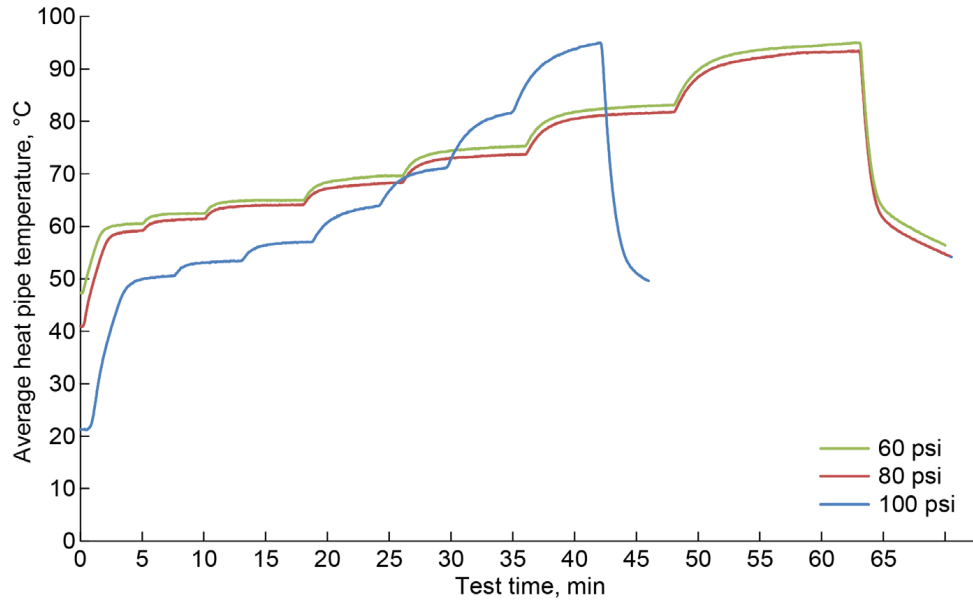


Figure 33.—Effect of plate force over condenser section on heat pipe 2 evaporator surface temperature from August 13 to 15, 2012, with Arctic Silver® paste, full condenser, multiple platen forces, 8 °C chiller setpoint, and horizontal operation.

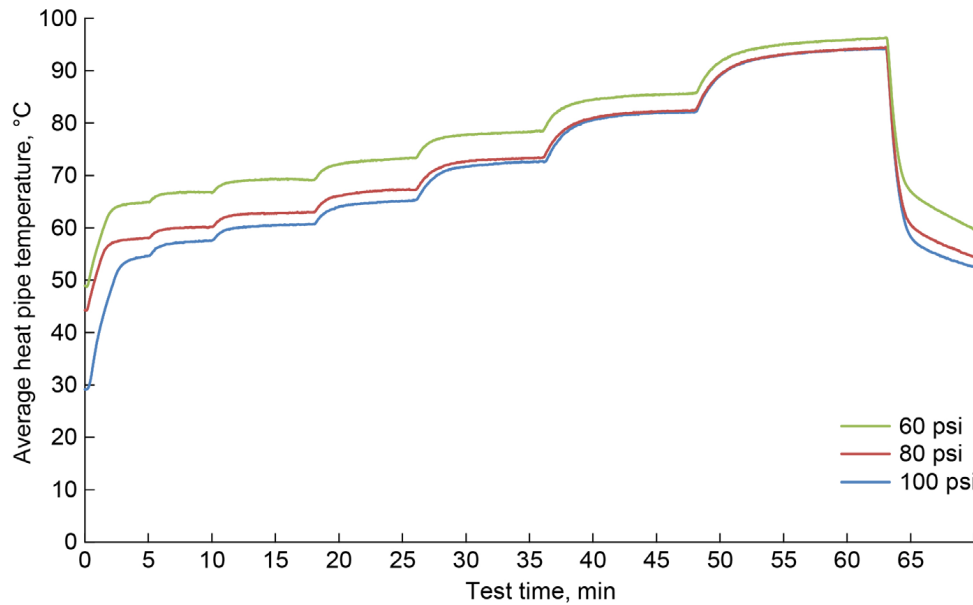


Figure 34.—Effect of plate force over condenser section on heat pipe 2 evaporator surface temperature from August 13 to 15, 2012, with Arctic Silver® paste, full condenser, multiple platen forces, 16 °C chiller setpoint, and horizontal operation.



## 5.4 Condenser Heat Transfer Area

The HP condenser length was decreased in 5-mm increments, from the full condenser length of 71 mm, until the HP could not achieve steady-state operation at 15 W of supplied heating power to evaluate the effect of the condenser area in the operation of the HP. Each 5 mm of condenser length corresponds to 4.1 cm<sup>2</sup> of condenser area. The same press force was maintained across all runs so the pressure (N/cm<sup>2</sup>) at 21 mm of condenser length was nearly 3.4 times greater than the pressure at the full 71-mm condenser length. Thus, when considering smaller condenser areas, performance declines may be somewhat mitigated by the increased contact pressure.

The results are shown in Figure 35 for reducing condenser heat transfer area in the platens with 100 lb of force applied. With the full condenser length chilled and in contact with the platens, the HP was able to transfer 75 W of heat applied to the evaporator section of the HP. This was the maximum heater power used during the testing. When 46 mm of condenser length was used, the HP could not transfer 55 W of heat without reaching evaporator surface temperatures of over 100 °C. Supplying 15 W of heat to the HP with only 21 mm of chilled condenser length, steady state is not reached prior to the evaporator surface temperature exceeding 100 °C. All of the tests were run with 100 lb of force and Arctic Silver® 5 paste applied to the condenser section of the HP. The chiller was set to 8 °C chiller and the HP was oriented horizontally in the press.

Similar to the trials with 100 lb of force applied, a series of tests were run with 60 lb of platen force. The results again showed that the HP capability to transfer heat decreases with reduced chilled condenser area, as presented in Figure 36. Chilling the full condenser length enables effective heat transfer of 75 W of heating power. When condenser length between press platens was reduced to 31 mm, it was not possible to reach steady-state evaporator temperature at 15-W heat load. All of this test series used 60 lb of force, Arctic Silver® 5 paste on the condenser, an 8 °C chiller setpoint, and horizontal operation.

For fuel cell operation, it is important to maintain a uniform temperature across the active area of a cell so the reaction proceeds at a similar rate in all locations. Higher temperatures promote reactant utilization and higher rates produce even more heat. Thus, an effective cooling strategy must minimize local variations. The maximum evaporator surface temperature differentials are shown in Figure 37 for a horizontally oriented HP with 100 lb of force on the condenser section, the chiller set to 8 °C as well as with and without Arctic Silver® 5 thermal compound. In general, the temperature difference was at most 1.4 to 2.0 °C for all cases utilizing Arctic Silver® 5 paste. For most of the condenser area tests, the differential increased slightly as tests progressed to greater heating loads. Beyond the 55-W step, and without the thermal compound, maximum temperature differences exceeded 2.5 °C. Although greater, such a differential is likely still acceptable for fuel cell operation.

A similar comparison was produced for the tests by using 60 lb of platen force as shown in Figure 38. These tests all utilized the Arctic Silver® 5 thermal paste with the chiller set to 8 °C and a horizontal orientation of the HP. The maximum temperature difference was between 1.1 and 1.8 °C for all recorded conditions. Again, the differential typically increased slightly as tests progressed to greater heating loads. The raw data, used to generate Figure 35 to Figure 38, is given in Figure A.2, Figure A.3, Figure A.12, and Figure A.16 to Figure A.33.

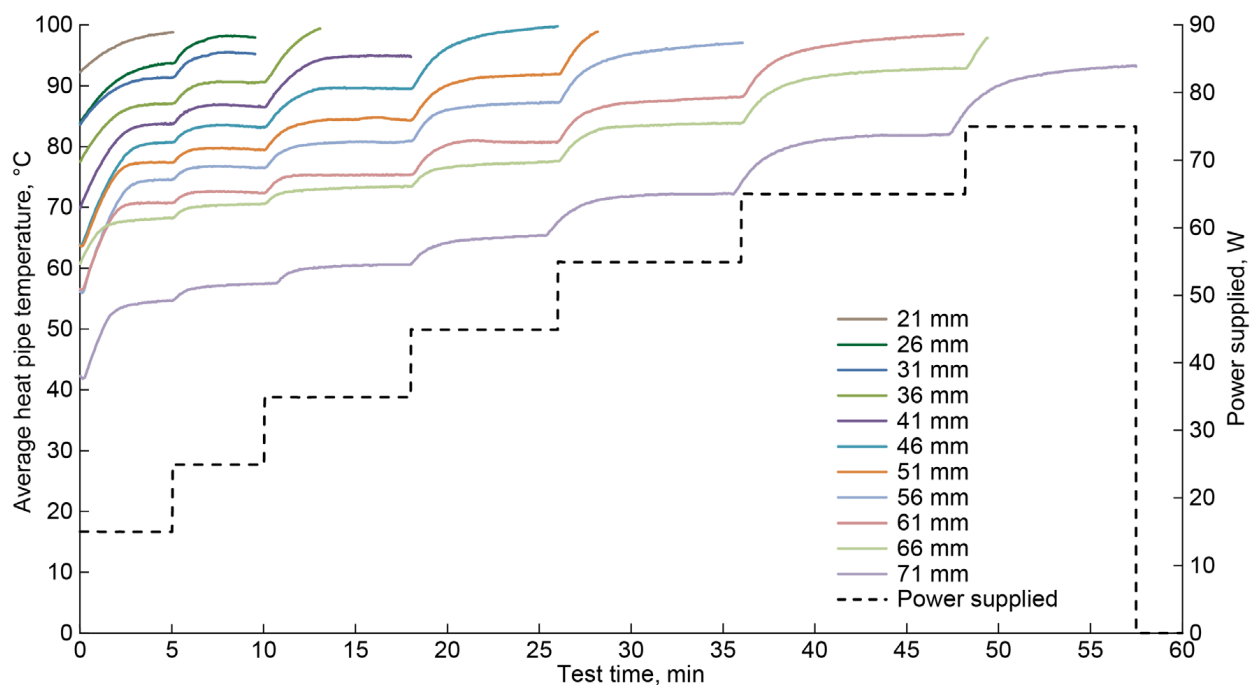


Figure 35.—Average heat pipe 2 surface temperature with varying lengths of condenser between the press platens on August 17, 2012, with Arctic Silver® paste, full condenser, 100-lb force, 8 °C chiller setpoint, and horizontal operation.

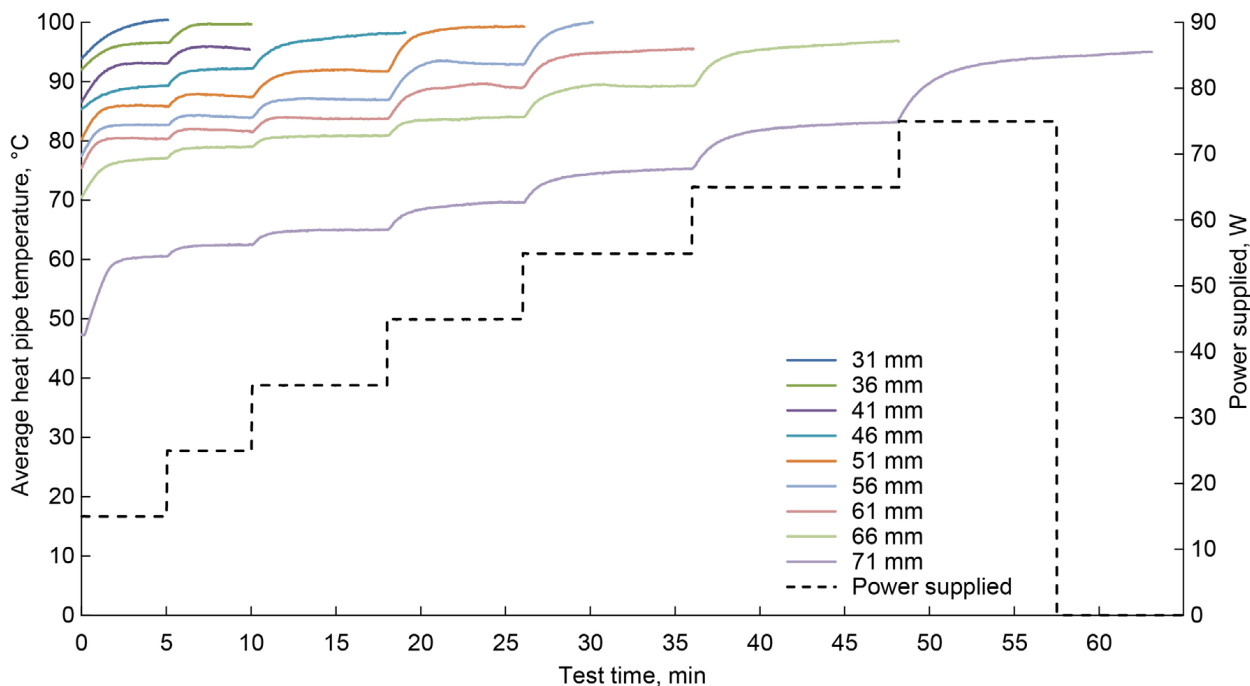


Figure 36.—Average heat pipe 2 surface temperature with varying lengths of condenser between press platens from August 20 to 21, 2012, with Arctic Silver® paste, full condenser, 60 lb-force, 8 °C chiller setpoint, and horizontal operation.

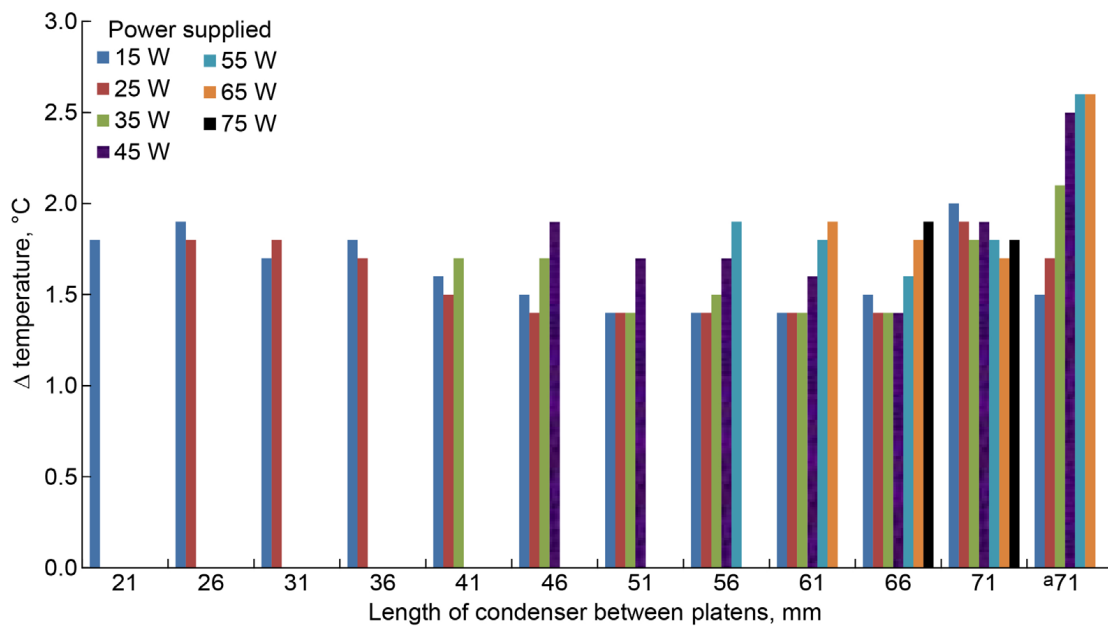


Figure 37.—Maximum steady-state temperature difference across heat pipe (HP) 2 evaporator surface at various supplied power levels excluding thermocouple 2 on August 17, 2012, with and without Arctic Silver® paste, with full condenser, 100-lb force, 8 °C chiller setpoint, and horizontal operation. <sup>a</sup>Without Arctic Silver® paste.

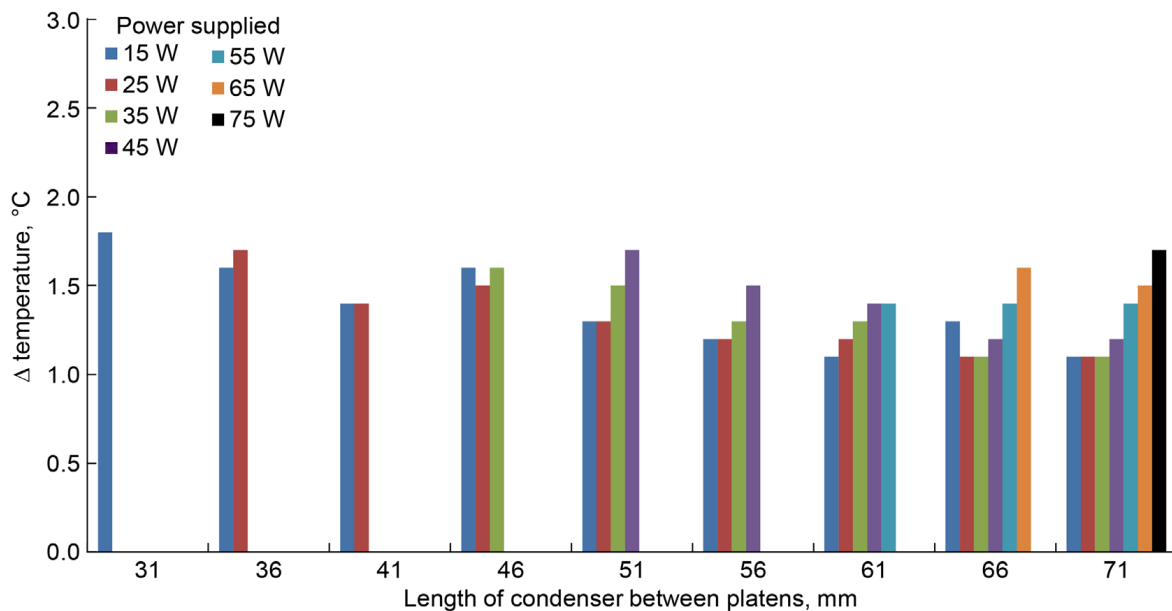


Figure 38.—Maximum steady-state temperature difference across heat pipe 2 surface at various supplied power levels from August 20 to 21, 2012, with Arctic Silver® paste, full condenser, 60-lb force, 8 °C chiller setpoint, and horizontal operation.

## 5.5 Heat Pipe (HP) Orientation

In order to evaluate how the positioning of the HP affects operation, the HPs were operated in four distinct orientations: condenser to the side, condenser on top of the evaporator section, condenser on bottom below evaporator, and HP situated horizontally. In the horizontal scenario, the previous test data was used where the HP performance was evaluated with the condenser in the previously described standard setup by using the press platens. For all other orientations, a set of copper plates, shown in Figure 25 to Figure 27, was used to produce the alternate orientations.

The average HP surface temperature is presented in Figure 39 for each orientation as heating power supplied was increased in 10-W steps starting from 15 W. Recorded temperatures were similar in the condenser on top and condenser to side cases. The condenser on bottom case neared 100 °C during the 45-W step and exhibited the poorest performance. This is likely due to the resistance in transporting liquid water against gravity from the relatively small cross-sectional area condenser section up to the evaporator to restore the heat transfer capacity of the HP.

The maximum evaporator surface temperature differentials are shown in Figure 40 for each tested orientation. Unlike the temperature differentials observed during condenser area testing, HP orientation appears to produce minimal evaporator surface temperature variation. All scenarios result in a maximum temperature differential between 1.0 and 1.4 °C. The individual TC temperature data, used to generate Figure 39 and Figure 40, are given by Figure A.34 to Figure A.38.

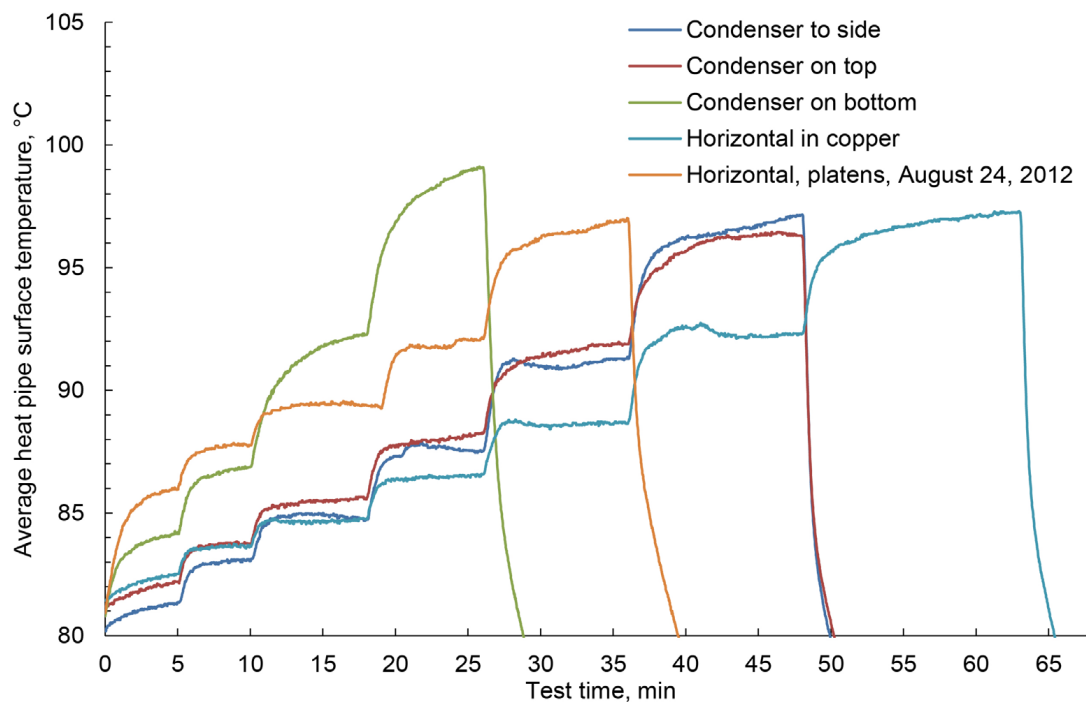


Figure 39.—Average heat pipe 2 surface temperature for various orientation over time from August 15 to 24, 2012, with Arctic Silver® paste, full condenser, 100-lb force, 8 °C chiller setpoint, and multiple orientation operation.

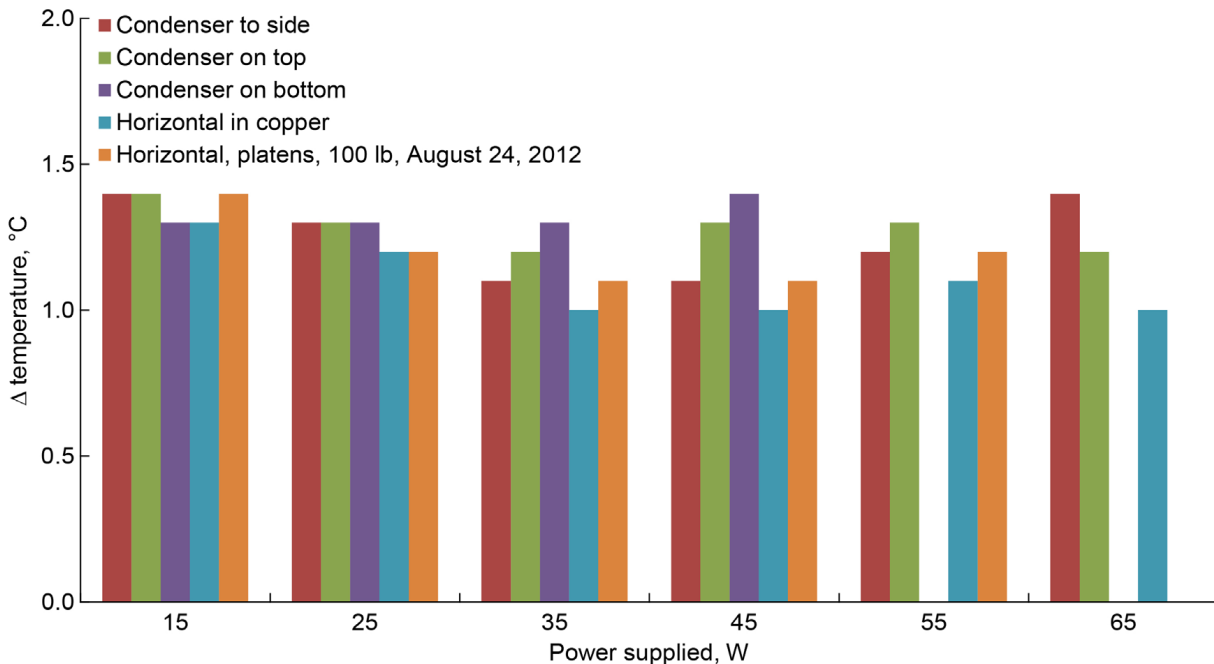


Figure 40.—Maximum temperature difference across heat pipe surface at steady state, excluding thermocouple 2 for each orientation.

## 5.6 Degradation

Further analysis of HP 2 data showed that there was apparent degradation of HP 2 during testing. After initially demonstrating the capability to transfer 75 W of heat, as depicted in Figure 41, the HP could only transfer 55 W nine calendar days later when set up in the same configuration. As the total operational time (TOT) on the HP increased, the operating temperature rose for all heating power levels. When supplying 55 W to the heater, the HP operating temperature when new was 72.5 °C. After nine days and approximately 106 h of operation with a supplied load between 15 and 75 W, the operating temperature at 55 W was 97.0 °C.

The rate of degradation slowed when the HP was not in use. Twelve days later with one further hour of usage, the operating temperature rose to 98.5 °C. On August 15, TOT was 3 h; on August 24, TOT was 109 h; and on September 5, TOT was 110 h. This indicates that usage of the HP affects the degradation rate more than inactive time. If there were a steady leak of working fluid from the HP, a more constant rate of increasing operating temperature could be expected regardless of TOT. All of these tests demonstrating the operational degradation utilized 100 lb of press force, Arctic Silver® 5 thermal compound on the condenser, an 8 °C chiller setpoint temperature, and a horizontal orientation.

It is possible that the condenser section was damaged during testing when installed and operated with the copper cooling plates. The most vulnerable location is the HP fill tube, which is the final sealing point during HP construction. Damage at this corner of the condenser could lead to overboard leakage and less internal water to transport heat. Alternatively, damage to flow pathways reduces heat transfer performance by preventing internal water flow.

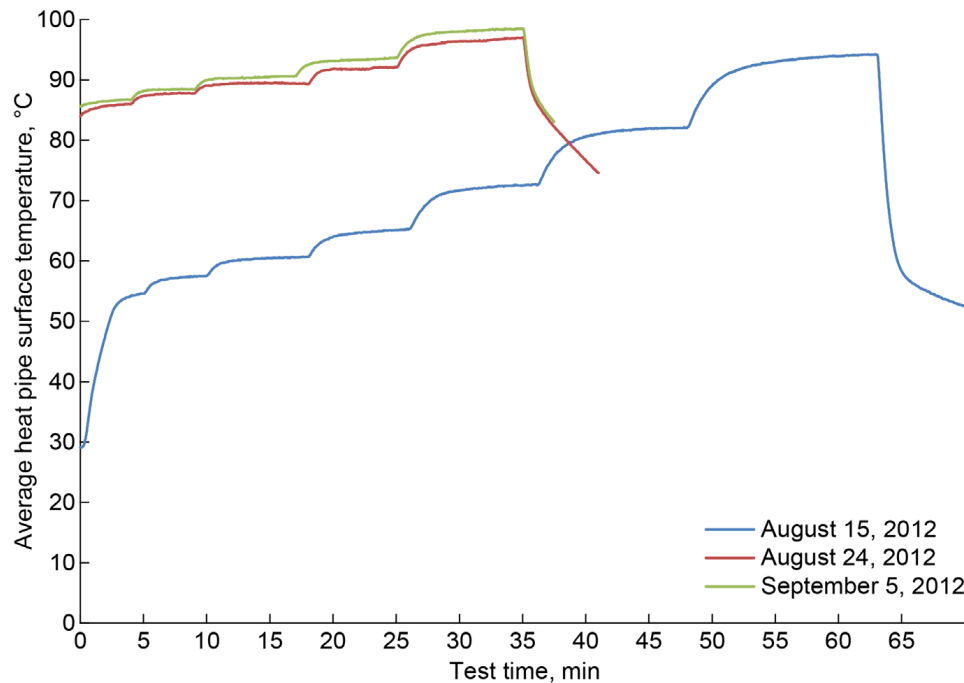


Figure 41.—Average heat pipe (HP) 2 evaporator section surface temperature as evidence of HP 2 performance degradation upon repeating test conditions for three different test days from August 15 to September 5, 2015, with Arctic Silver® paste, full condenser, 100-lb force, 8 °C chiller setpoint, and horizontal operation.

## 5.7 Performance Variability

In addition to the characterization of HP 2, the six additional HPs were operated in a standard configuration to observe unit-to-unit variability and repeatability of performance, as shown in Figure 42 to Figure 47 for HPs A to F, respectively. The average evaporator plate temperatures are plotted for each HP as the heater power is stepped from 15 to 75 W over an 85-min period. Three test runs were performed with each HP, except for HP A on which four test runs were performed. All test runs utilized 100 lb of force, Arctic Silver® paste, the full condenser length (71 mm) held in the press platens, a 10 °C chiller setpoint, and horizontal operation.

HP B was consistent during all three test runs. All five other HPs showed performance that varied each time a unit was tested. HPs A and C both improved with further operational time. At heater power levels beyond 35 W, HPs D and F showed the lowest evaporator temperatures during test 2. In early test runs, HPs D and F showed the lowest temperatures during test 1 runs. HP E had the best performance and showed the lowest temperature in test 1. It subsequently exhibited the highest temperature and worst performance in test 2.

At nearly all heating power levels for each individual HP, the average plate temperature varied by less than 10 °C across the test trials. The HPs were less consistent when comparing different units. In Figure 48, the maximum recorded temperature is shown from test 2 for HPs A to F when supplying 15 W of heating power. While four of the HPs operated between 32 and 38 °C in these conditions, the remaining two HPs exhibited evaporator temperatures exceeding 52 °C. The TC data, used to generate the results shown in Figure 42 to Figure 48, are given in Figure A.39 to Figure A.57.

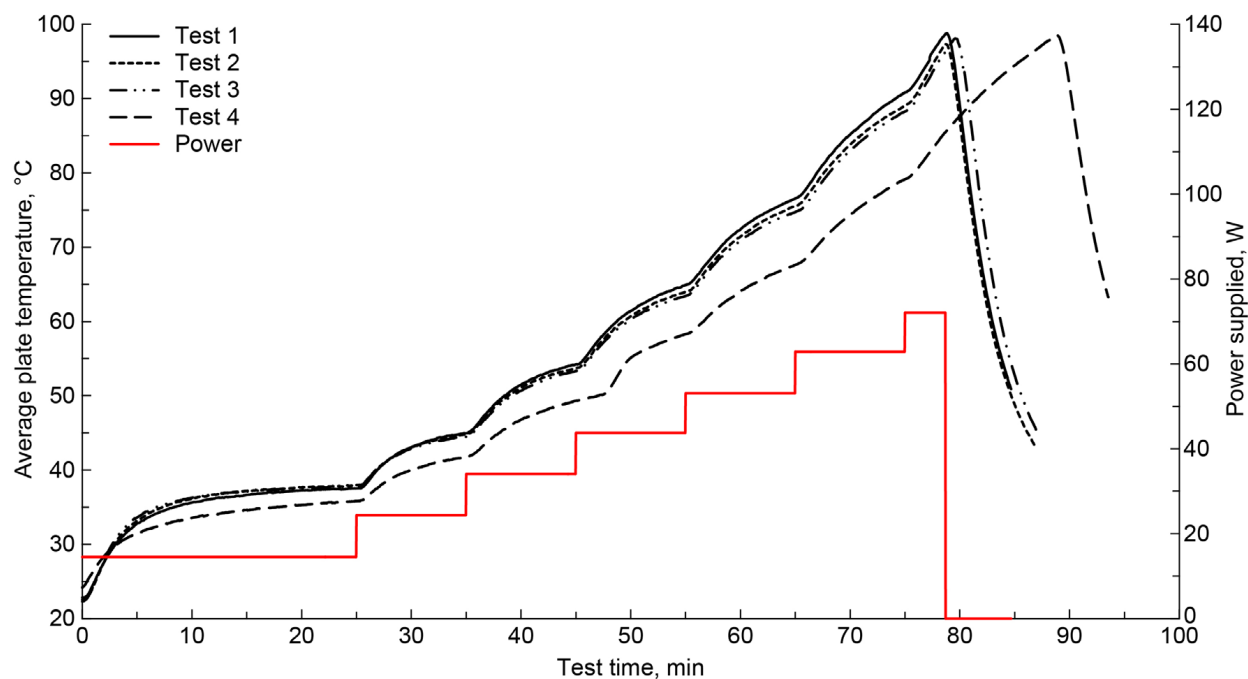


Figure 42.—Average heat pipe (HP) A surface temperature for four test runs of identical configuration from August 12 to 19, 2013, with Arctic Silver® paste, full condenser, 10-lb force, 10 °C chiller setpoint, and horizontal operation.

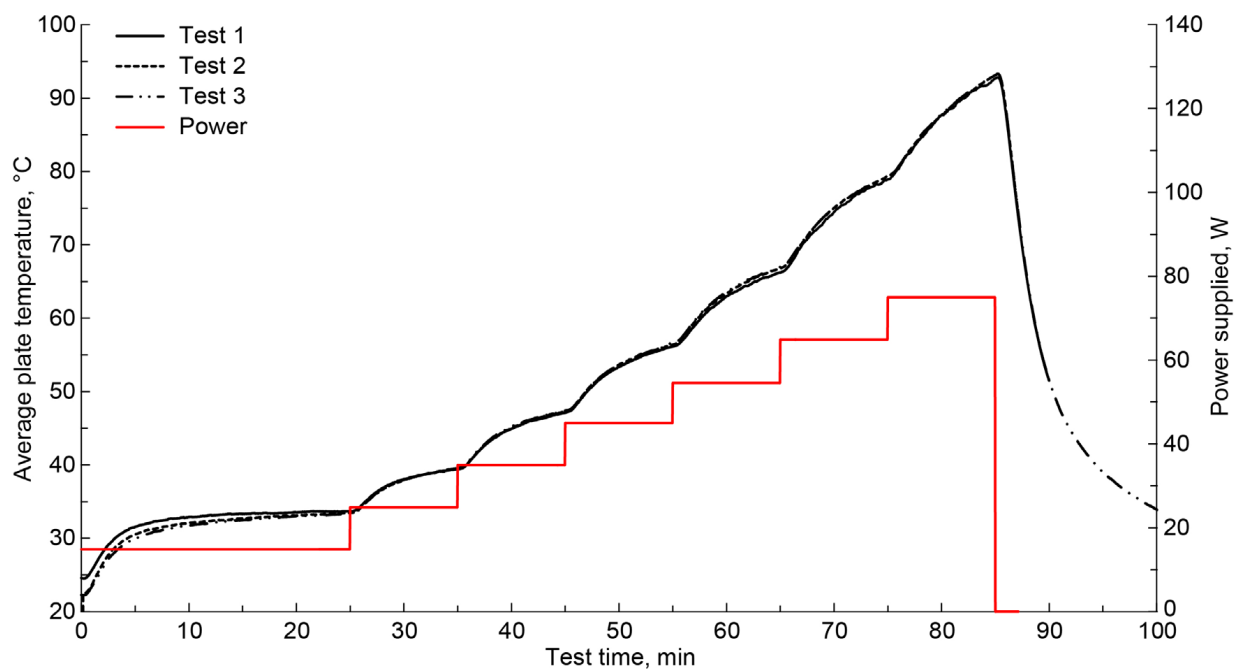


Figure 43.—Average heat pipe (HP) B surface temperature for three test runs of identical configuration on August 14, 2013, with Arctic Silver® paste, full condenser, 100-lb force, 10 °C chiller setpoint, and horizontal operation.

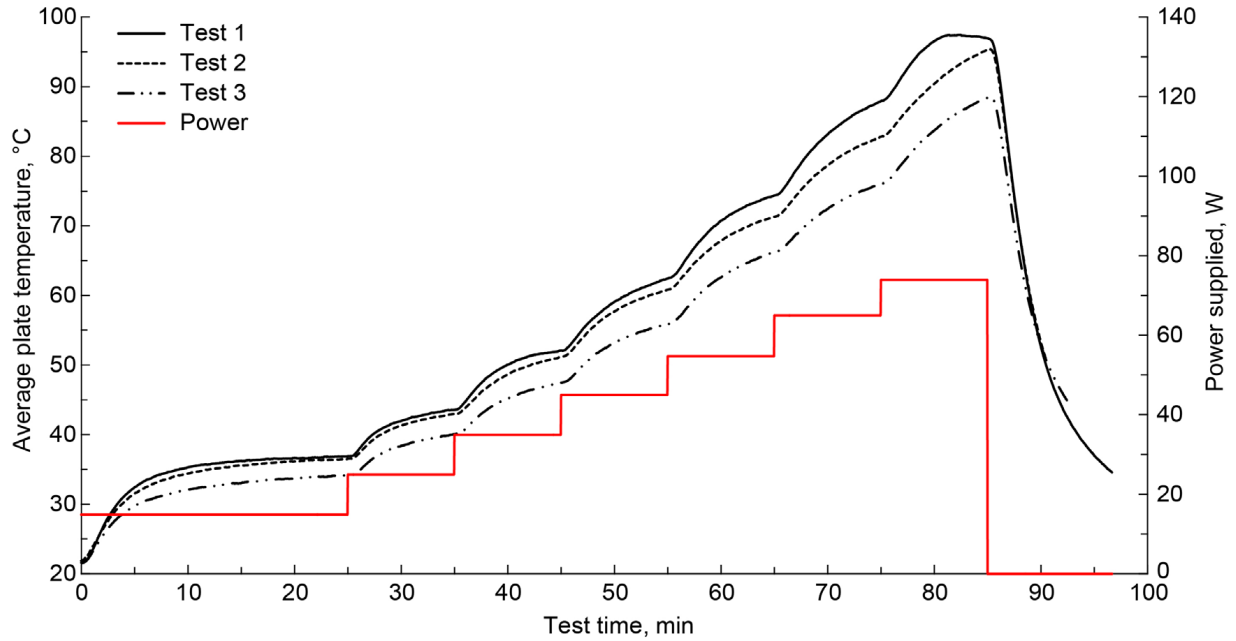


Figure 44.—Average heat pipe (HP) C surface temperature for four test runs of identical configuration from August 14 to 15, 2013, with Arctic Silver<sup>®</sup> paste, full condenser, 100-lb force, 10 °C chiller setpoint, and horizontal operation.

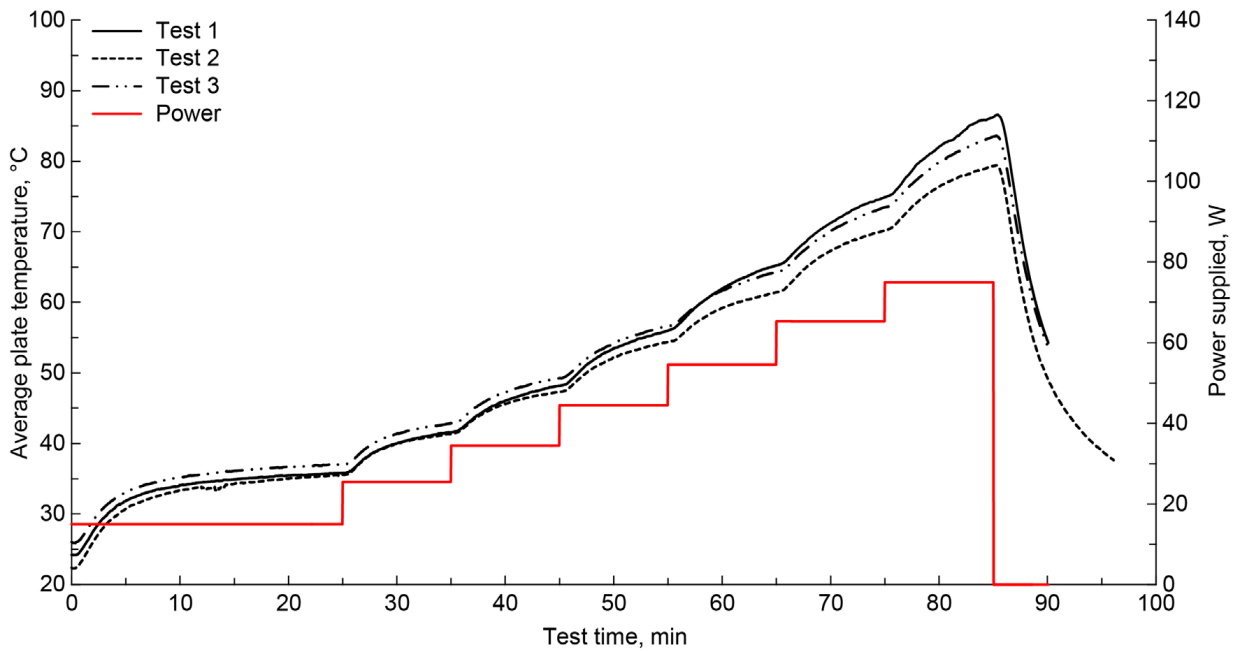


Figure 45.—Average heat pipe (HP) D surface temperature for four test runs of identical configuration from August 15 to 19, 2013, with Arctic Silver<sup>®</sup> paste, full condenser, 100-lb force, 10 °C chiller setpoint, and horizontal operation.



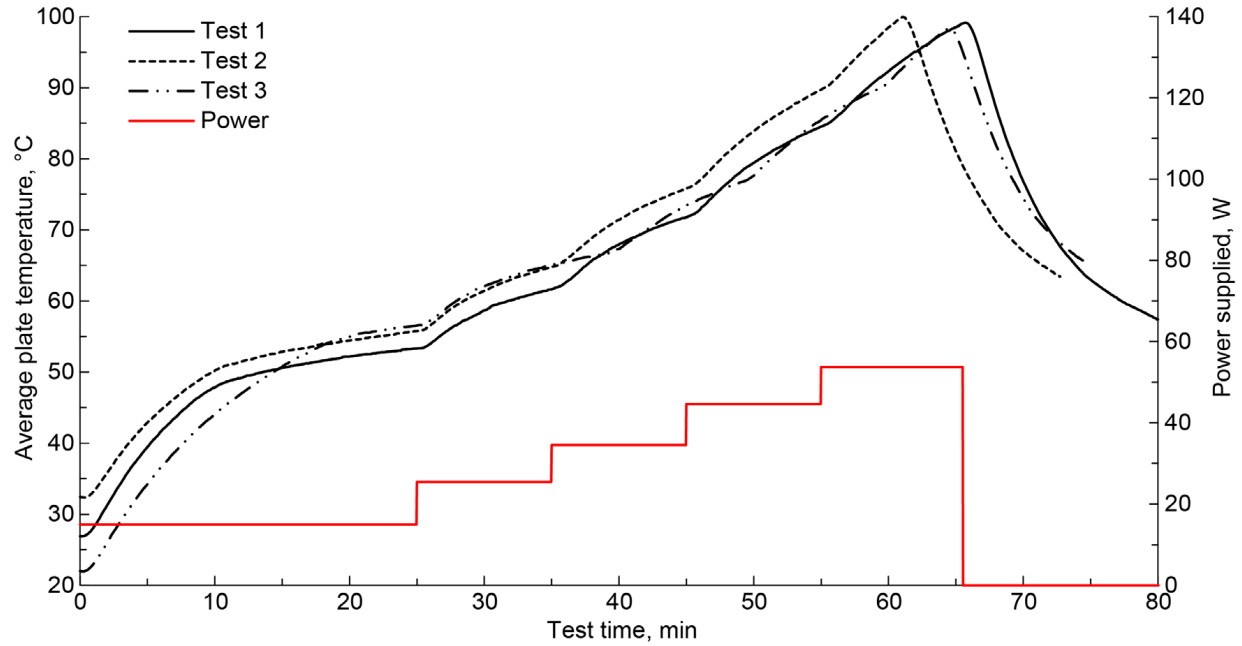


Figure 46.—Average heat pipe (HP) E surface temperature for four test runs of identical configuration from August 16 to 19, 2013, with Arctic Silver® paste, full condenser, 100-lb force, 10 °C chiller setpoint, and horizontal operation.

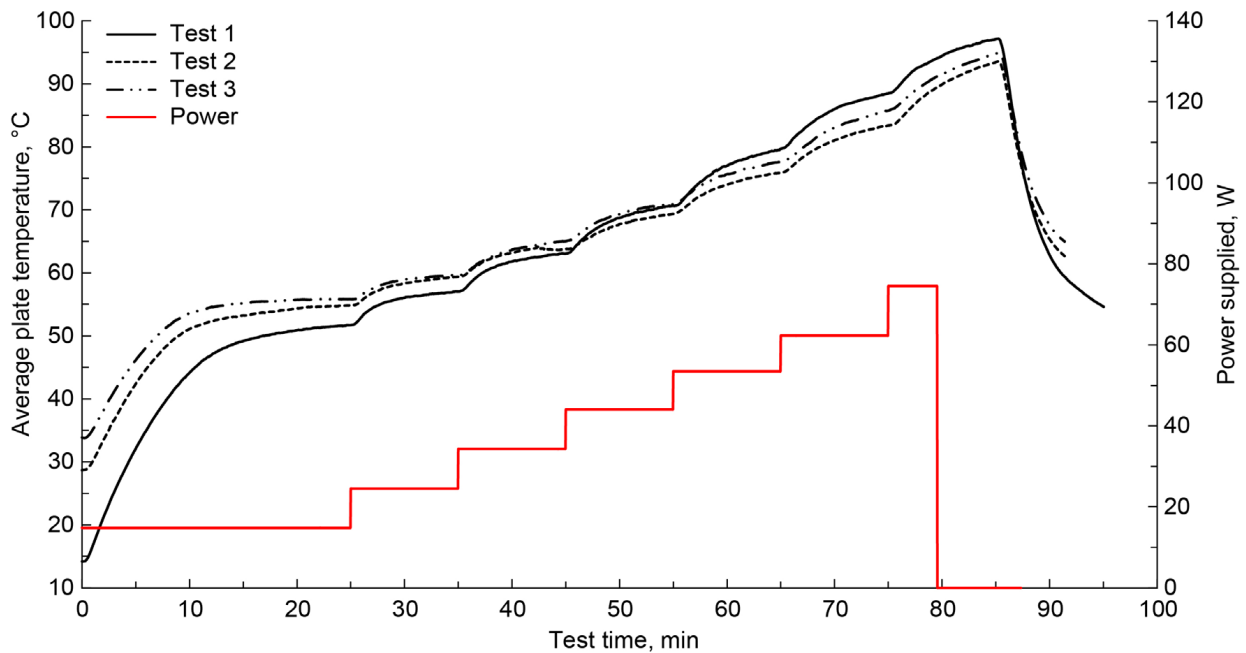


Figure 47.—Average heat pipe (HP) F surface temperature for three test runs of identical configuration from August 12 to 14, 2013, with Arctic Silver® paste, full condenser, 100-lb force, 10 °C chiller setpoint, and horizontal operation.

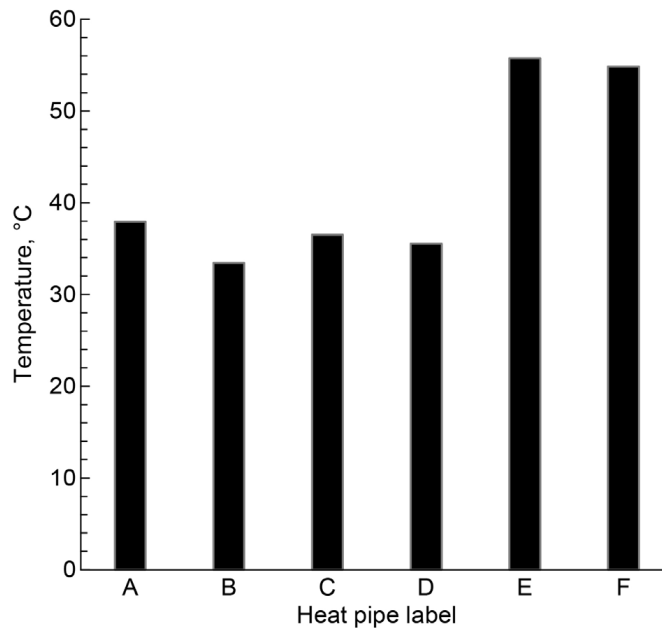


Figure 48.—Comparison of average evaporator plate surface temperature for six heat pipes at end of the 15-W power supplied step from test 2 runs with Arctic Silver® paste, full condenser, 100-lb force, 10 °C chiller setpoint, and horizontal orientation.

## 5.8 Quantification of External Heat Loss

Although the HPs are insulated, it remains desirable to identify the heat lost through the polyester insulation to the surroundings. The thermal power lost through the insulation, calculated from Equations (4) and (5), is plotted in Figure 49 and Figure 50 for two different tests of HP 2. These tests utilized 100 lb of platen force with the HP oriented horizontally and an 8 °C chiller coolant temperature. The experimental results correspond to the test cases shown in Figure A.3 and Figure A.16 in addition to the insulation temperatures shown in Figure A.58 and Figure A.59.

Depending upon test room conditions and insulation fiber degradation due to heat cycling and HP handling, approximately 8 to 12 percent of the thermal power supplied was lost through the insulation to the surroundings. Many of the exterior insulation temperature measurements taken were not at steady state due to leftover heat from previous trials. The radiation estimate appears noisier due to the use of a single TC to measure ambient air temperature. There is also a significant time delay in attaining steady-state temperature at the exterior insulation surface. Though this temperature is a parameter in both calculation methods, it appears to more greatly affect the radiation estimate early in a test run, resulting in perhaps an underestimation of heat lost at lower power input levels.

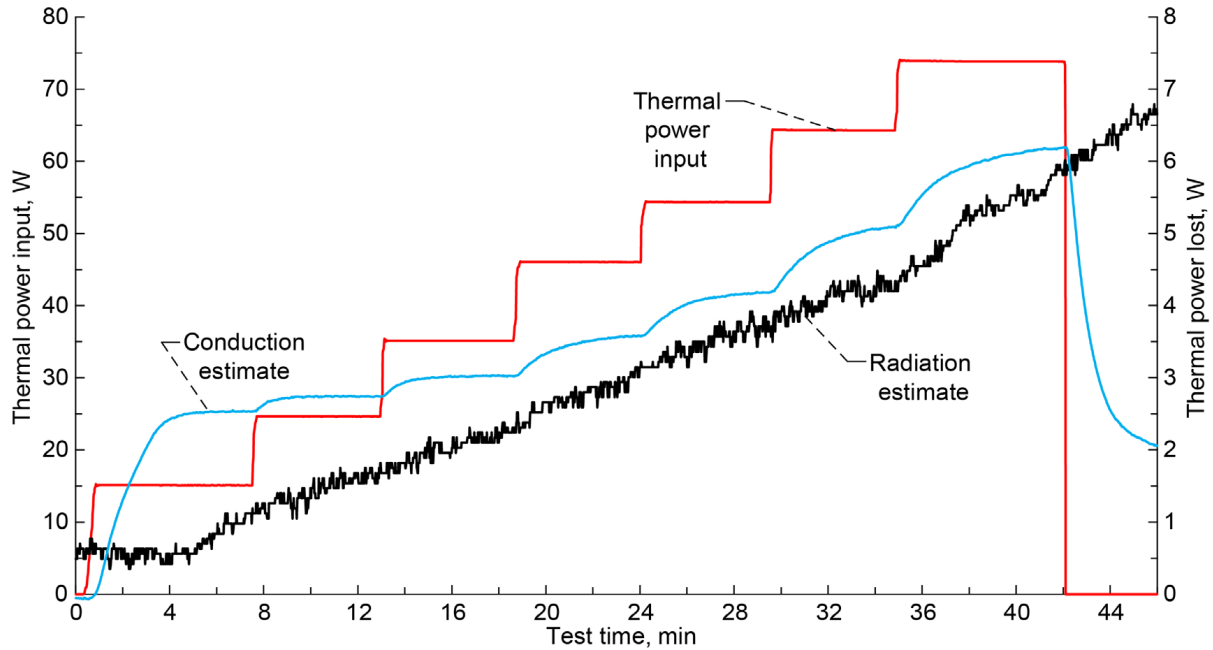


Figure 49.—Conduction and radiation heat loss with increasing thermal heater power over test duration for heat pipe 2 on August 13, 2013, with Arctic Silver® paste, full condenser length, 100-lb force, 8 °C chiller setpoint, and horizontal operation.

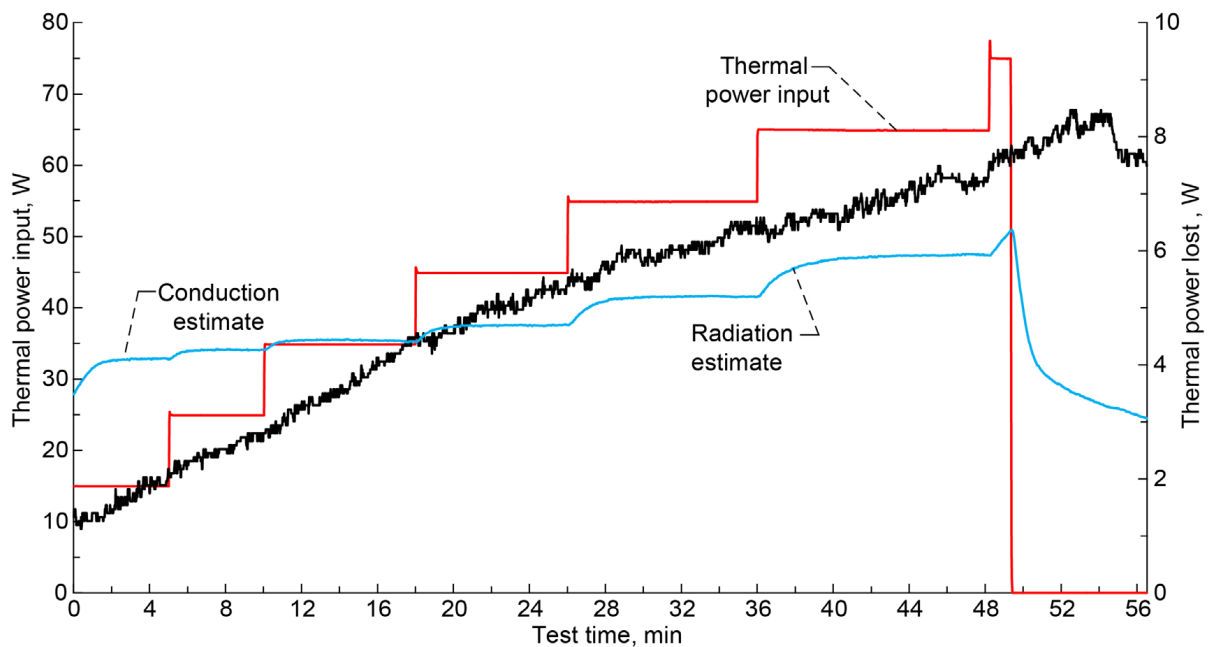


Figure 50.—Second case of conduction and radiation heat loss with increasing thermal heater power over test duration for heat pipe 2 on August 17, 2012, with Arctic Silver® paste, 66-mm condenser length, 100-lb force, 8 °C chiller setpoint, and horizontal operation.

## 6.0 Conclusions and Recommendations

Heat pipe (HP) degradation and performance inconsistencies precluded development of a universal correlation relating operating temperature to heat load, contact pressure, condenser heat sink temperature, or physical orientation. It remained possible to confirm that improved condenser and heat sink contact through increased pressure and thermal contact coating, greater condenser area utilization, and colder heat sink temperature considerably enhance HP performance. Higher initial HP temperature and greater age or operation time reduce HP capabilities. HP orientation results in minimal evaporator plate temperature variation with the exemption of placing the condenser lower than the evaporator. Condensing fluid in the lower section reduces heat transfer capacity.

Experimental control could be improved by directly monitoring condenser temperature, then varying coolant temperature and flow rate. In the setup described here, no thermocouples (TCs) are placed on the condenser directly to avoid destruction on the TC and an increase in contact resistance between the condenser and the platens and cold plates. The platen temperature does not necessarily equal the condenser temperature and coolant temperature frequently drifted or varied by several tenths of a degree Celsius during a test run.

For integration of HPs into a fuel cell, it will be necessary to improve quality control so that the HPs all operate within a narrower range of evaporator plate temperatures. HPs must also be designed to match with the expected steady-state operational load. Lower power generation will result in cooler than optimal operating temperatures that reduce fuel cell efficiency and may eventually degrade the membranes.

## Appendix A.—Raw Data and Charts

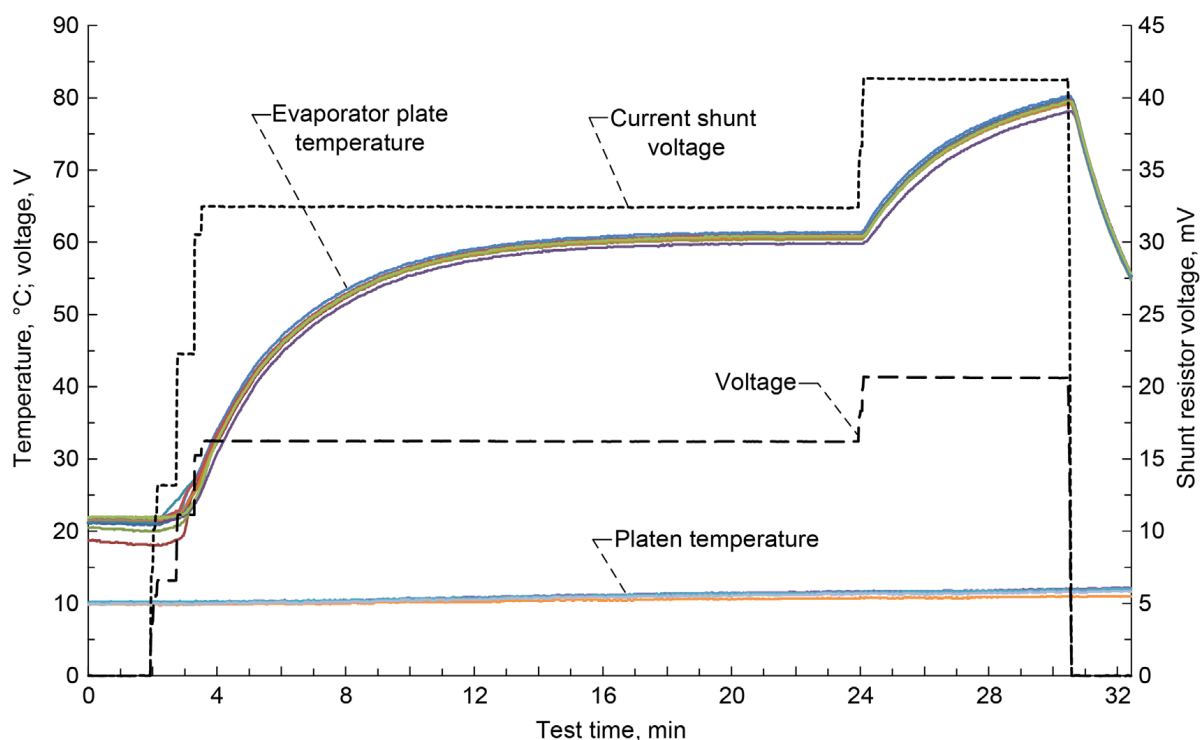


Figure A.1.—Heat pipe 1 on August 7, 2012, without Arctic Silver® paste, with full condenser, 100-lb platen force, 8 °C chiller setpoint, and horizontal operation.

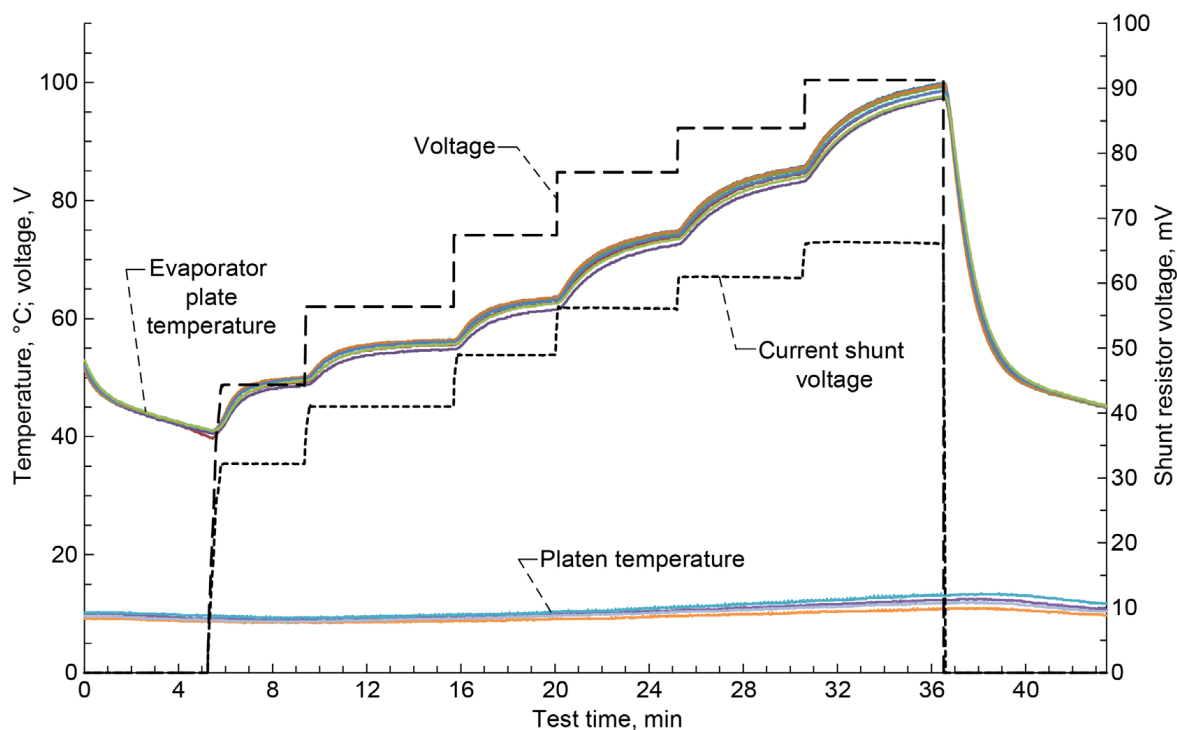


Figure A.2.—Heat pipe 2 on August 9, 2012, without Arctic Silver® paste, with full condenser, 100-lb platen force, 8 °C chiller setpoint, and horizontal operation.

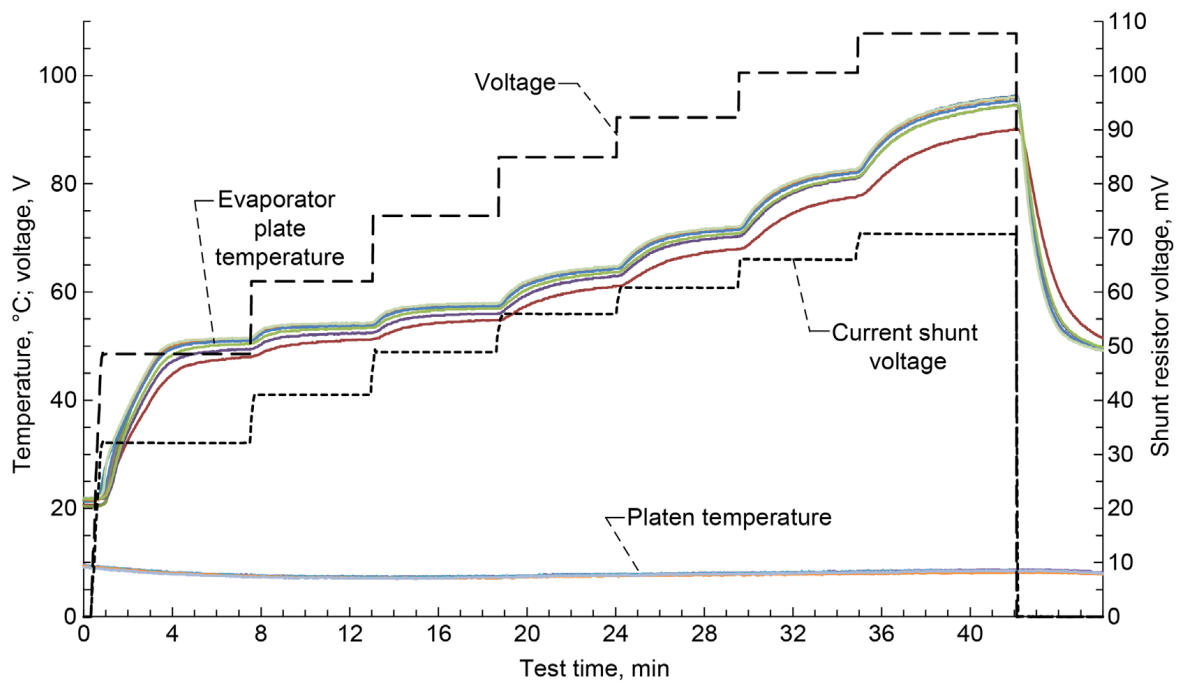


Figure A.3.—Heat pipe 2 on August 13, 2012, with Arctic Silver® paste, full condenser, 100-lb platen force, 8 °C chiller setpoint, and horizontal operation.

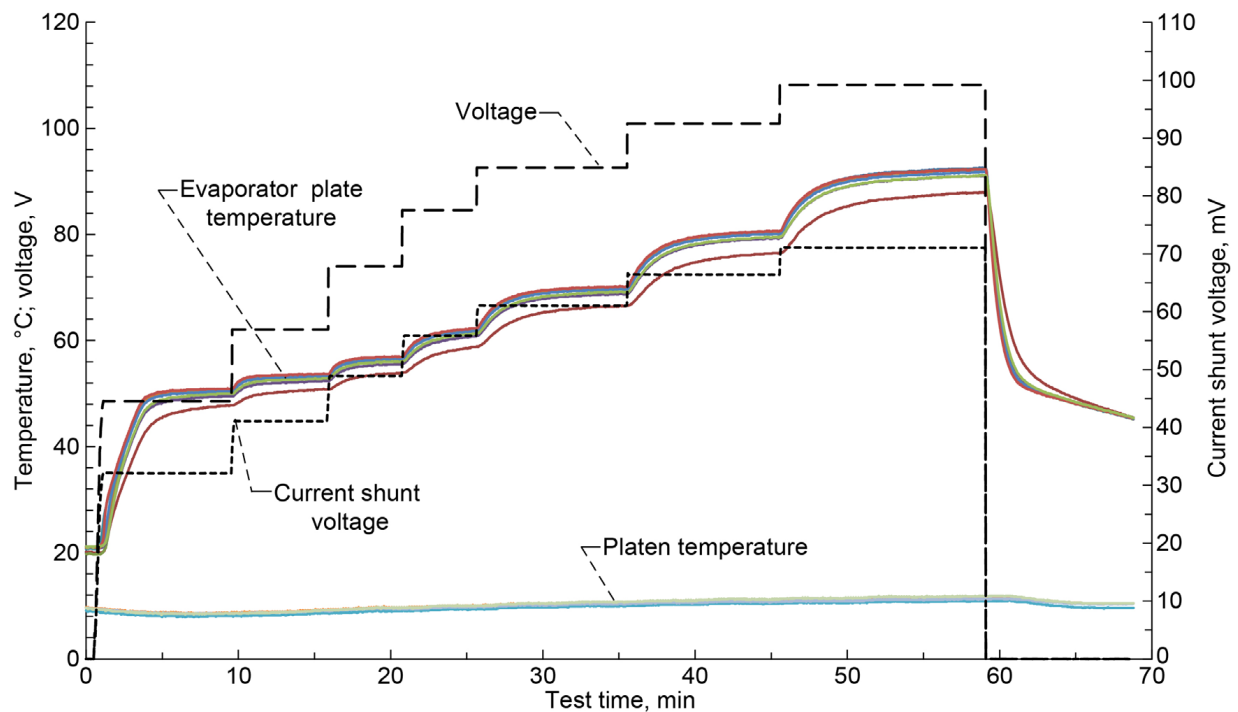


Figure A.4.—Heat pipe 2 on August 13, 2012, with Arctic Silver® paste, full condenser, 100-lb platen force, 10 °C chiller setpoint, and horizontal operation.

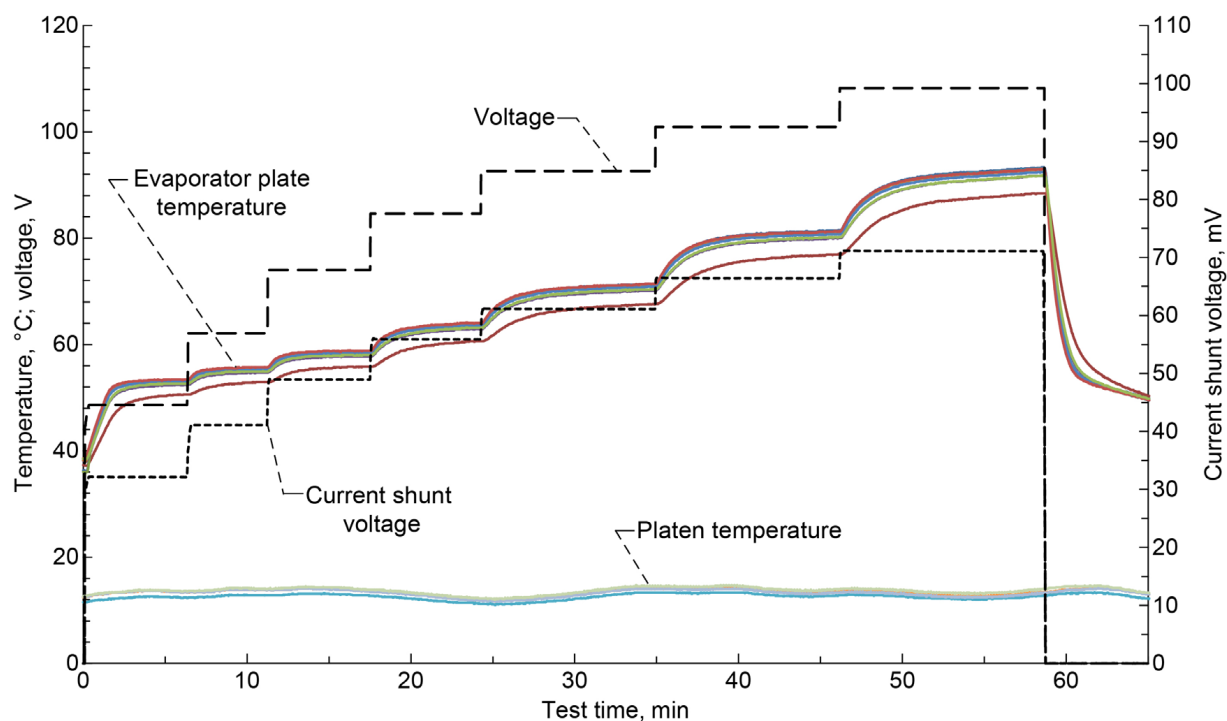


Figure A.5.—Heat pipe 2 on August 13, 2012, with Arctic Silver® paste, full condenser, 100-lb platen force, 12 °C chiller setpoint, and horizontal operation.

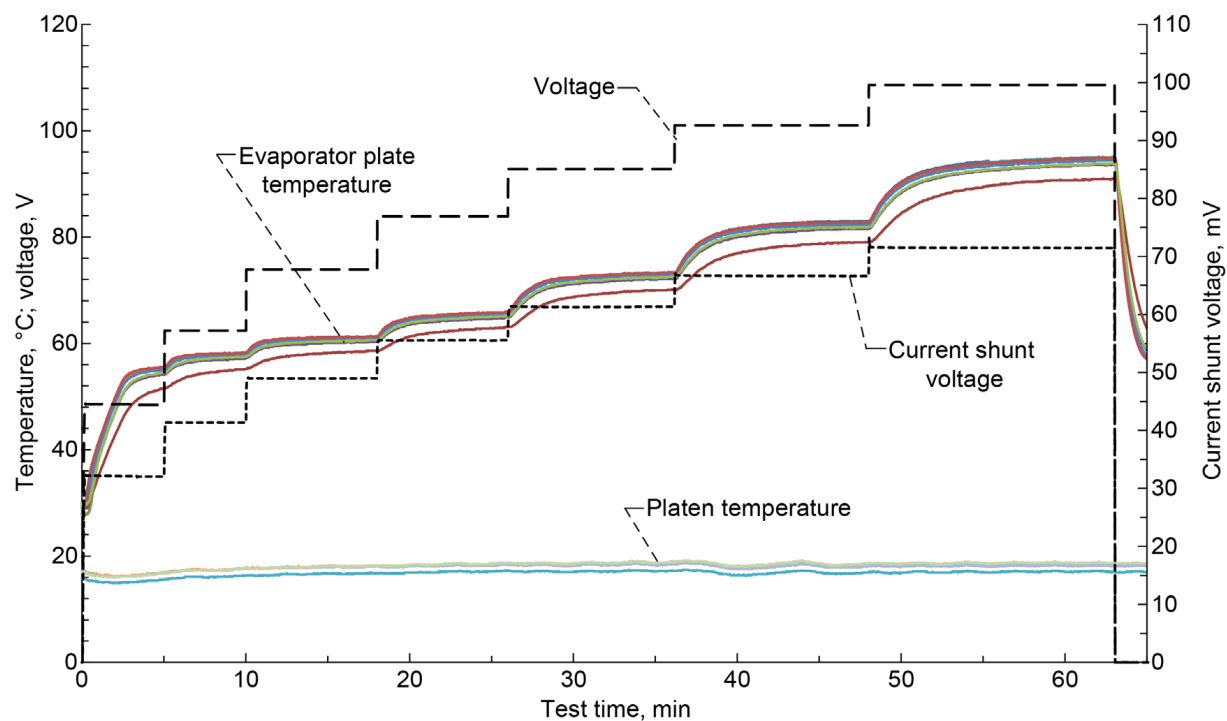


Figure A.6.—Heat pipe 2 on August 15, 2012, with Arctic Silver® paste, full condenser, 100-lb platen force, 16 °C chiller setpoint, and horizontal operation.



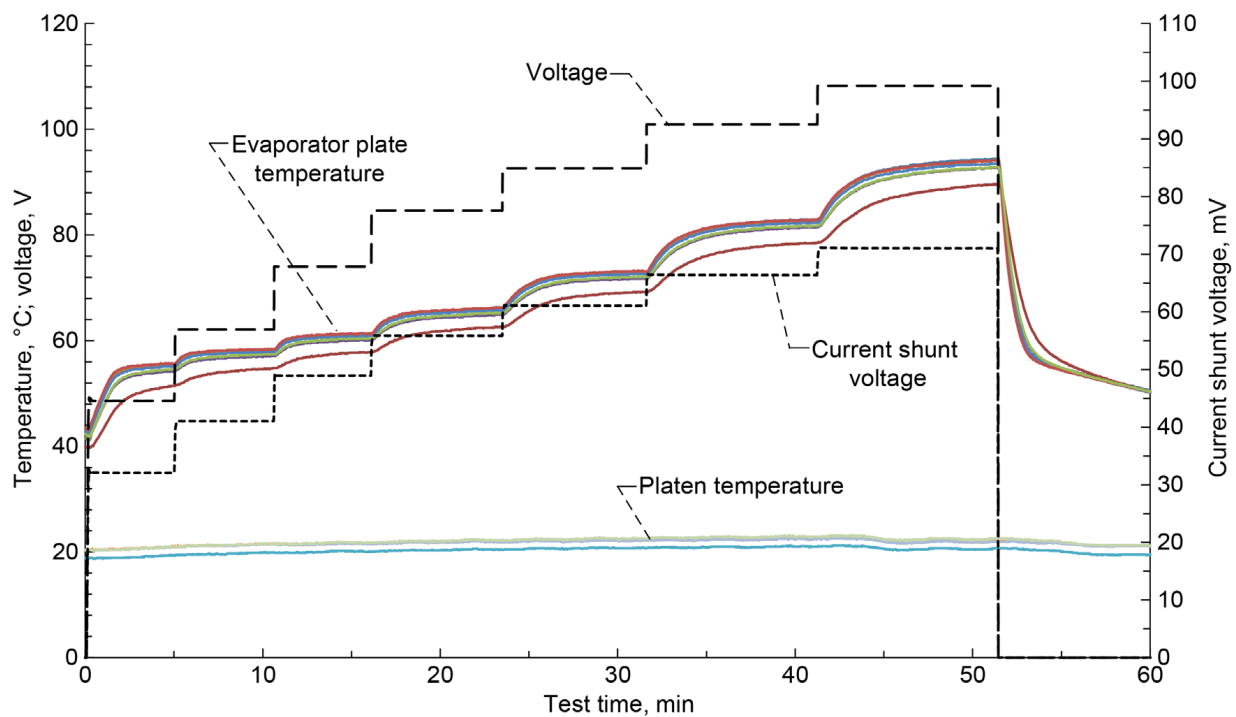


Figure A.7.—Heat pipe 2 on August 14, 2012, with Arctic Silver® paste, full condenser, 100-lb platen force, 20 °C chiller setpoint, and horizontal operation.

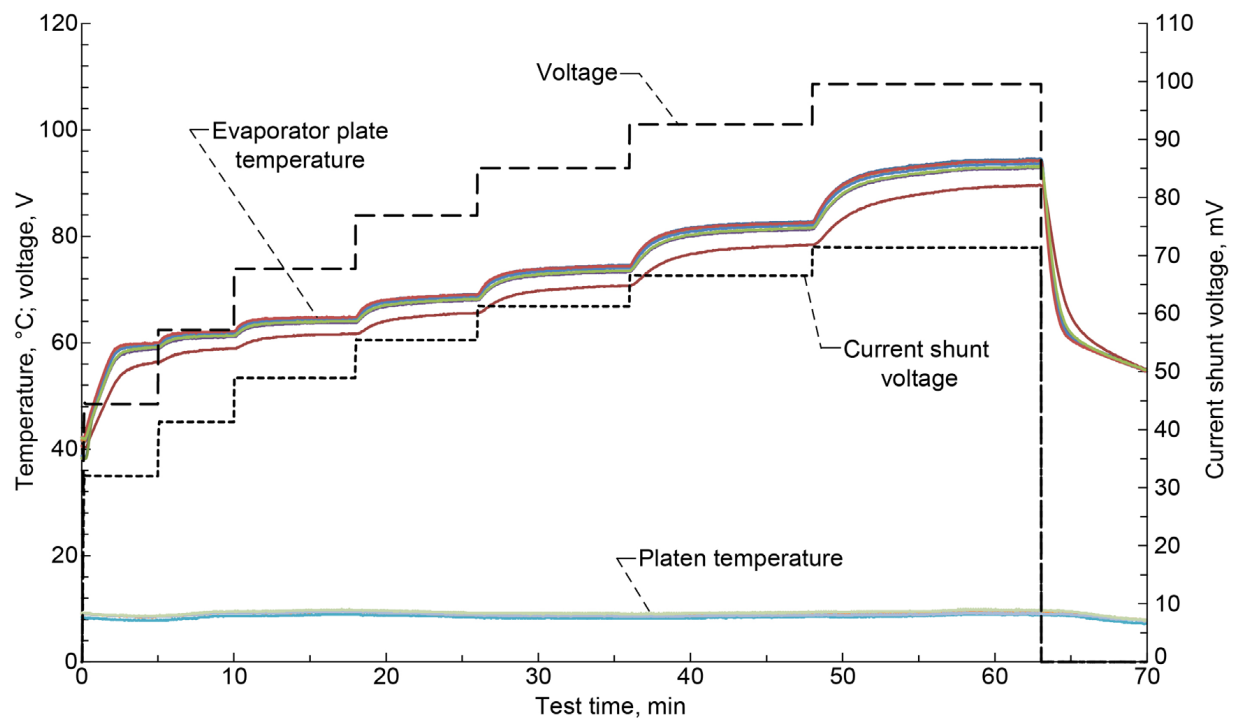


Figure A.8.—Heat pipe 2 on August 15, 2012, with Arctic Silver® paste, full condenser, 80-lb platen force, 8 °C chiller setpoint, and horizontal operation.

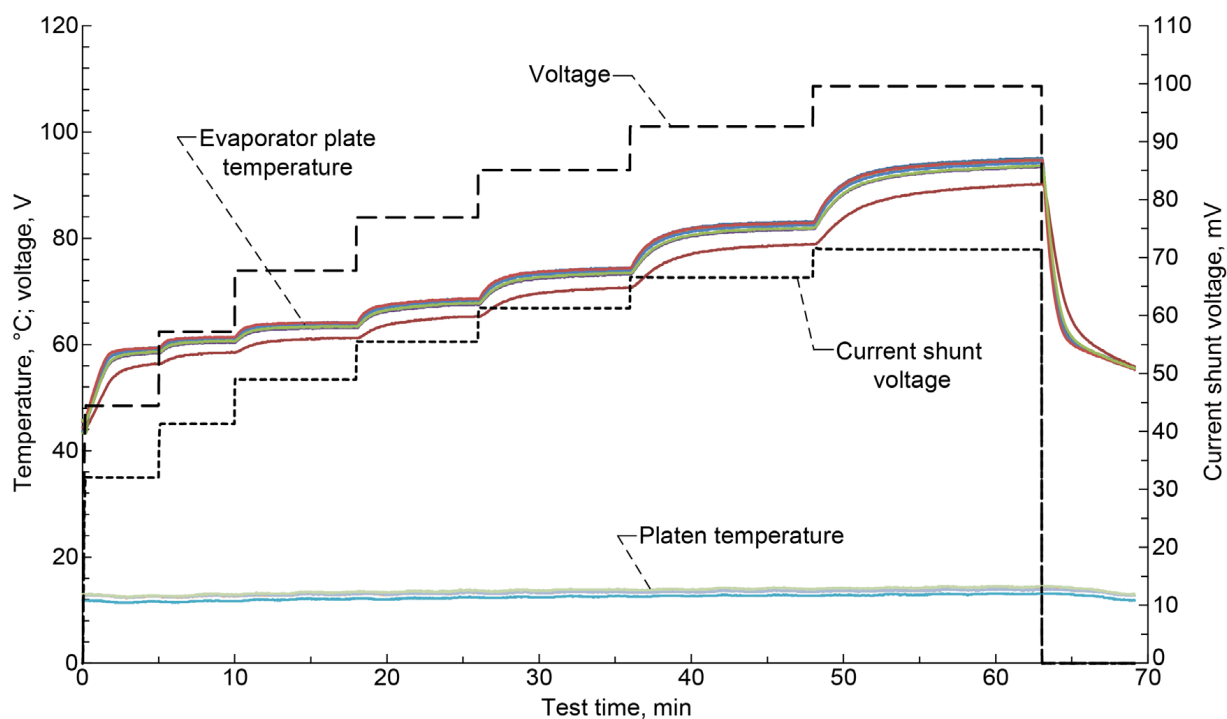


Figure A.9.—Heat pipe 2 on August 15, 2012, with Arctic Silver® paste, full condenser, 80-lb platen force, 12 °C chiller setpoint, and horizontal operation.

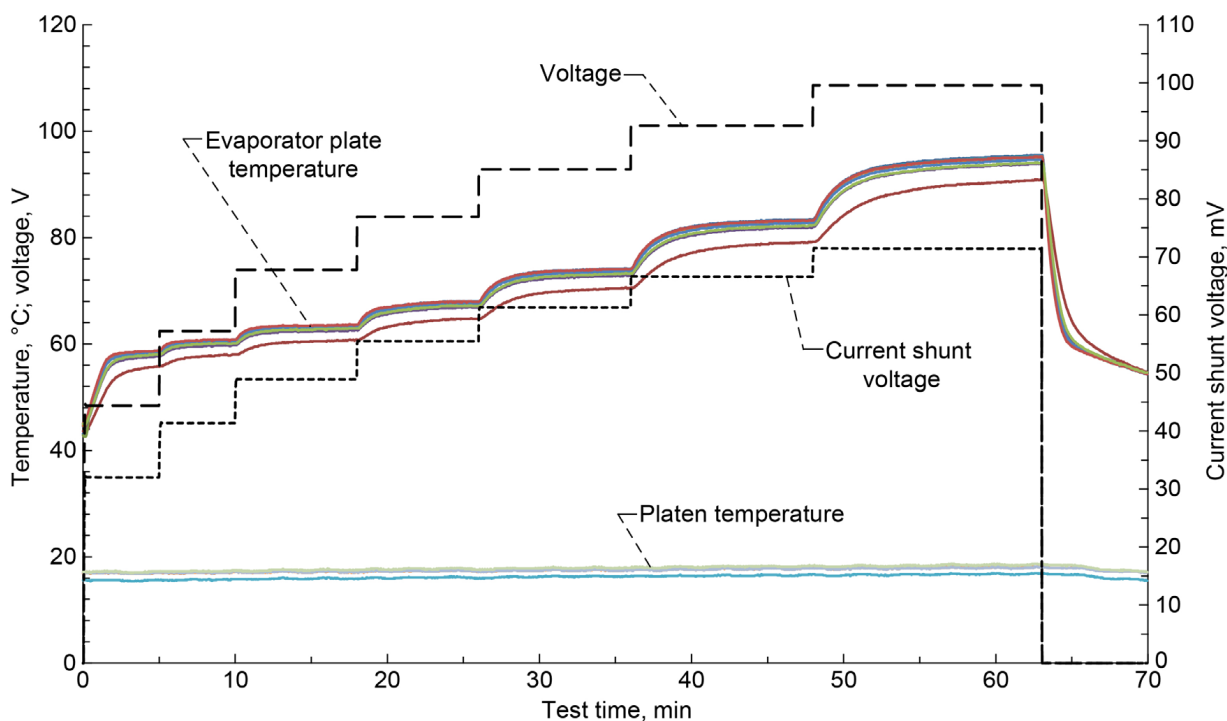


Figure A.10.—Heat pipe 2 on August 15, 2012, with Arctic Silver® paste, full condenser, 80-lb platen force, 16 °C chiller setpoint, and horizontal operation.

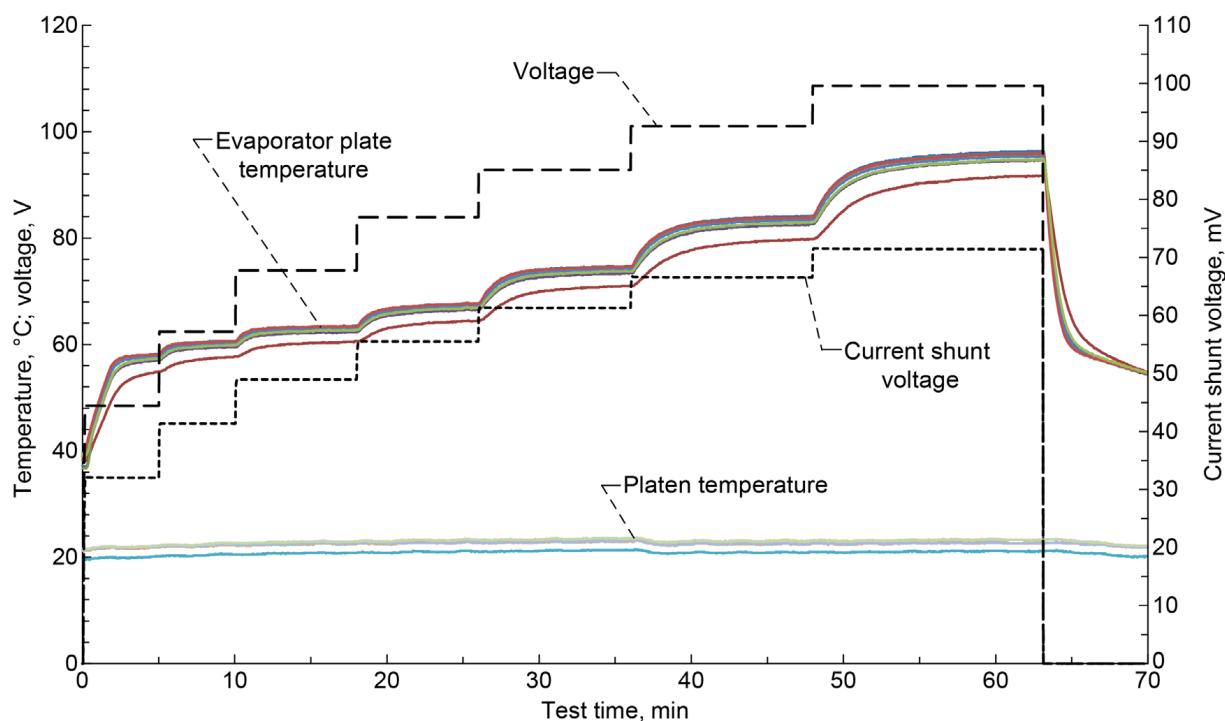


Figure A.11.—Heat pipe 2 on August 15, 2012, with Arctic Silver® paste, full condenser, 80-lb platen force, 20 °C chiller setpoint, and horizontal operation.

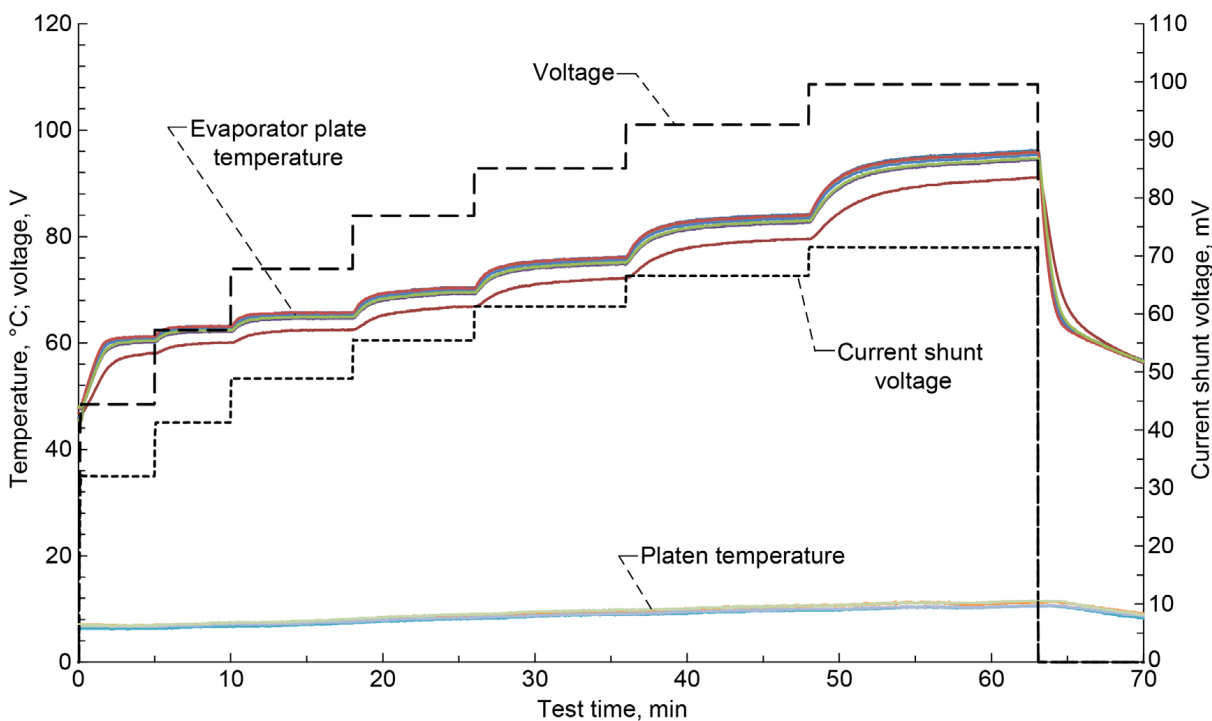


Figure A.12.—Heat pipe 2 on August 15, 2012, with Arctic Silver® paste, full condenser, 60-lb platen force, 8 °C chiller setpoint, and horizontal operation.

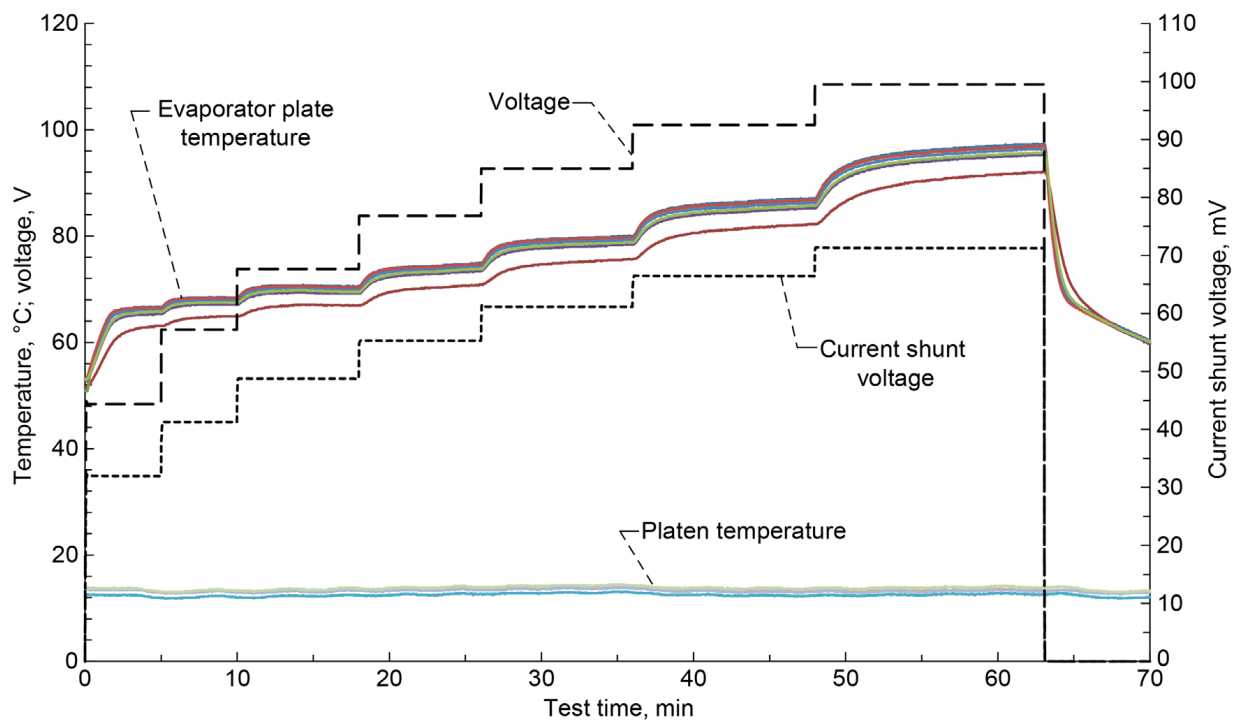


Figure A.13.—Heat pipe 2 on August 16, 2012, with Arctic Silver® paste, full condenser, 60-lb platen force, 12 °C chiller setpoint, and horizontal operation.

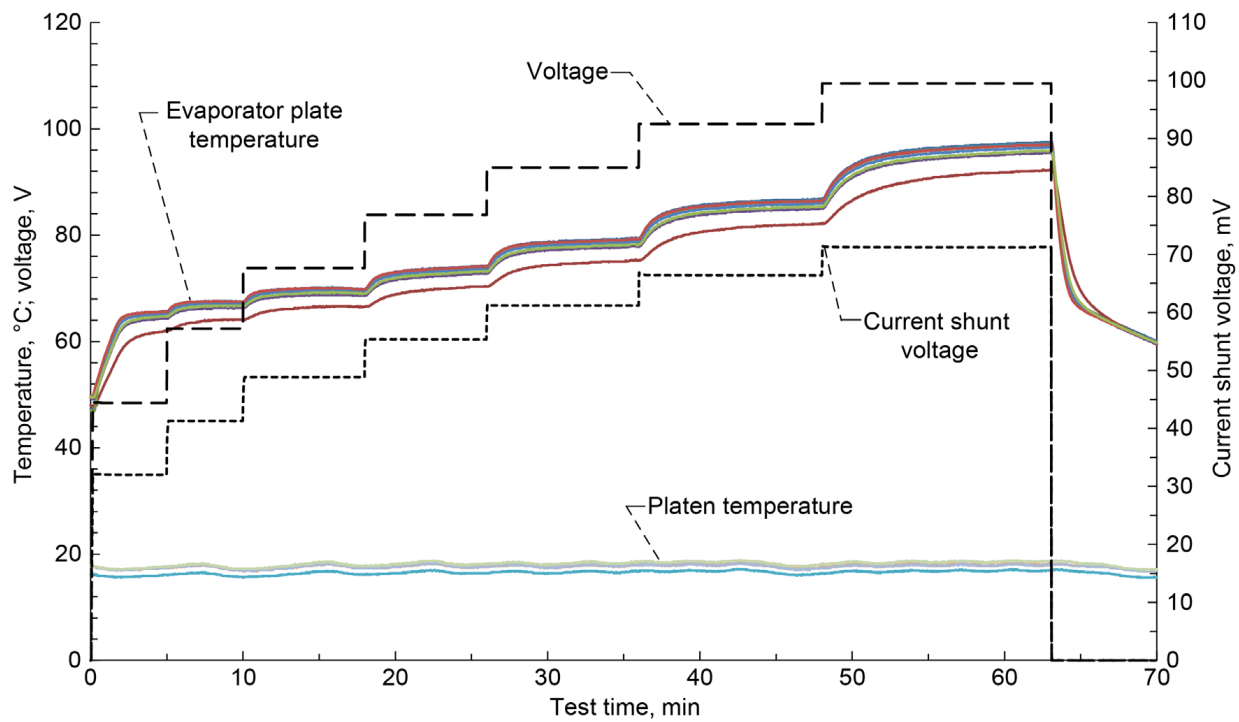


Figure A.14.—Heat pipe 2, test 2 on August 16, 2012, with Arctic Silver® paste, full condenser, 60-lb platen force, 16 °C chiller setpoint, and horizontal operation.

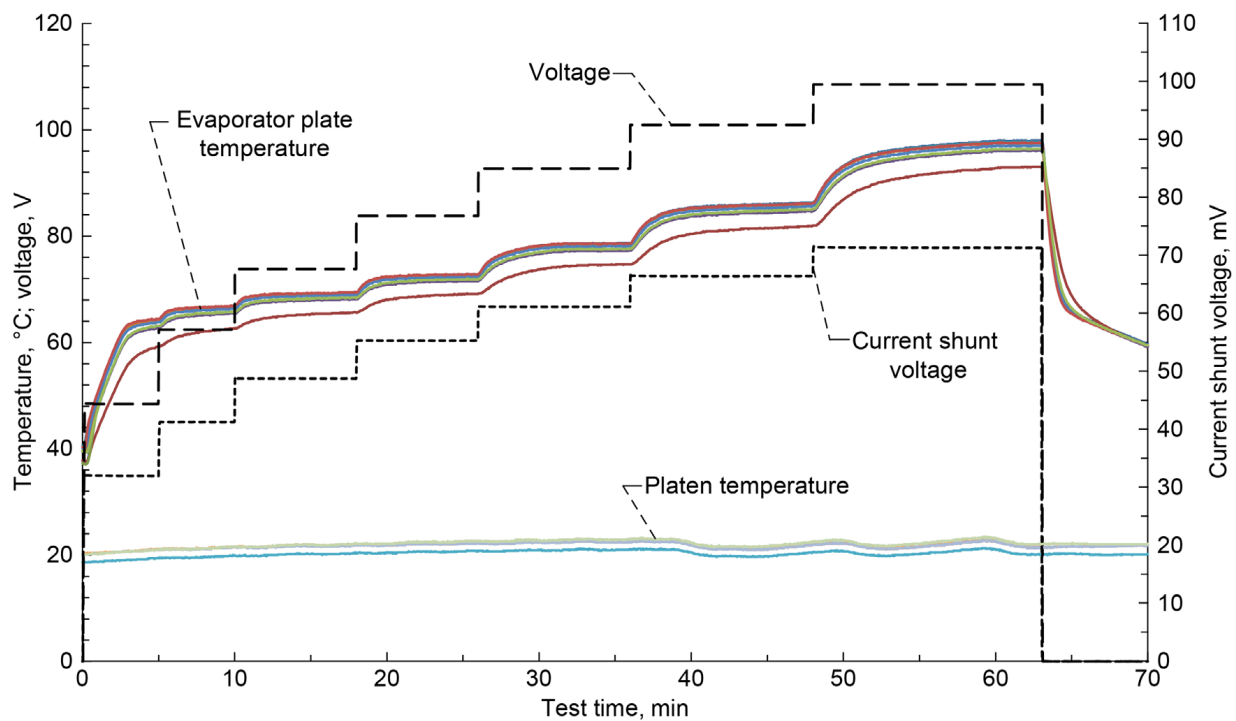


Figure A.15.—Heat pipe 2 on August 16, 2012, with Arctic Silver® paste, full condenser, 60-lb platen force, 20 °C chiller setpoint, and horizontal operation.

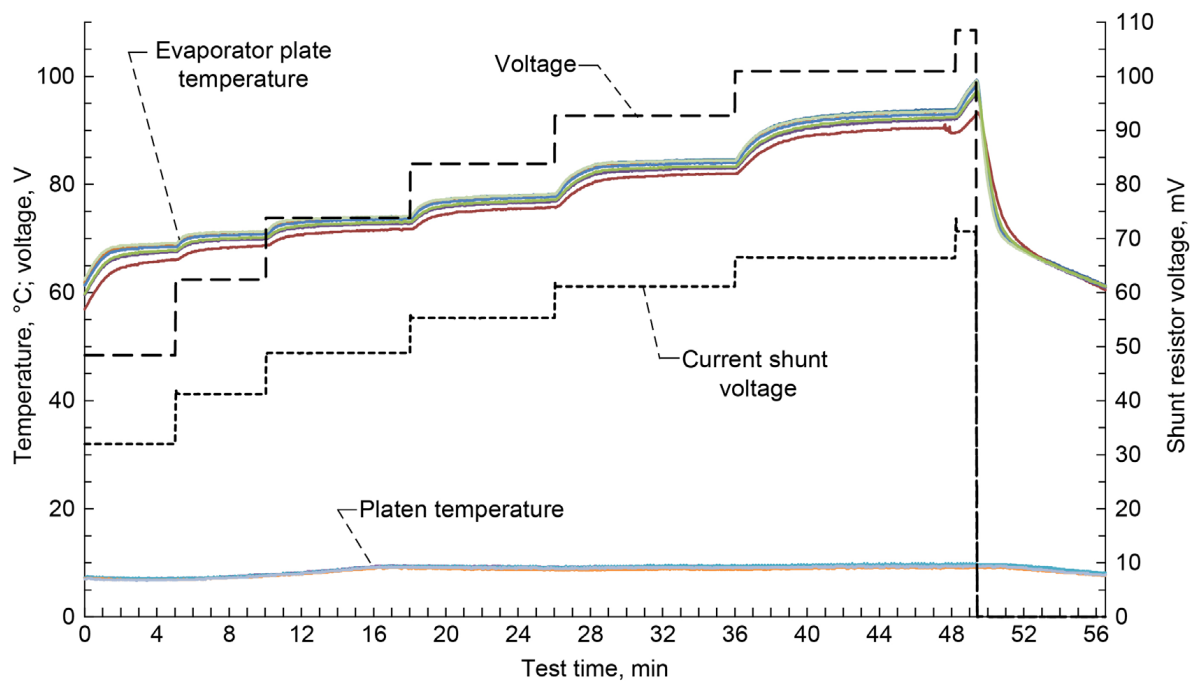


Figure A.16.—Heat pipe 2 on August 17, 2012, with Arctic Silver® paste, 66-mm condenser length, 100-lb platen force, 8 °C chiller setpoint, and horizontal operation.

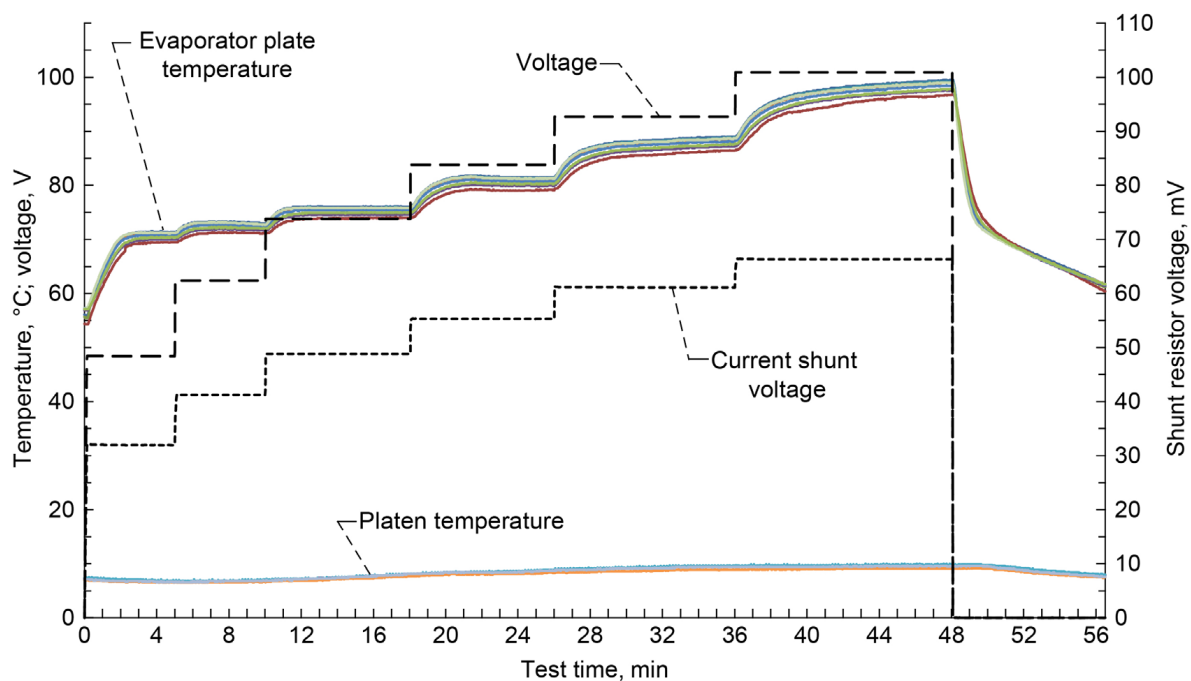


Figure A.17.—Heat pipe 2 on August 17, 2012, with Arctic Silver® paste, 61-mm condenser length, 100-lb platen force, 8 °C chiller setpoint, and horizontal operation.

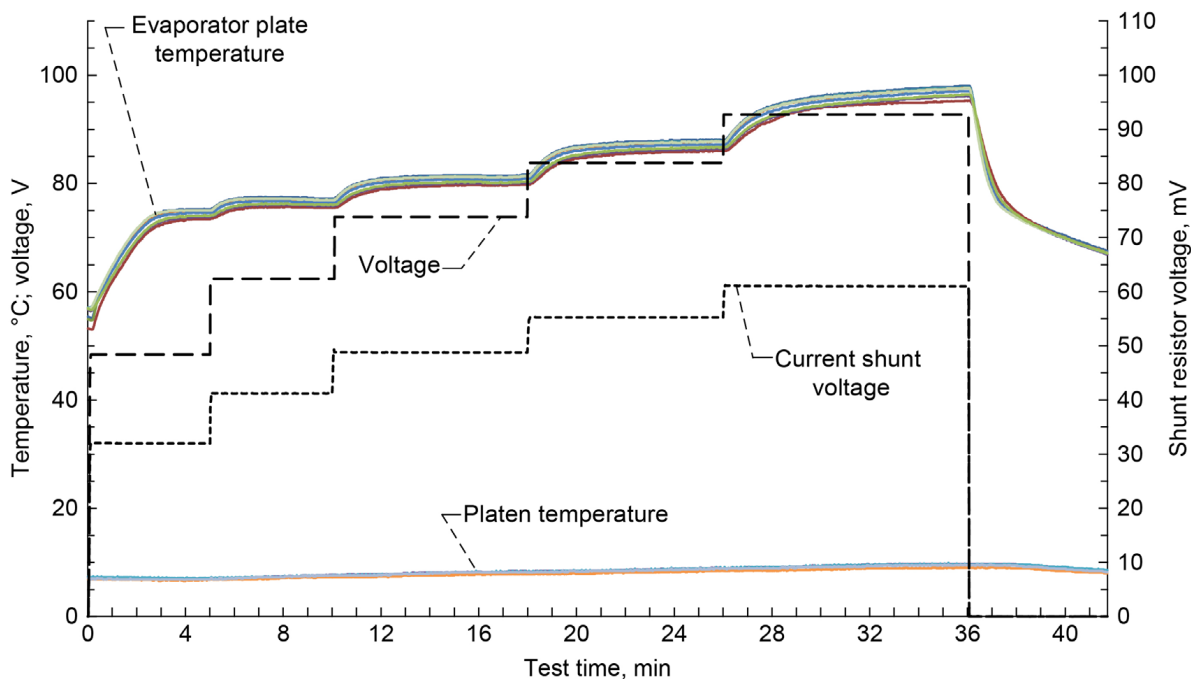


Figure A.18.—Heat pipe 2 on August 17, 2012, with Arctic Silver® paste, 56-mm condenser length, 100-lb platen force, 8 °C chiller setpoint, and horizontal operation.

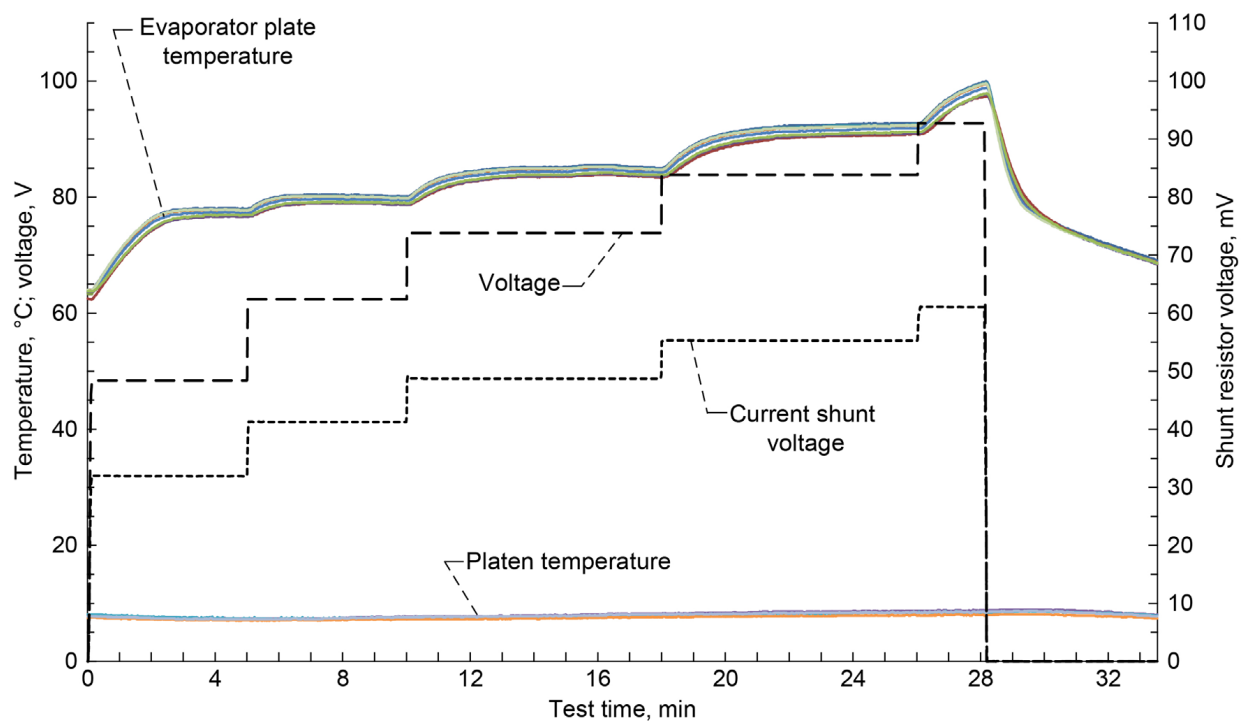


Figure A.19.—Heat pipe 2 on August 17, 2012, with Arctic Silver® paste, 51-mm condenser length, 100-lb platen force, 8 °C chiller setpoint, and horizontal operation.

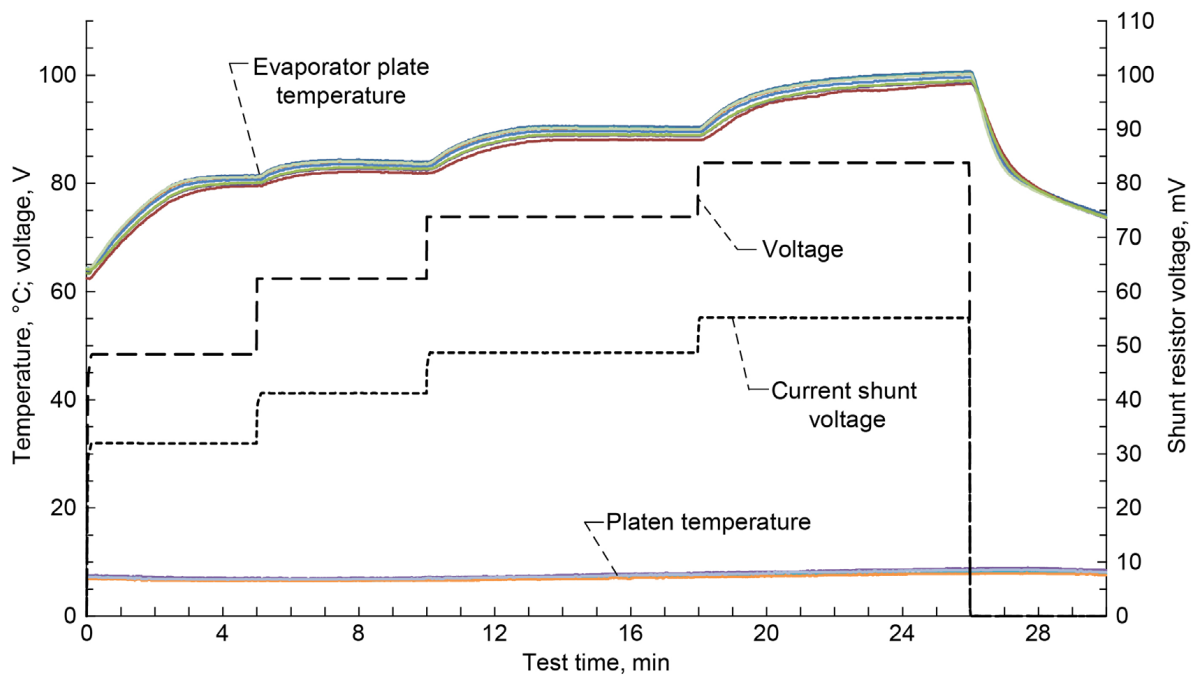


Figure A.20.—Heat pipe 2 on August 17, 2012, with Arctic Silver® paste, 46-mm condenser length, 100-lb platen force, 8 °C chiller setpoint, and horizontal operation.



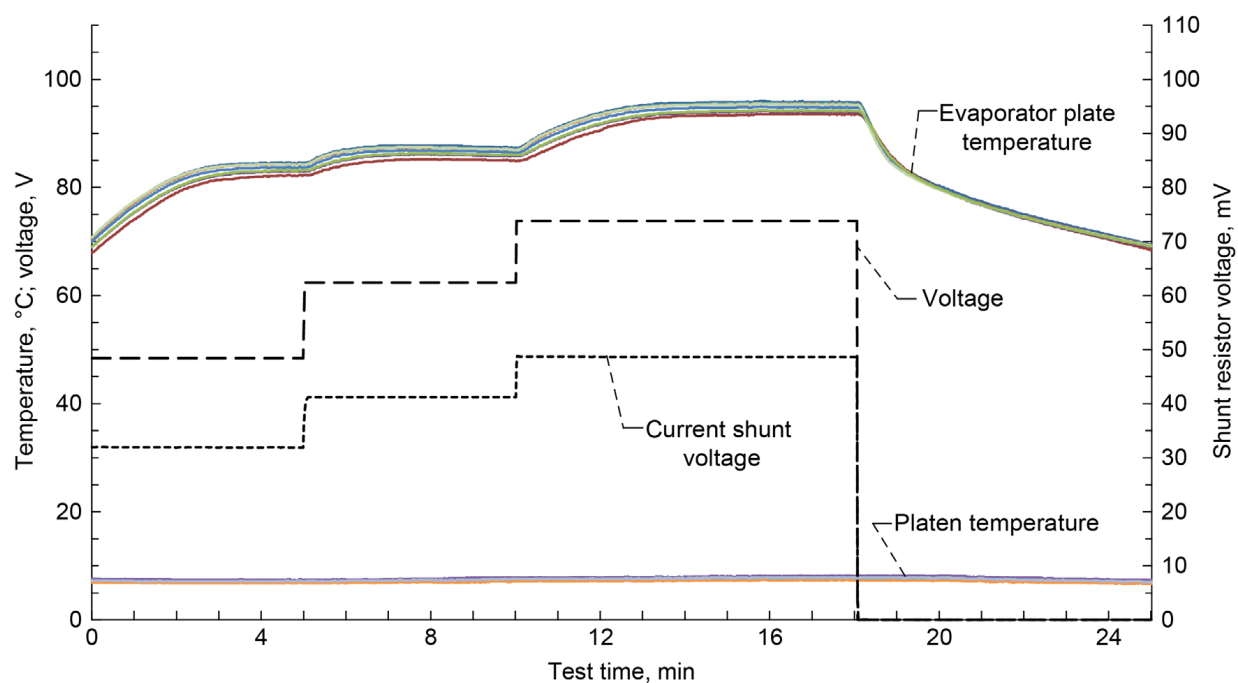


Figure A.21.—Heat pipe 2 on August 17, 2012, with Arctic Silver® paste, 41-mm condenser length, 100-lb platen force, 8 °C chiller setpoint, and horizontal operation.

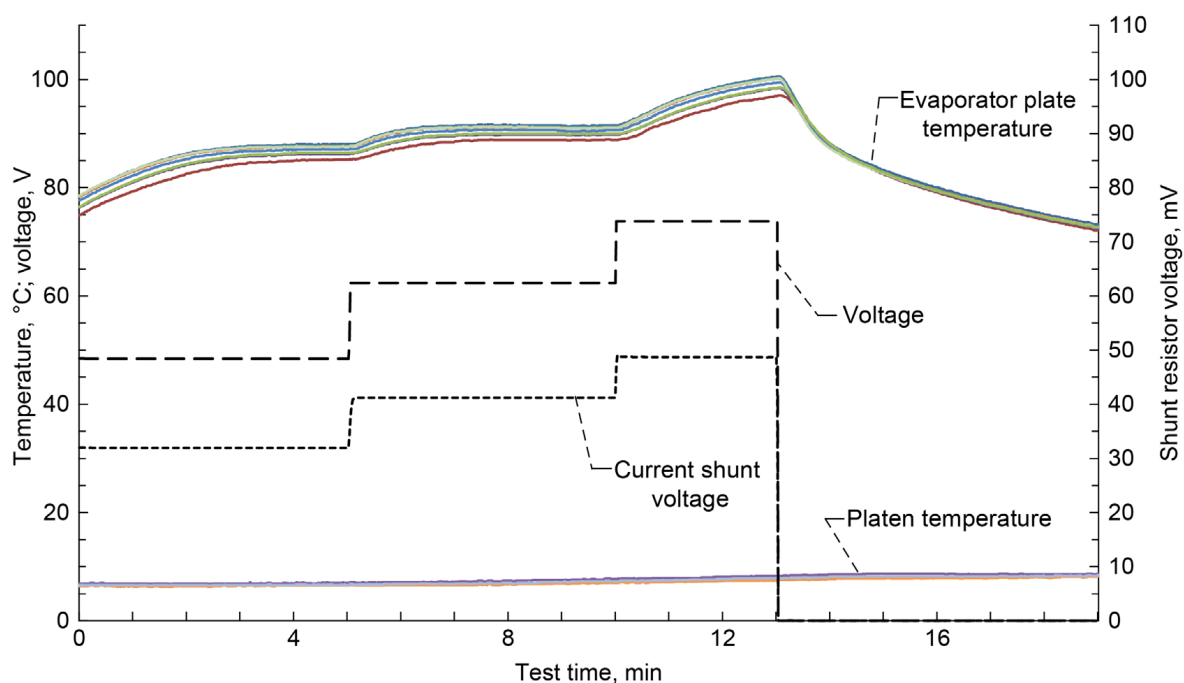


Figure A.22.—Heat pipe 2 on August 17, 2012, with Arctic Silver® paste, 36-mm condenser length, 100-lb platen force, 8 °C chiller setpoint, and horizontal operation.

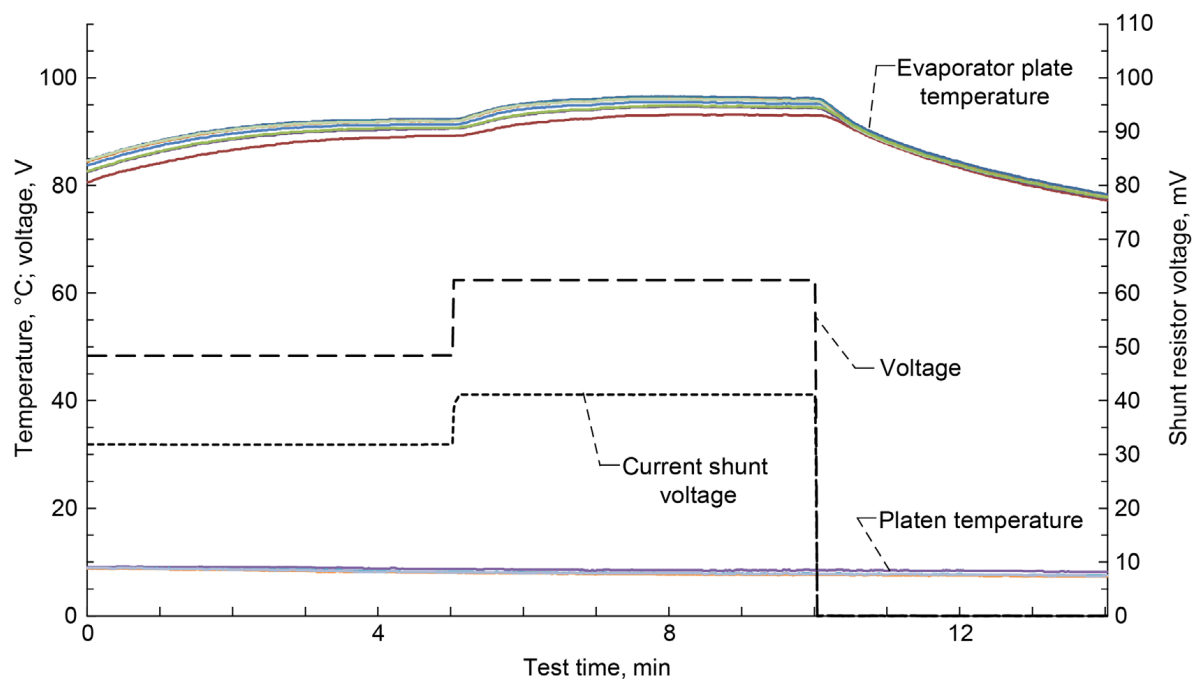


Figure A.23.—Heat pipe 2 on August 17, 2012, with Arctic Silver® paste, 31-mm condenser length, 100-lb platen force, 8 °C chiller setpoint, and horizontal operation.

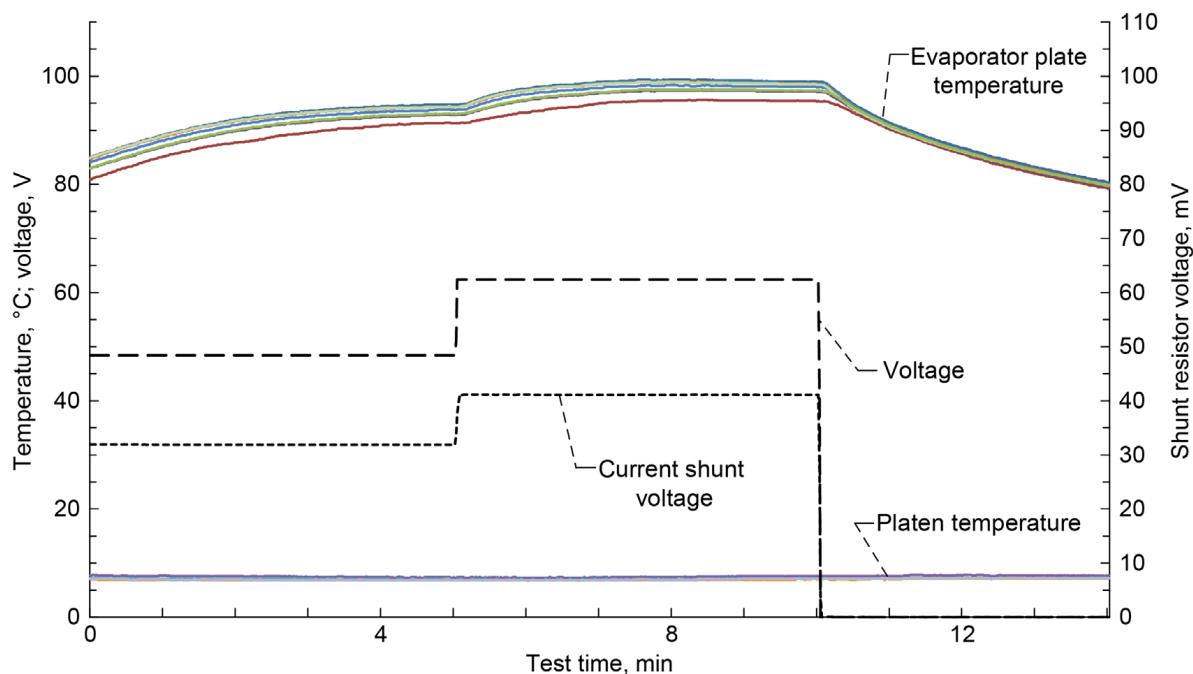


Figure A.24.—Heat pipe 2 on August 17, 2012, with Arctic Silver® paste, 26-mm condenser length, 100-lb platen force, 8 °C chiller setpoint, and horizontal operation.

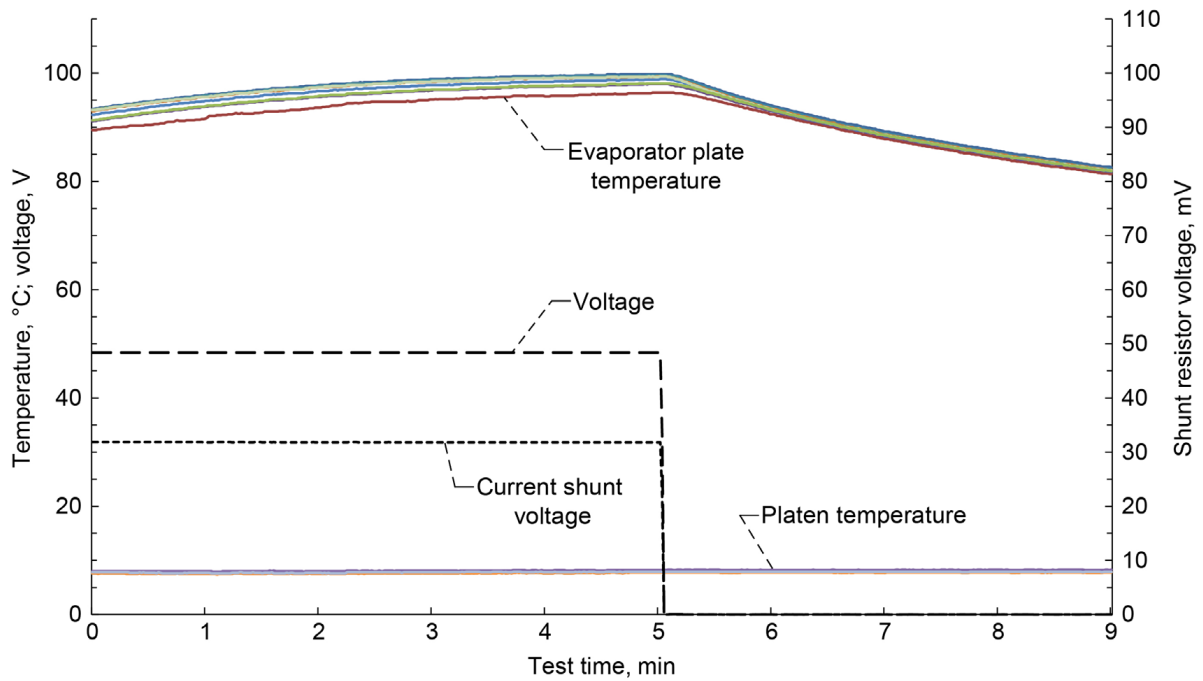


Figure A.25.—Heat pipe 2 on August 17, 2012, with Arctic Silver® paste, 21-mm condenser length, 100-lb platen force, 8 °C chiller setpoint, and horizontal operation.

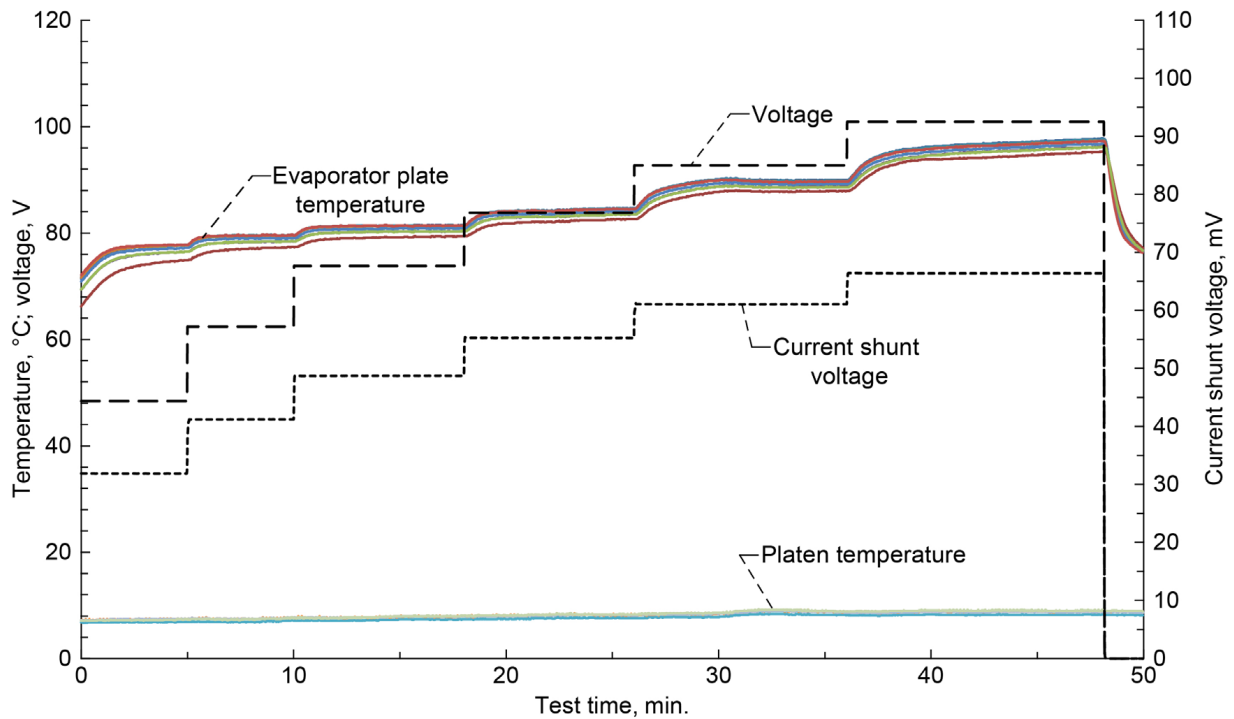


Figure A.26.—Heat pipe 2 on August 20, 2012, with Arctic Silver® paste, 66-mm condenser length, 60-lb platen force, 8 °C chiller setpoint, and horizontal operation.

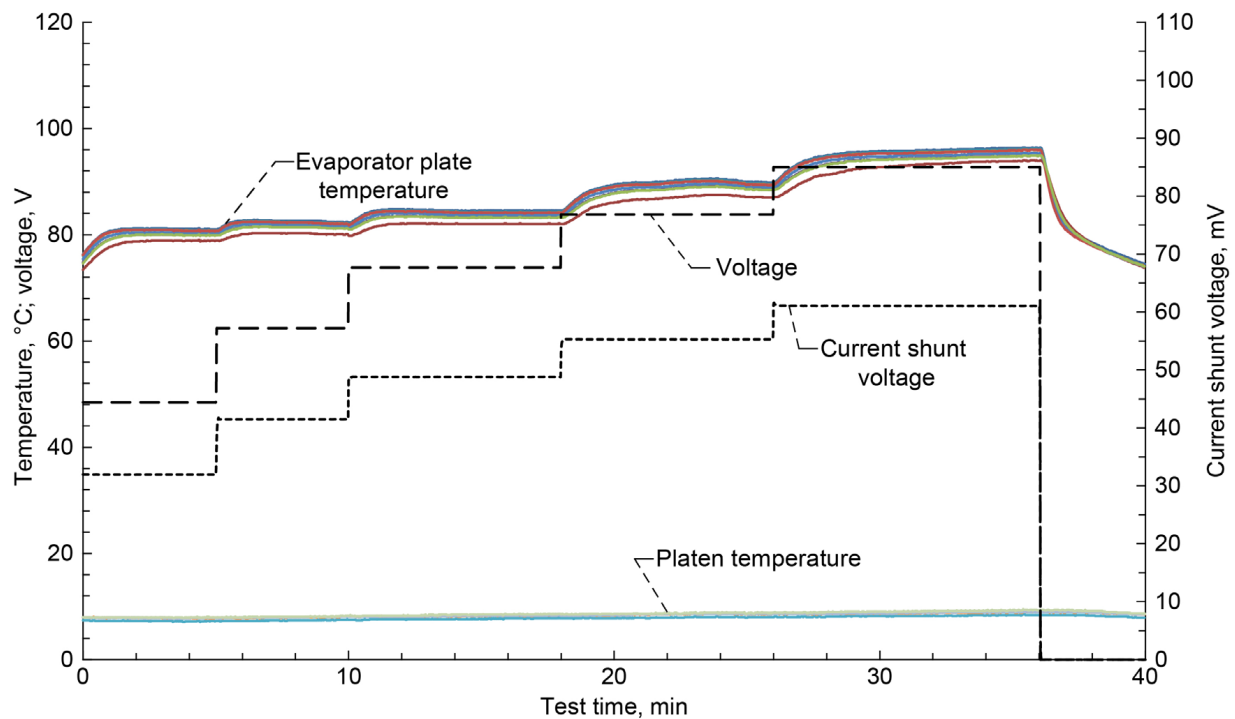


Figure A.27.—Heat pipe 2 on August 20, 2012, with Arctic Silver® paste, 61-mm condenser length, 60-lb platen force, 8 °C chiller setpoint, and horizontal operation.

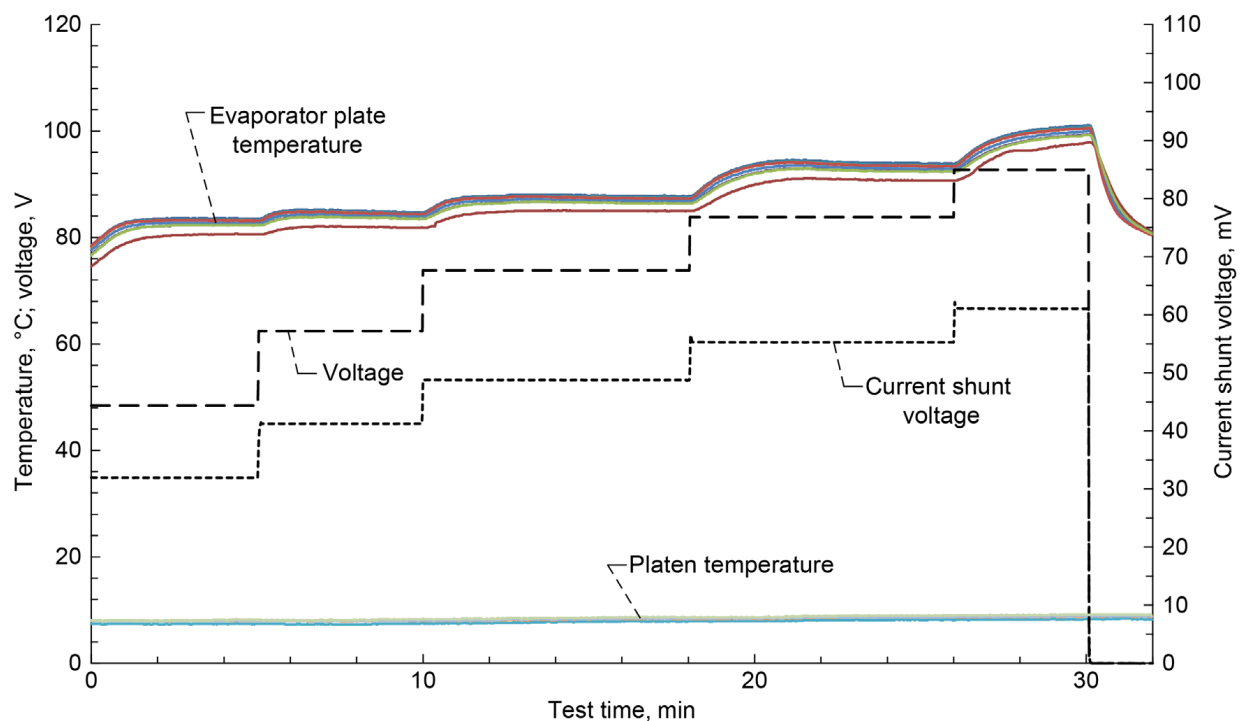


Figure A.28.—Heat pipe 2 on August 20, 2012, with Arctic Silver® paste, 56-mm condenser length, 60-lb platen force, 8 °C chiller setpoint, and horizontal operation.

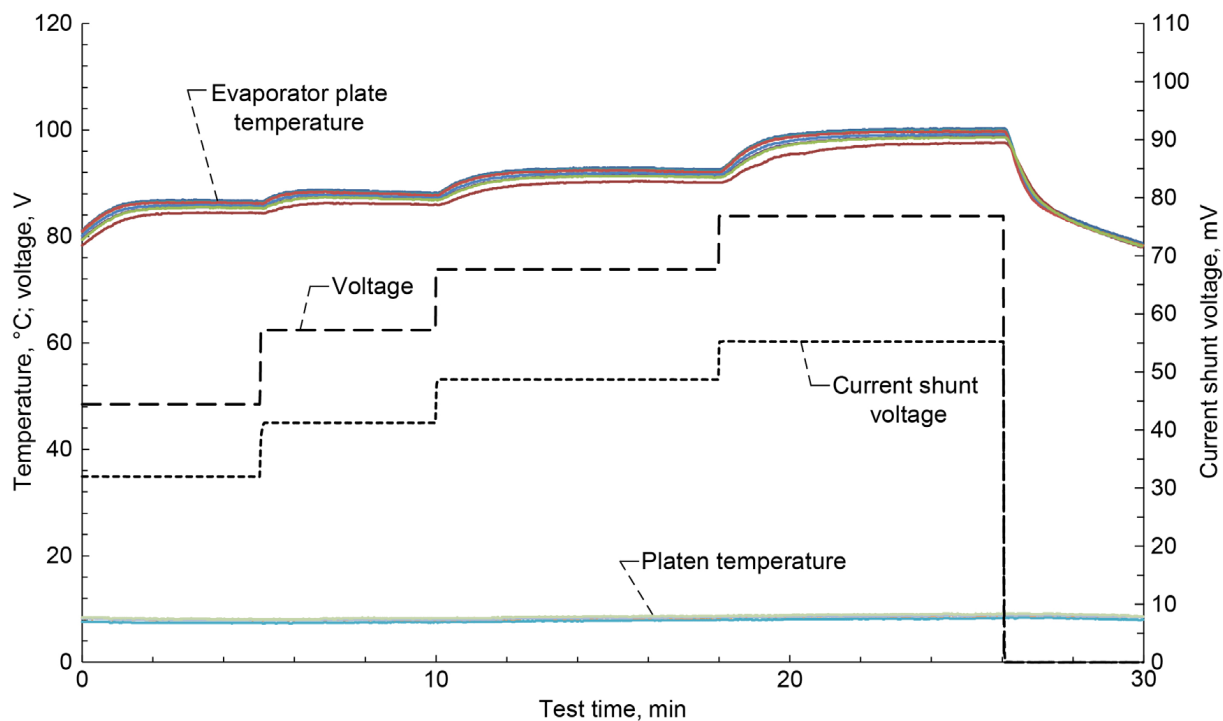


Figure A.29.—Heat pipe 2 on August 20, 2012, with Arctic Silver® paste, 51-mm condenser length, 60-lb platen force, 8 °C chiller setpoint, and horizontal operation.

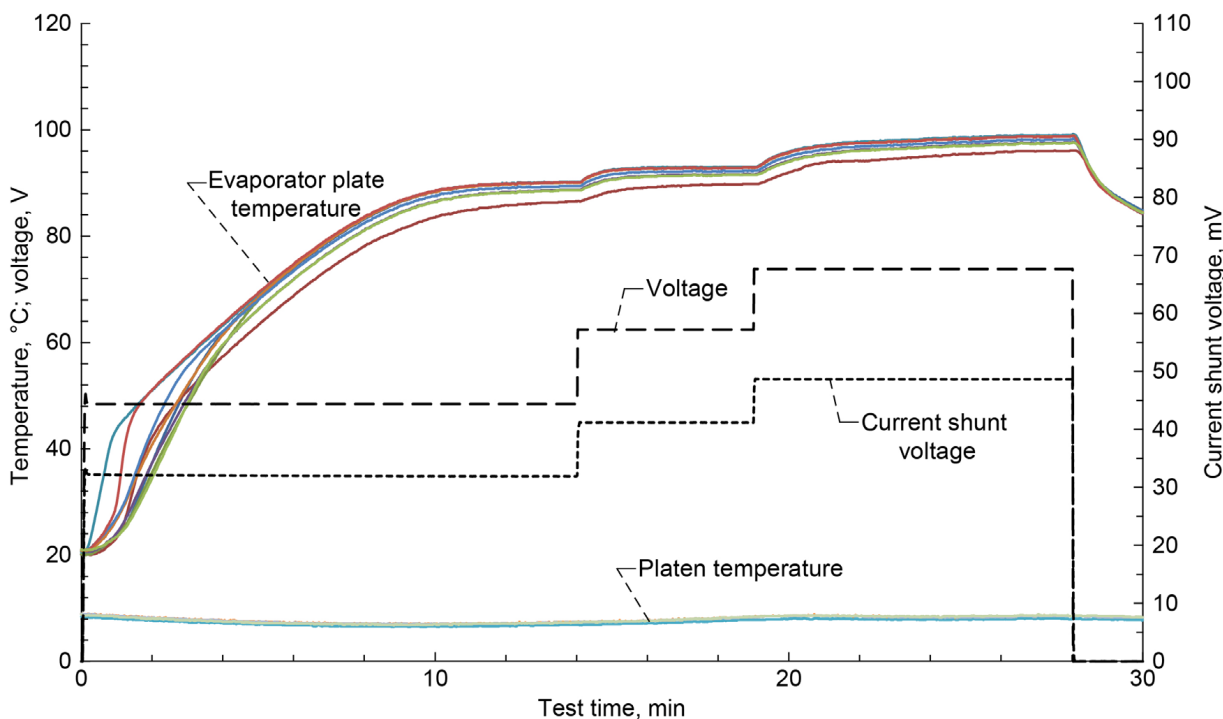


Figure A.30.—Heat pipe 2 on August 20, 2012, with Arctic Silver® paste, 46-mm condenser length, 60-lb platen force, 8 °C chiller setpoint, and horizontal operation.

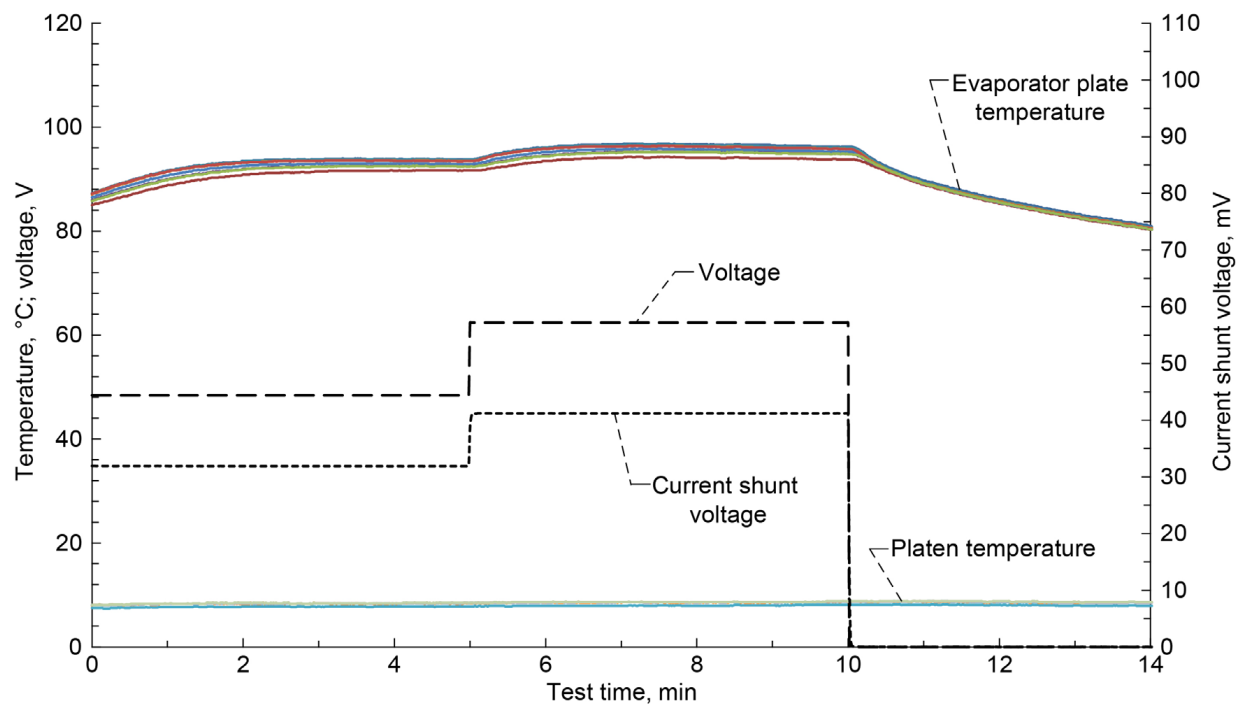


Figure A.31.—Heat pipe 2 on August 20, 2012, with Arctic Silver® paste, 41-mm condenser length, 60-lb platen force, 8 °C chiller setpoint, and horizontal operation.

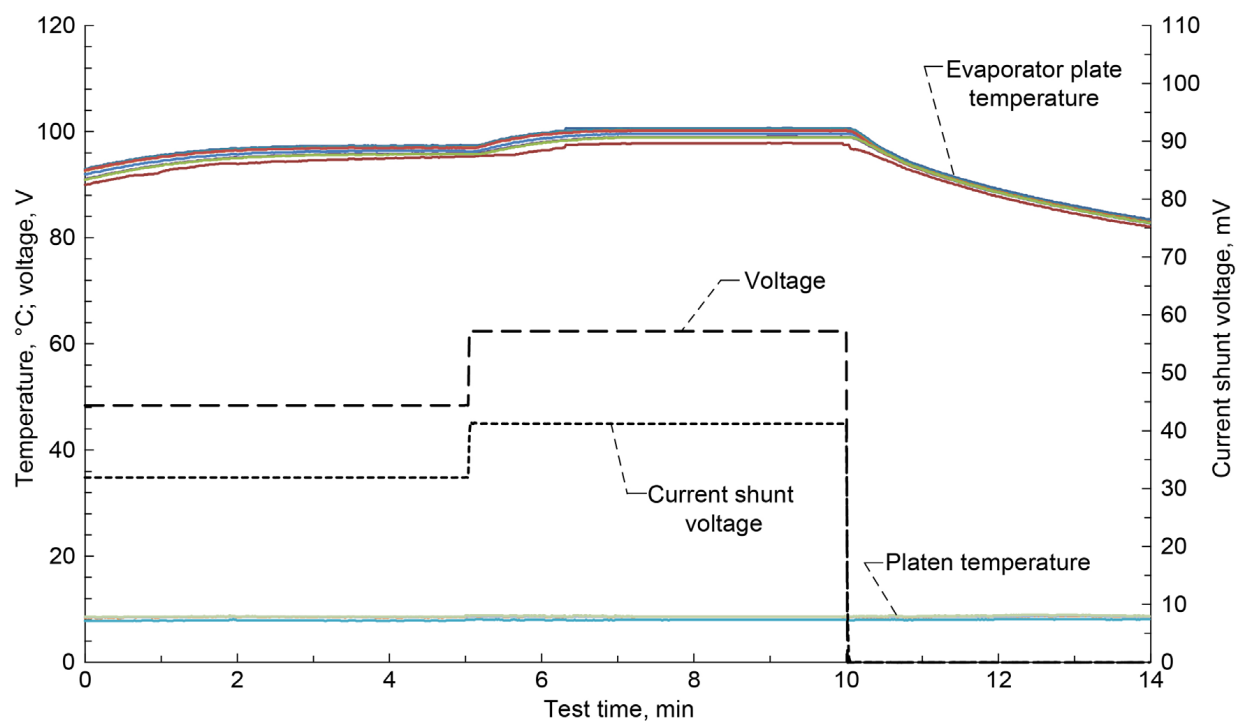


Figure A.32.—Heat pipe 2 on August 20, 2012, with Arctic Silver® paste, 36-mm condenser length, 60-lb platen force, 8 °C chiller setpoint, and horizontal operation.

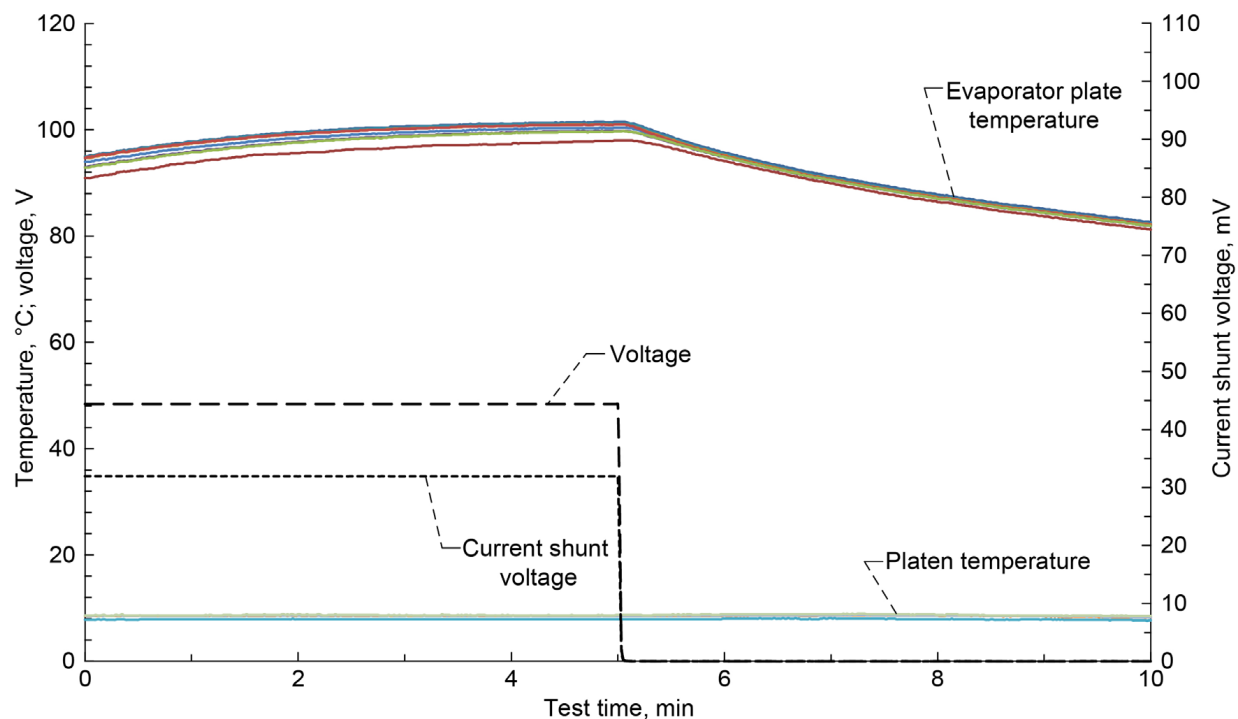


Figure A.33.—Heat pipe 2 on August 20, 2012, with Arctic Silver® paste, 31-mm condenser length, 60-lb platen force, 8 °C chiller setpoint, and horizontal operation.

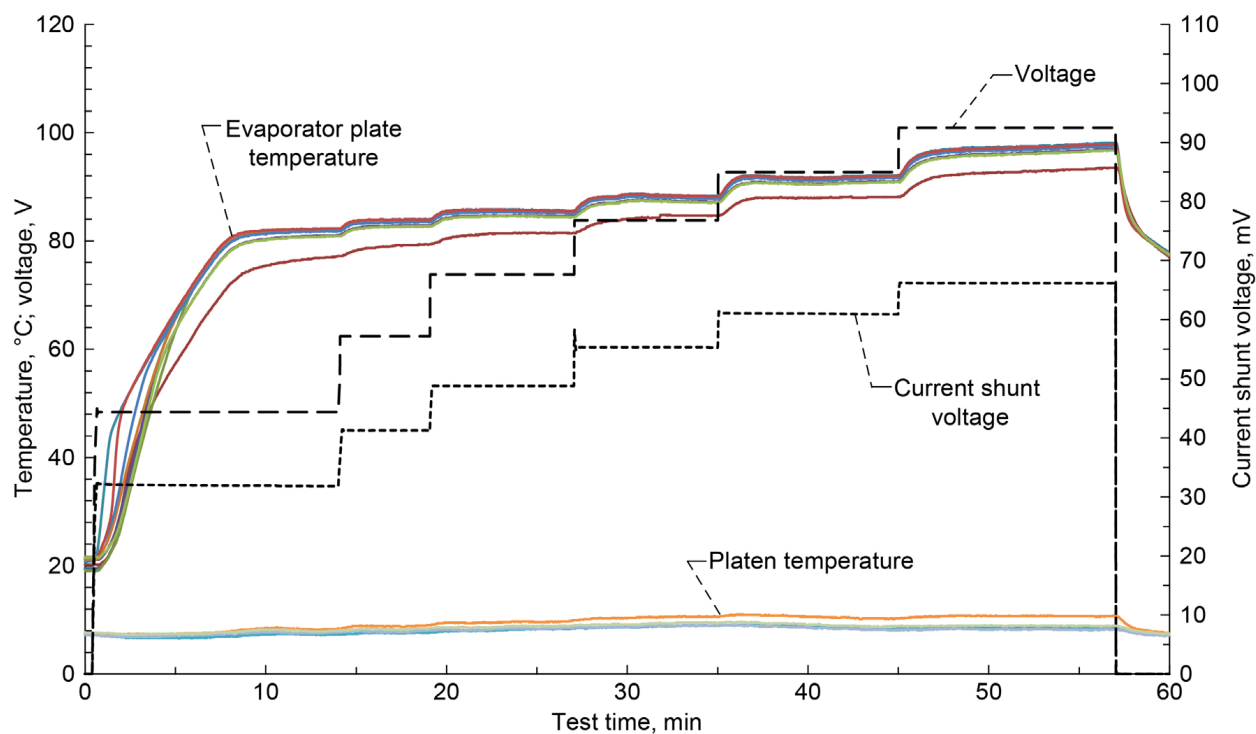


Figure A.34.—Heat pipe 2 on August 22, 2012, with Arctic Silver® paste, full-condenser length, 100-lb platen force, 8 °C chiller setpoint, and condenser-to-side operation in copper platens.



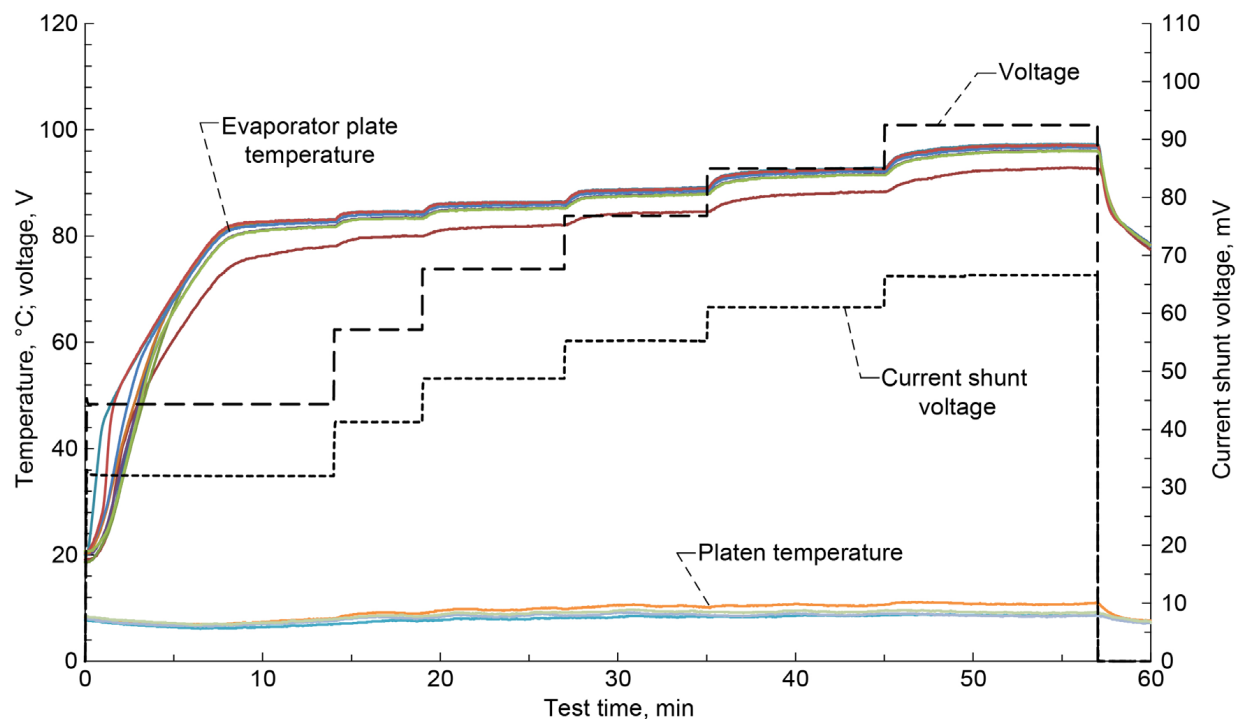


Figure A.35.—Heat pipe 2 on August 23, 2012, with Arctic Silver® paste, full-condenser length, 100-lb platen force, 8 °C chiller setpoint, and condenser on top operation in copper platens.

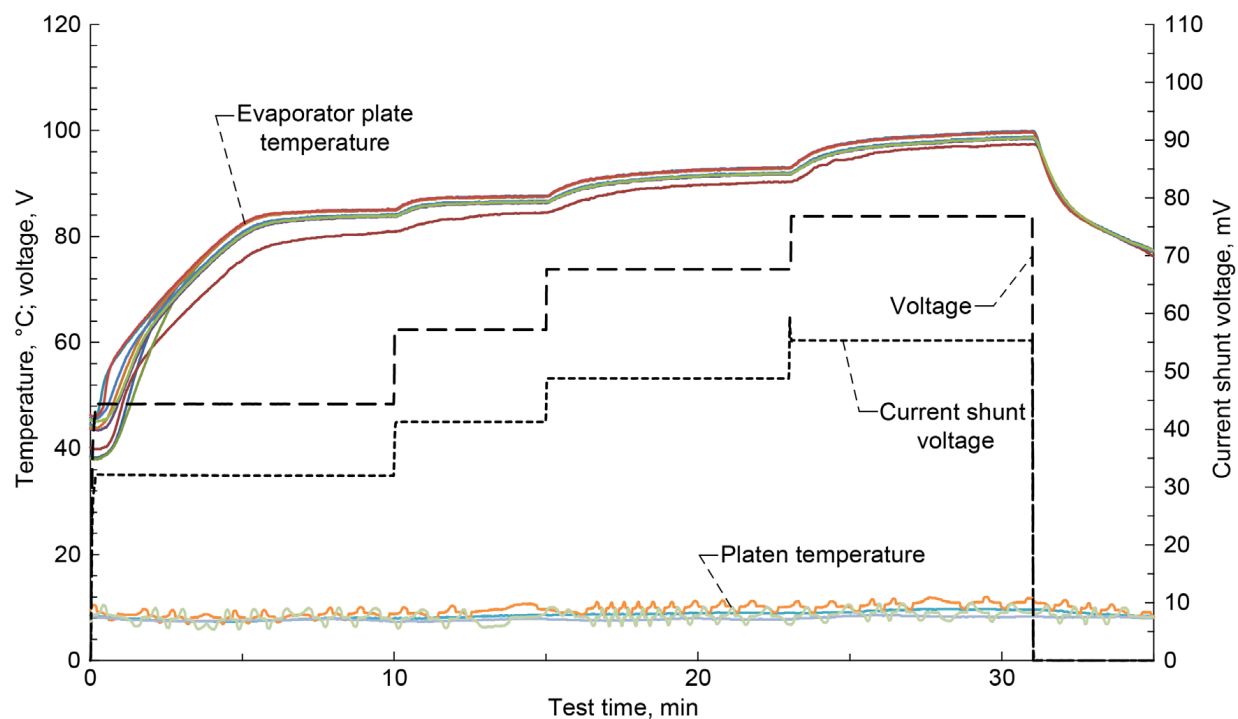


Figure A.36.—Heat pipe 2 on August 23, 2012, with Arctic Silver® paste, full-condenser length, 100-lb platen force, 8 °C chiller setpoint, and condenser on bottom operation in copper platens.

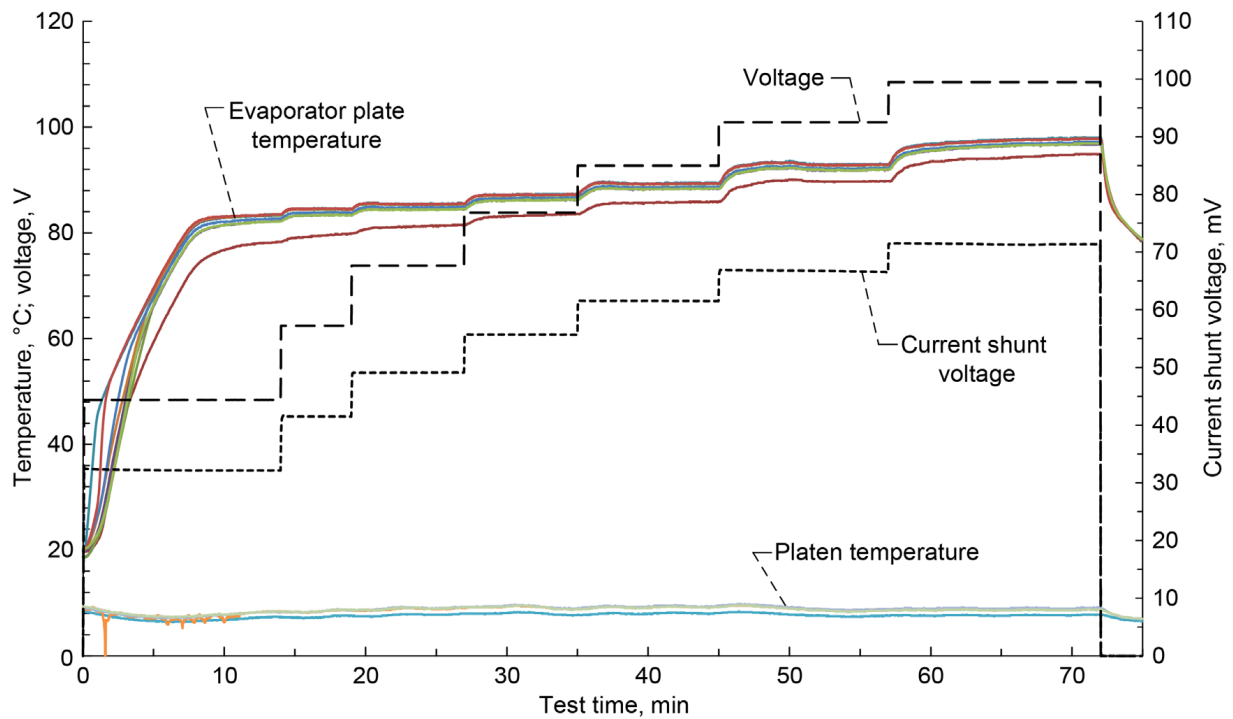


Figure A.37.—Heat pipe 2 on August 24, 2012, with Arctic Silver® paste, full-condenser length, 100-lb platen force, 8 °C chiller setpoint, and horizontal operation in copper platens.

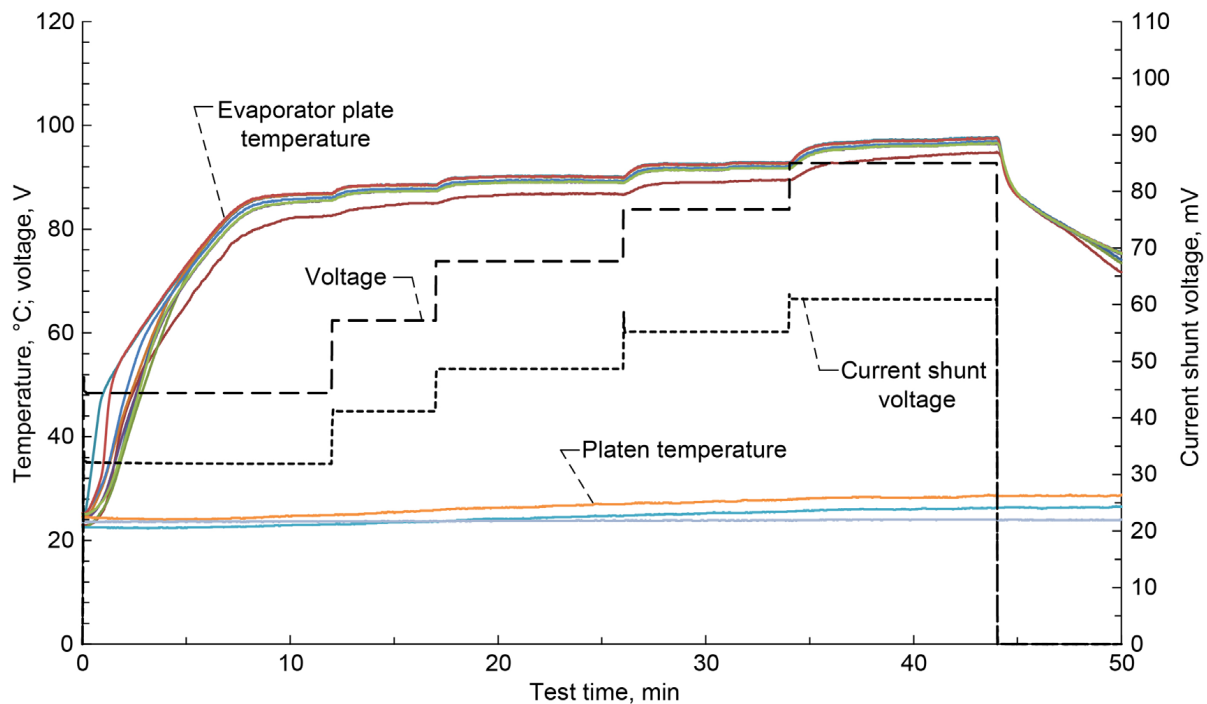


Figure A.38.—Heat pipe 2 on August 24, 2012, with Arctic Silver® paste, full-condenser length, 100-lb platen force, 8 °C chiller setpoint, and horizontal operation.

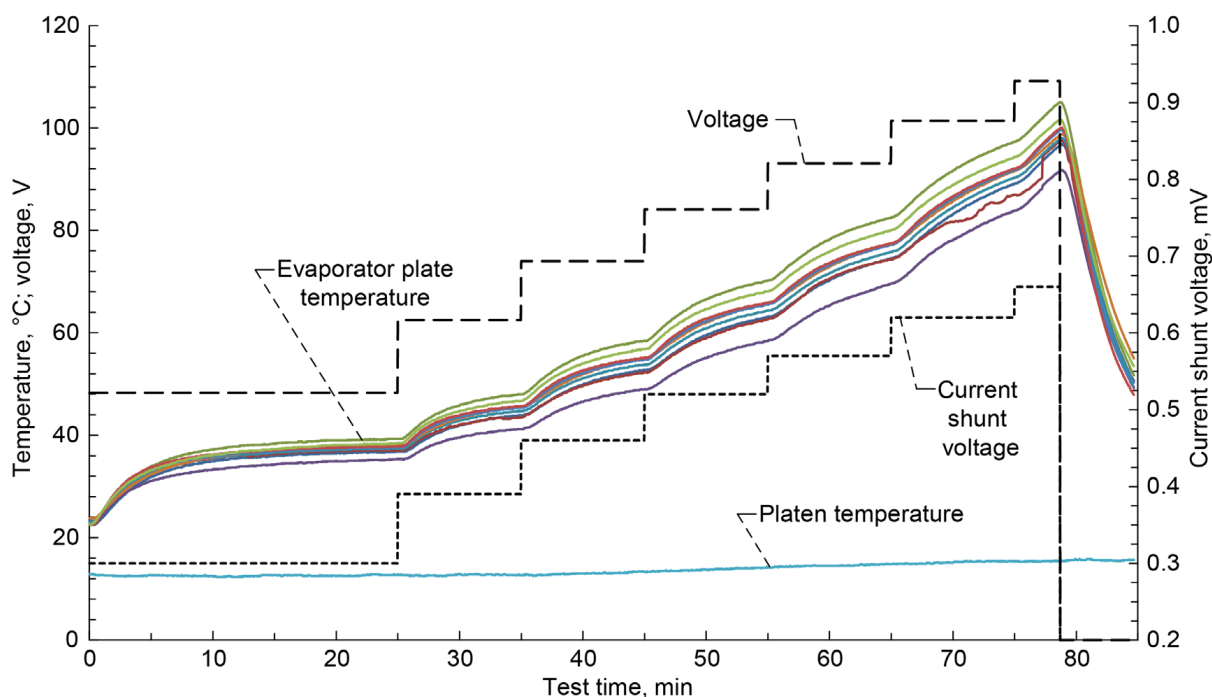


Figure A.39.—Heat pipe A test run 1, on August 12, 2013, with Arctic Silver<sup>®</sup> paste, full-condenser length, 100-lb platen force, 10 °C chiller setpoint, and horizontal operation.

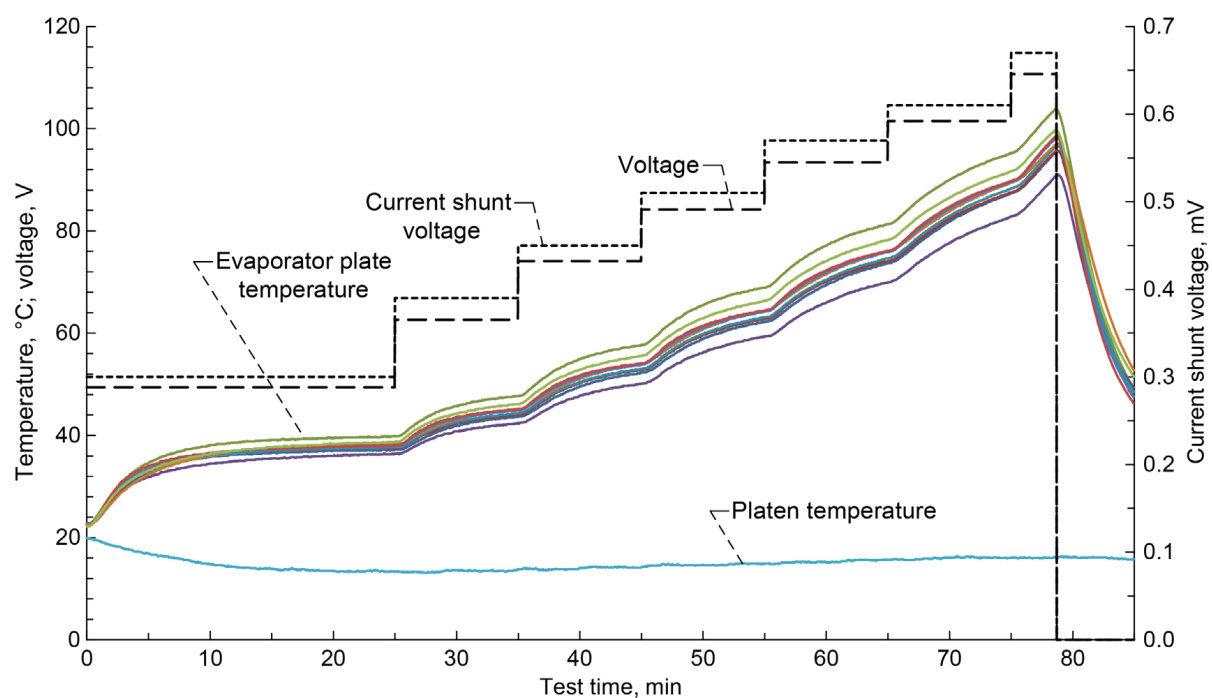


Figure A.40.—Heat pipe A, test run 2 on August 13, 2013, with Arctic Silver<sup>®</sup> paste, full-condenser length, 100-lb platen force, 10 °C chiller setpoint, and horizontal operation.

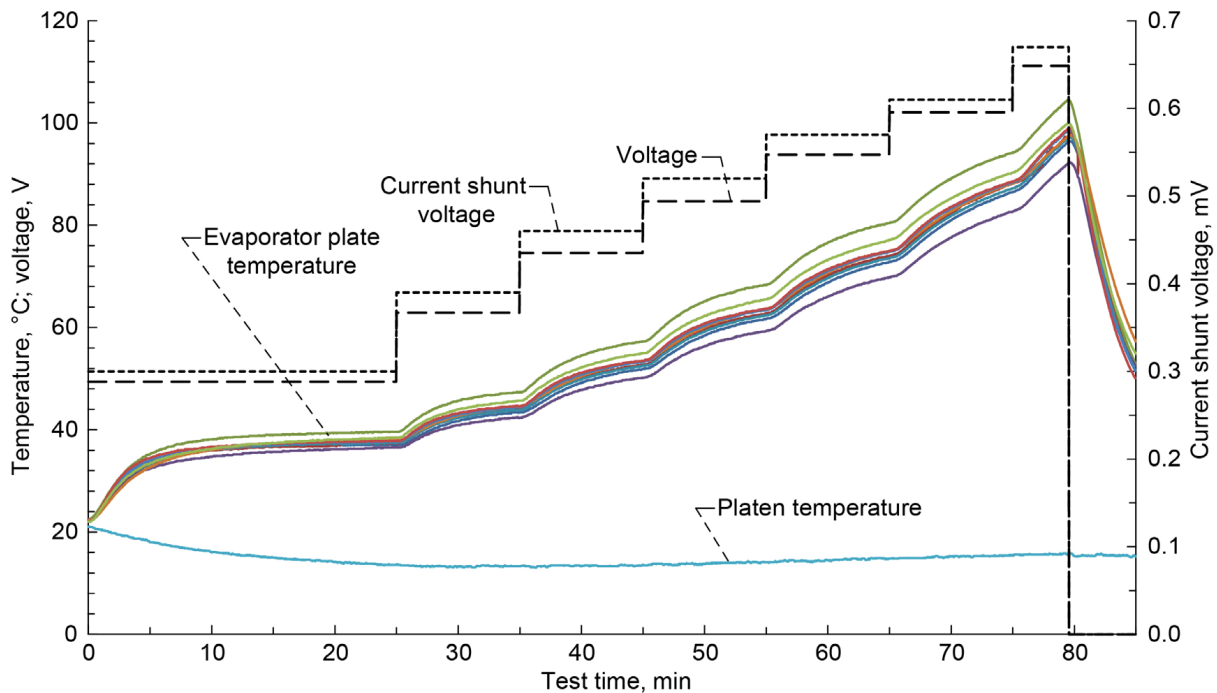


Figure A.41.—Heat pipe A, test run 3 on August 13, 2013, with Arctic Silver<sup>®</sup> paste, full-condenser length, 100-lb platen force, 10 °C chiller setpoint, and horizontal operation.

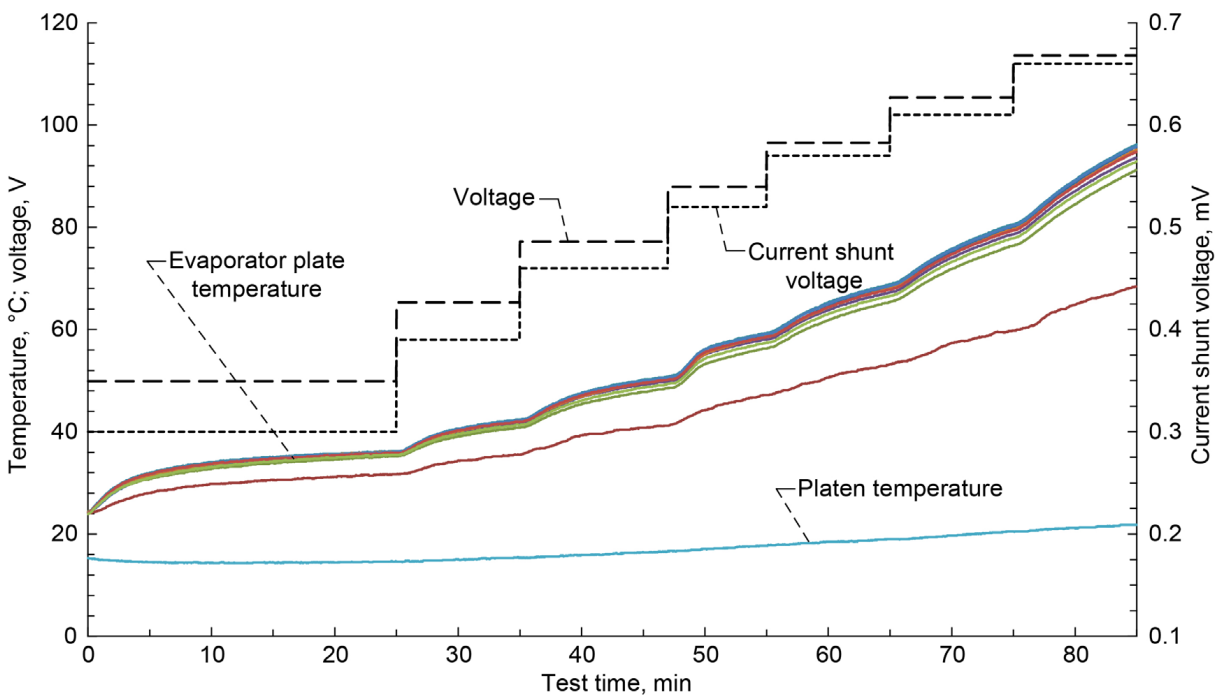


Figure A.42.—Heat pipe A, test run 4 on August 19, 2013, with Arctic Silver<sup>®</sup> paste, full condenser length, 100-lb platen force, 10 °C chiller setpoint, and horizontal operation.

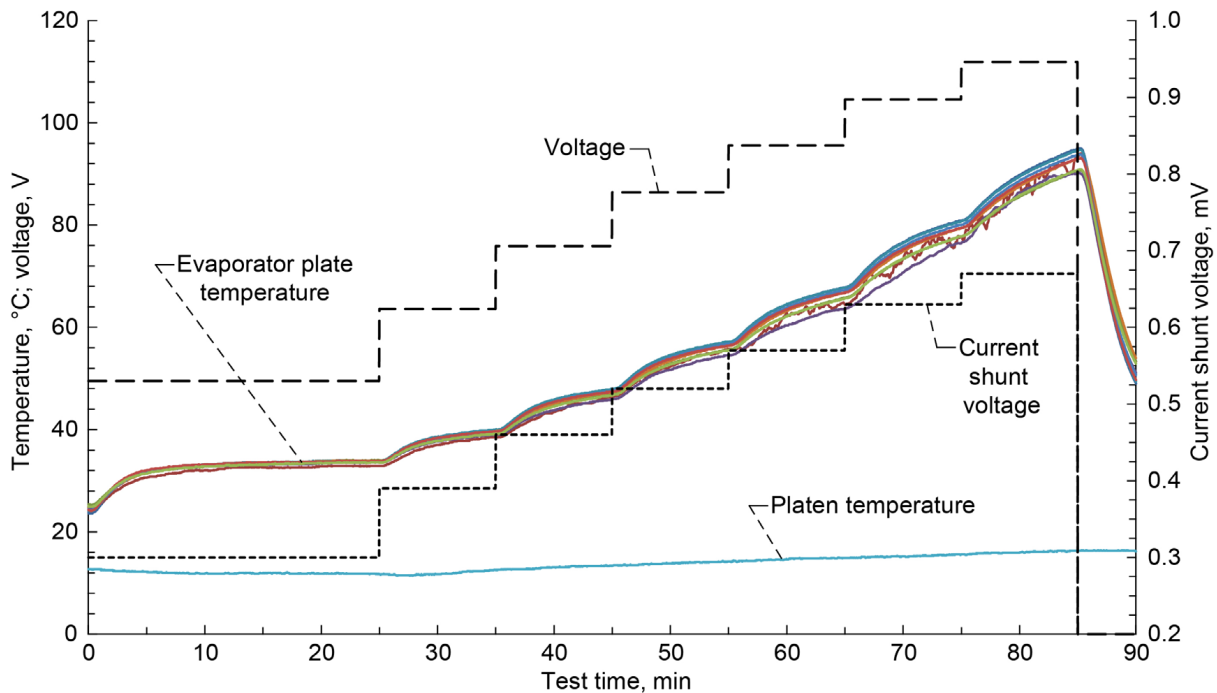


Figure A.43.—Heat pipe B, test run 1 on August 14, 2013, with Arctic Silver® paste, full condenser length, 100-lb platen force, 10 °C chiller setpoint, and horizontal operation.

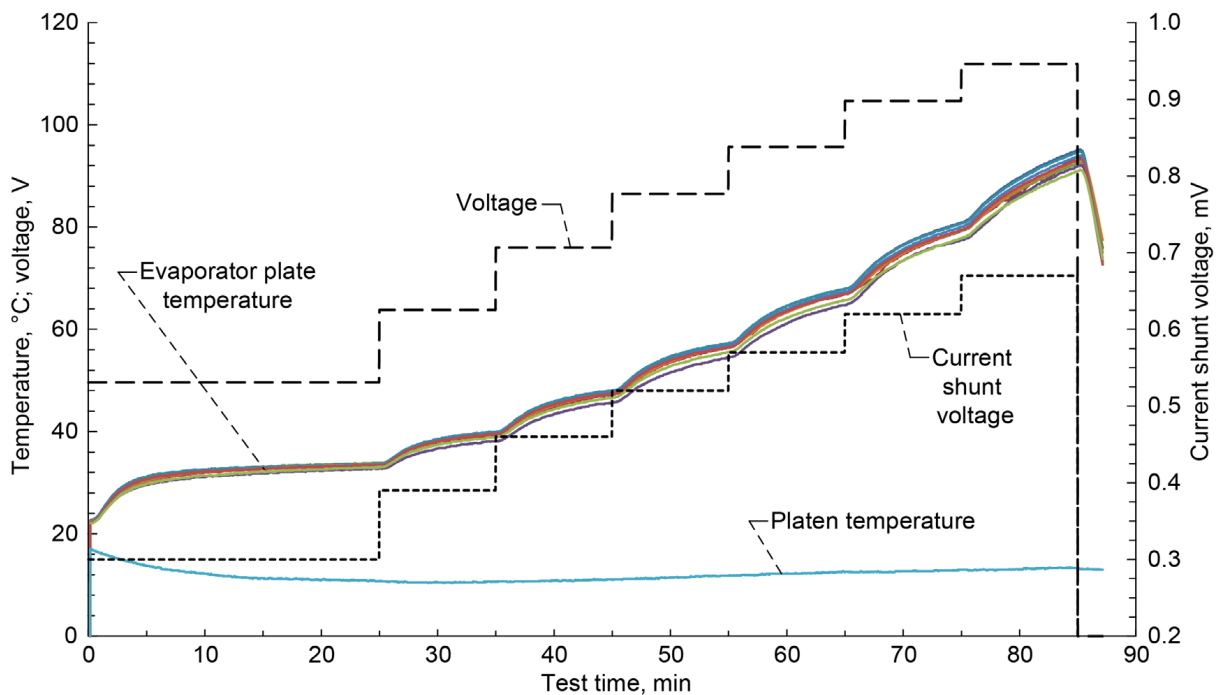


Figure A.44.—Heat pipe B, test run 2 on August 14, 2013, with Arctic Silver® paste, full condenser length, 100-lb platen force, 10 °C chiller setpoint, and horizontal operation



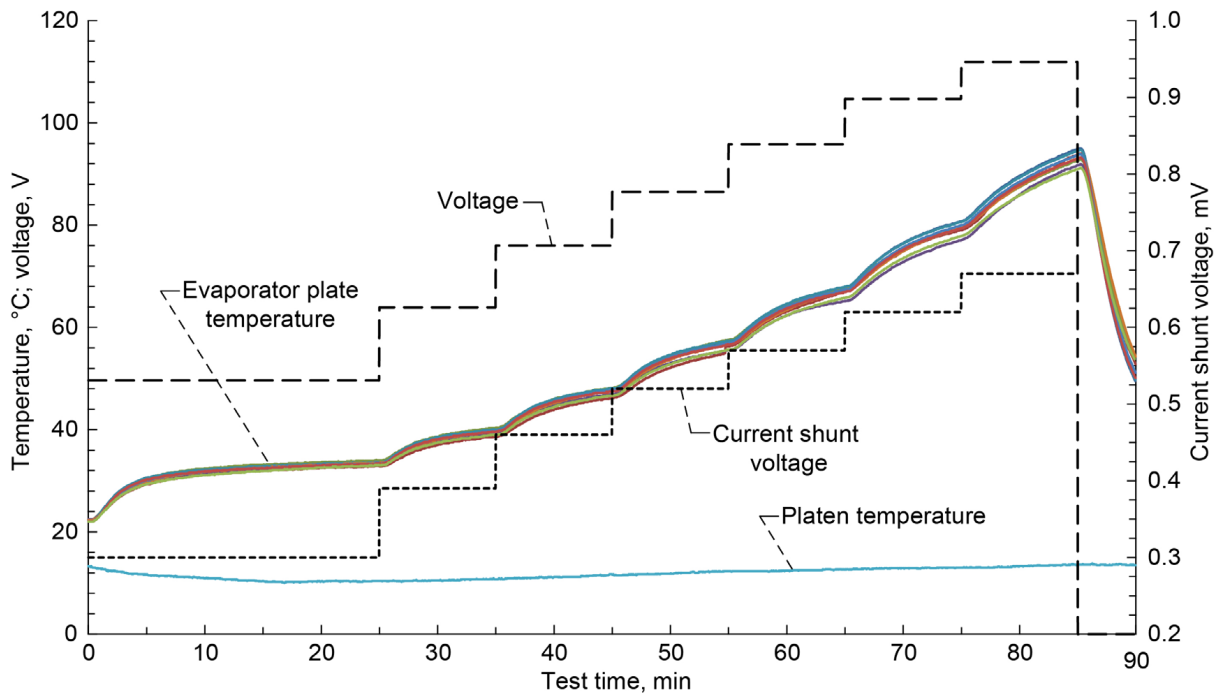


Figure A.45.—Heat pipe B, test run 3 on August 14, 2013, with Arctic Silver® paste, full condenser length, 100-lb platen force, 10 °C chiller setpoint, and horizontal operation.

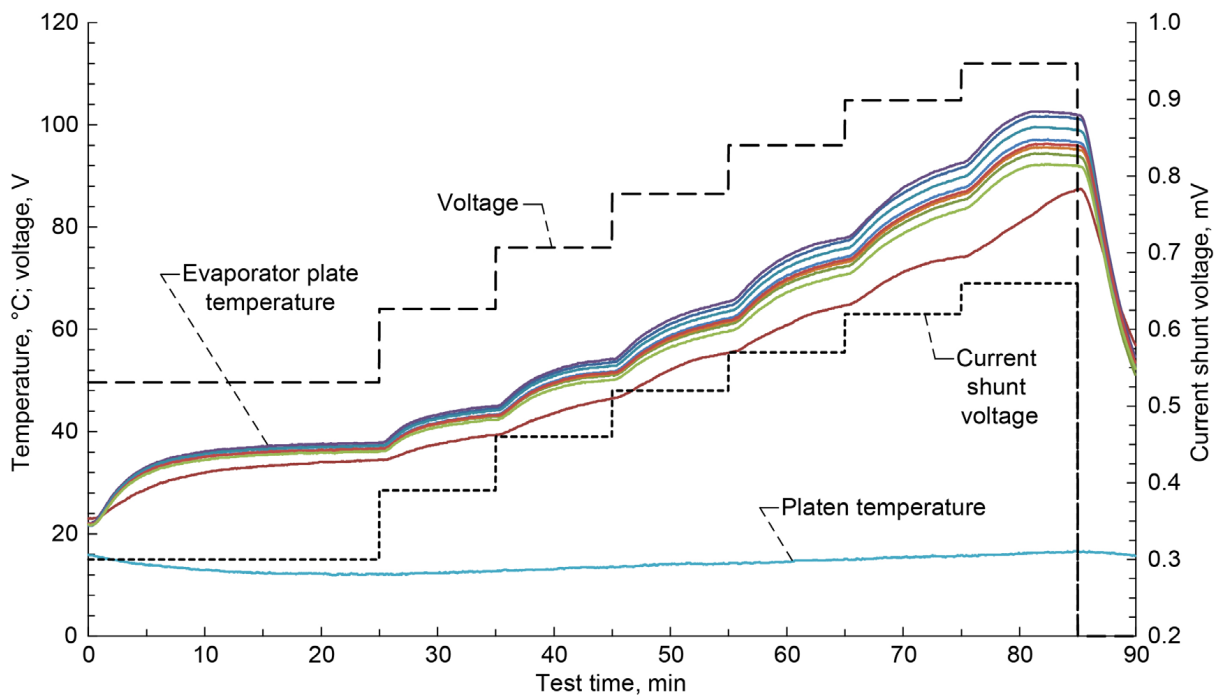


Figure A.46.—Heat pipe C, test run 1 on August 14, 2013, with Arctic Silver® paste, full condenser length, 100-lb platen force, 10 °C chiller setpoint, and horizontal operation.

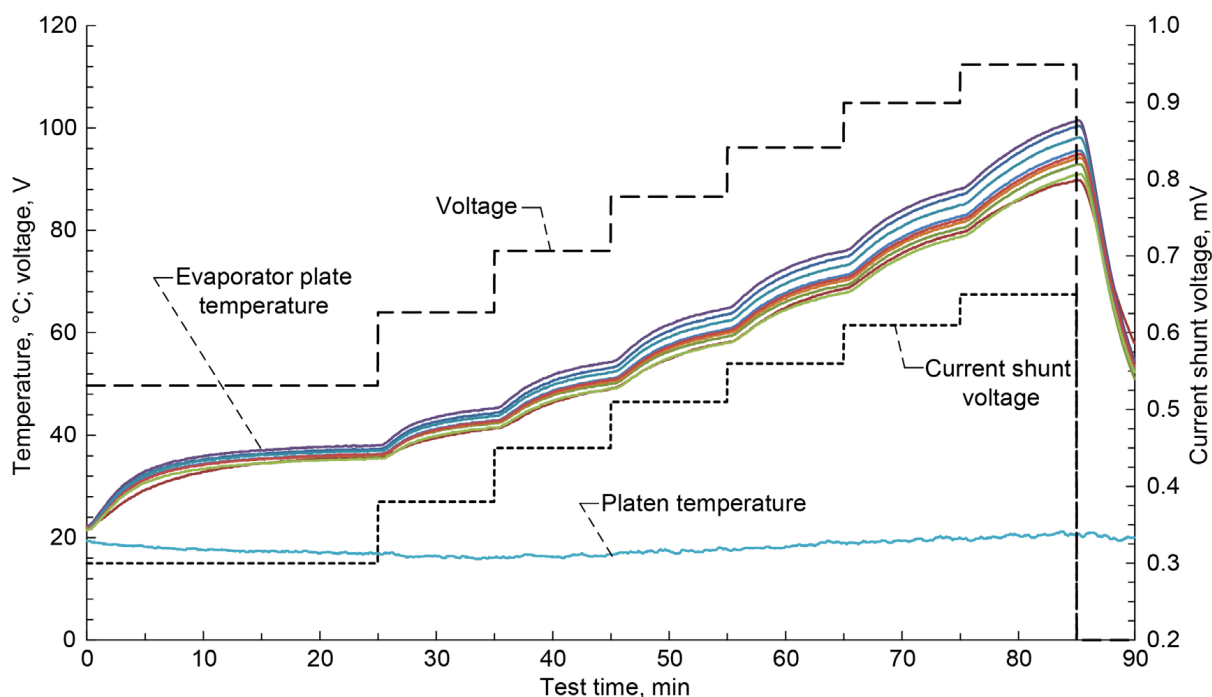


Figure A.47.—Heat pipe C, test run 2 on August 15, 2013, with Arctic Silver® paste, full condenser length, 100-lb platen force, 10 °C chiller setpoint, and horizontal operation.

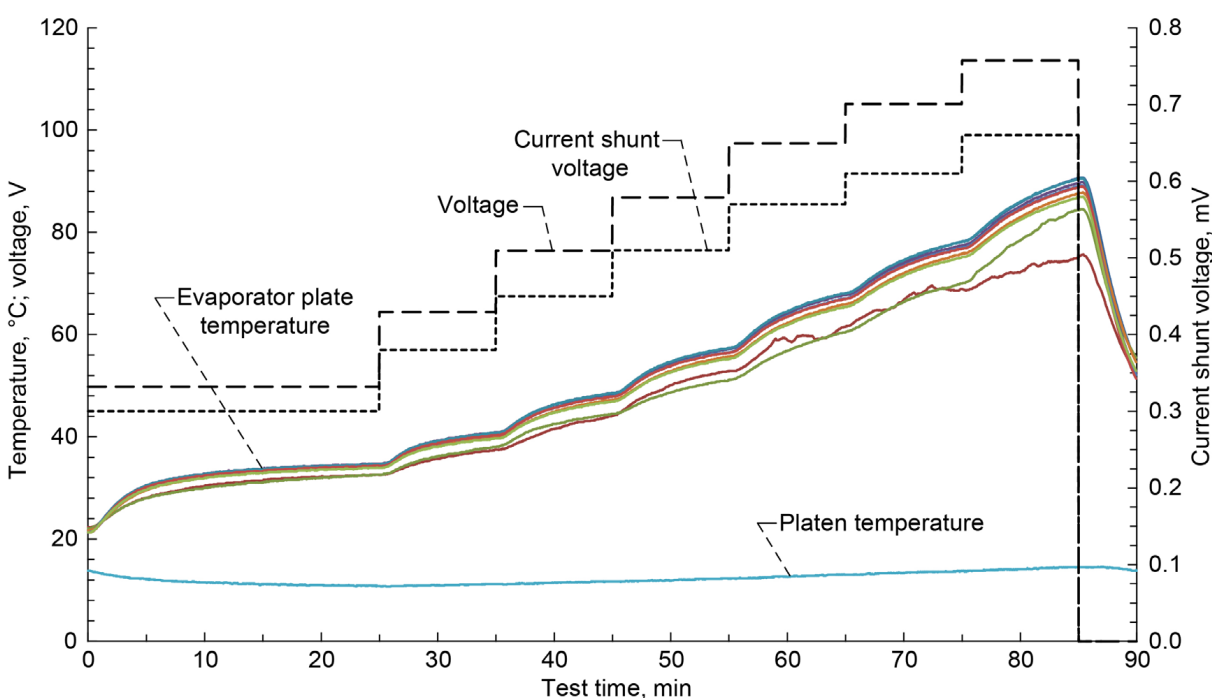


Figure A.48.—Heat pipe C, test run 3 on August 15, 2013, with Arctic Silver® paste, full condenser length, 100-lb platen force, 10 °C chiller setpoint, and horizontal operation.

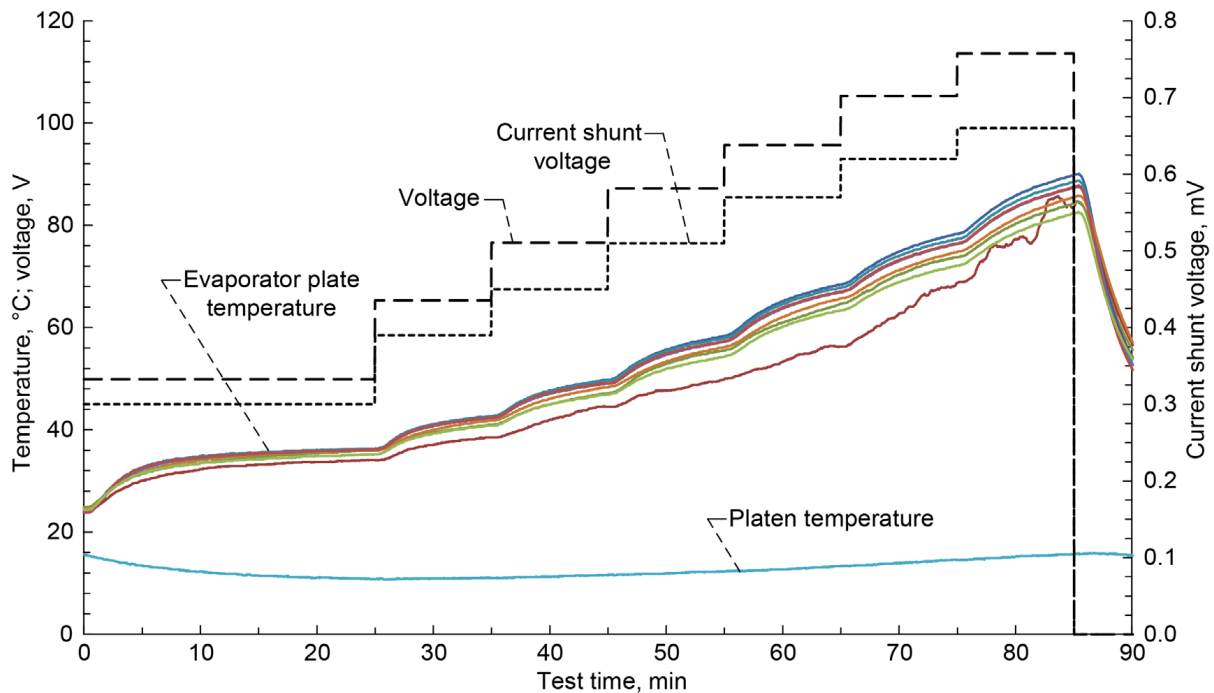


Figure A.49.—Heat pipe D, test run 1 on August 15, 2013, with Arctic Silver<sup>®</sup> paste, full condenser length, 100-lb platen force, 10 °C chiller setpoint, and horizontal operation.

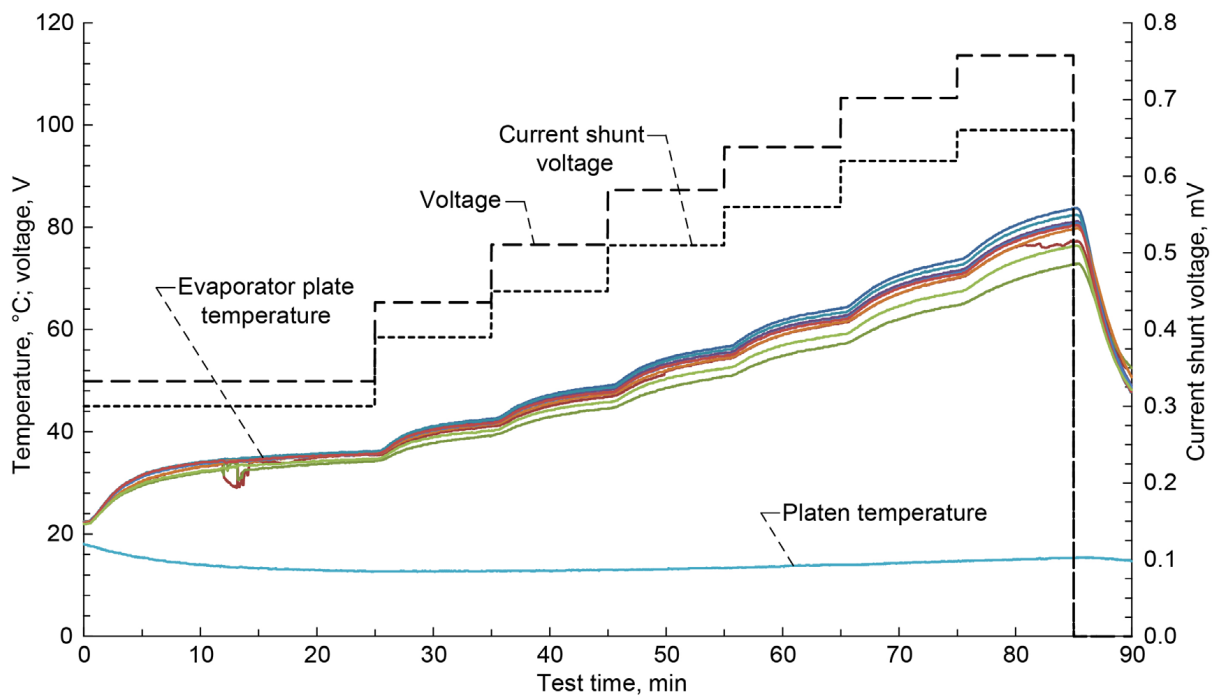


Figure A.50.—Heat pipe D, test run 2 on August 16, 2013, with Arctic Silver<sup>®</sup> paste, full condenser length, 100-lb platen force, 10 °C chiller setpoint, and horizontal operation.

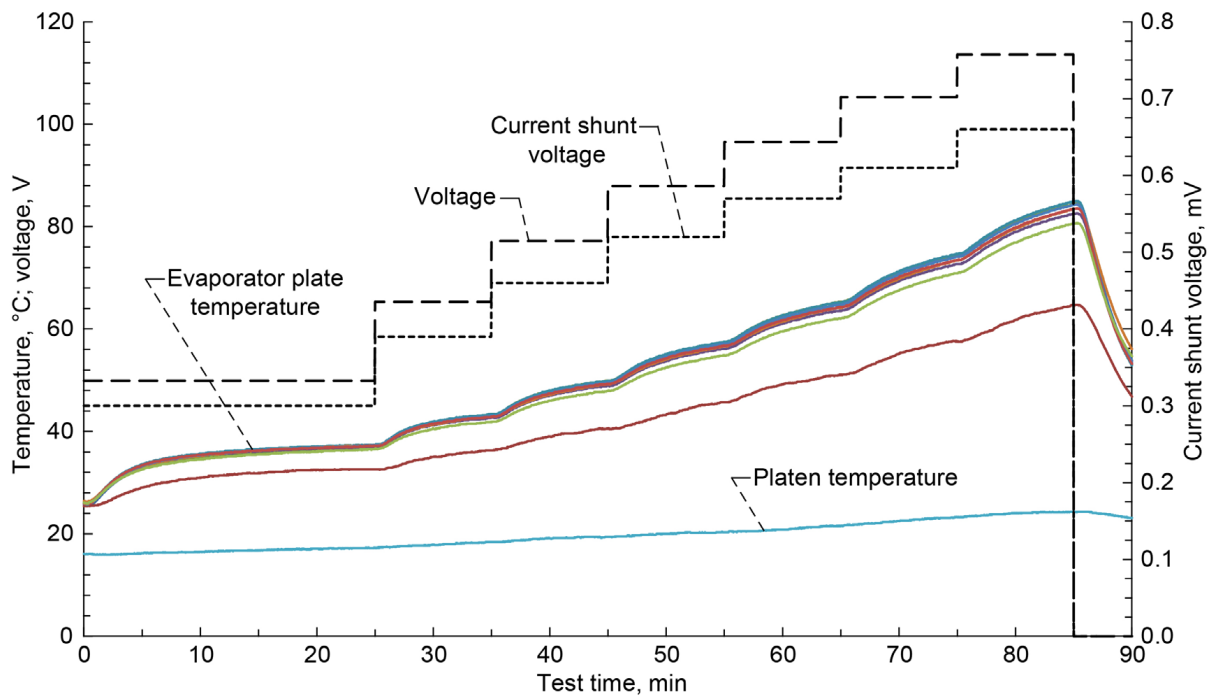


Figure A.51.—Heat pipe D, test run 3 on August 19, 2013, with Arctic Silver<sup>®</sup> paste, full condenser length, 100-lb platen force, 10 °C chiller setpoint, and horizontal operation.

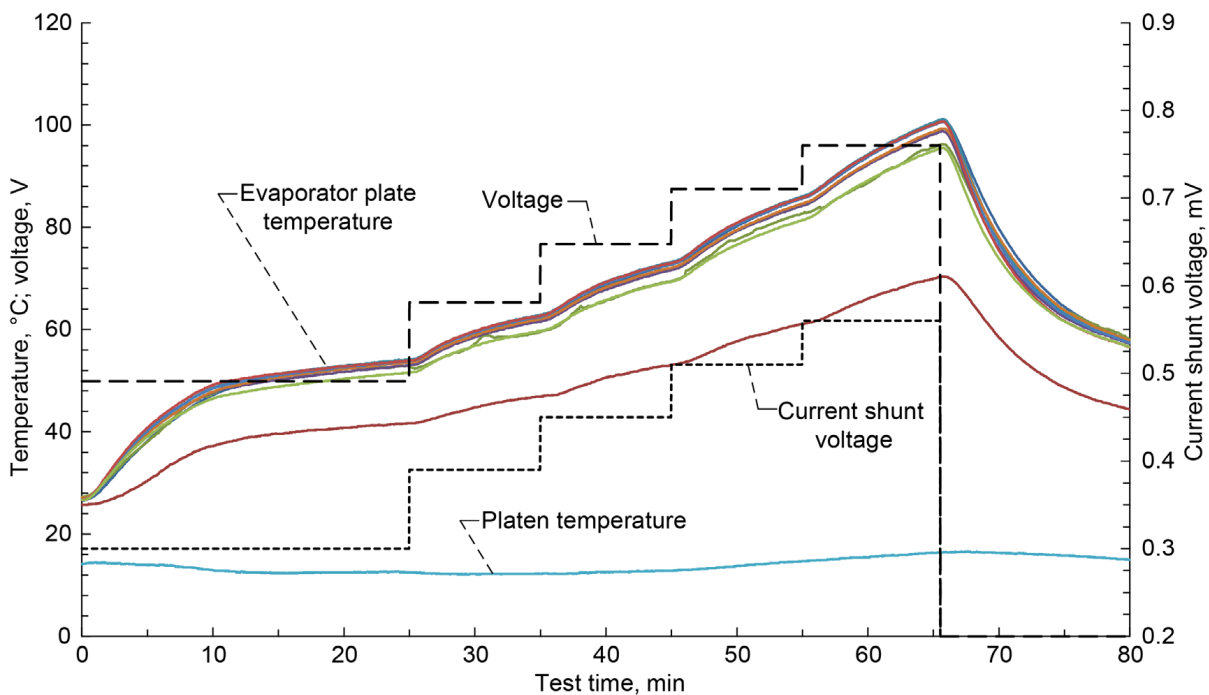


Figure A.52.—Heat pipe E, test run 1 on August 16, 2013, with Arctic Silver<sup>®</sup> paste, full condenser length, 100-lb platen force, 10 °C chiller setpoint, and horizontal operation.

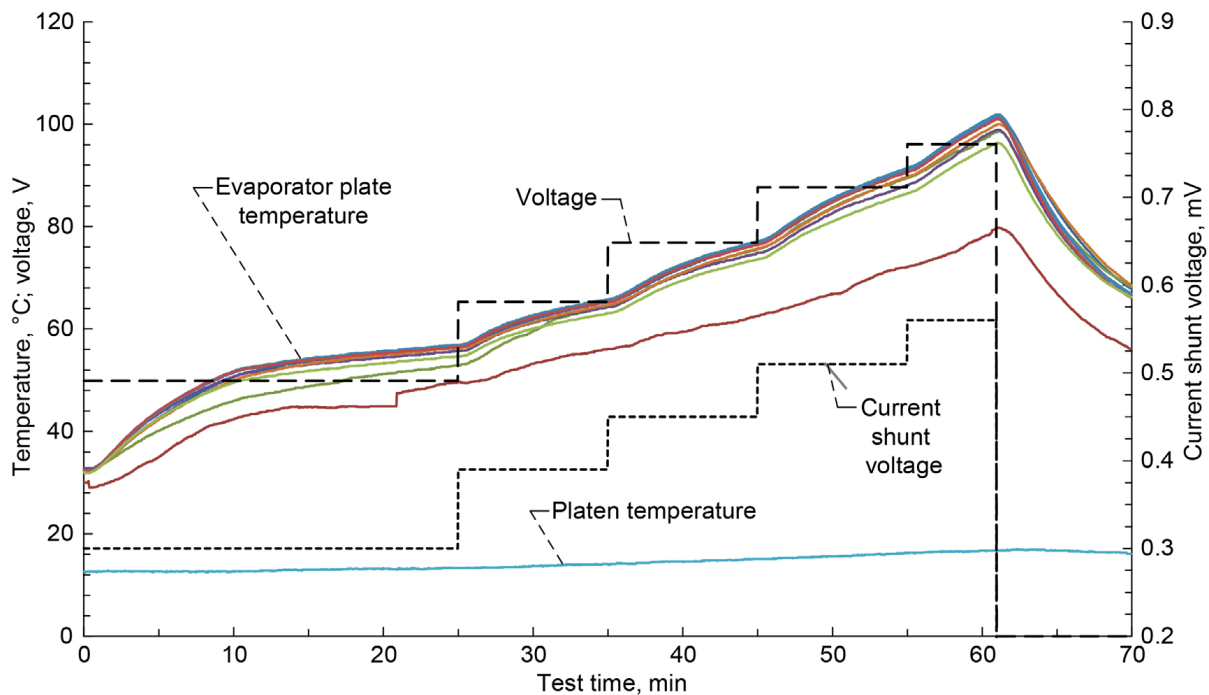


Figure A.53.—Heat pipe E, test run 2 on August 16, 2013, with Arctic Silver<sup>®</sup> paste, full condenser length, 100-lb platen force, 10 °C chiller setpoint, and horizontal operation.

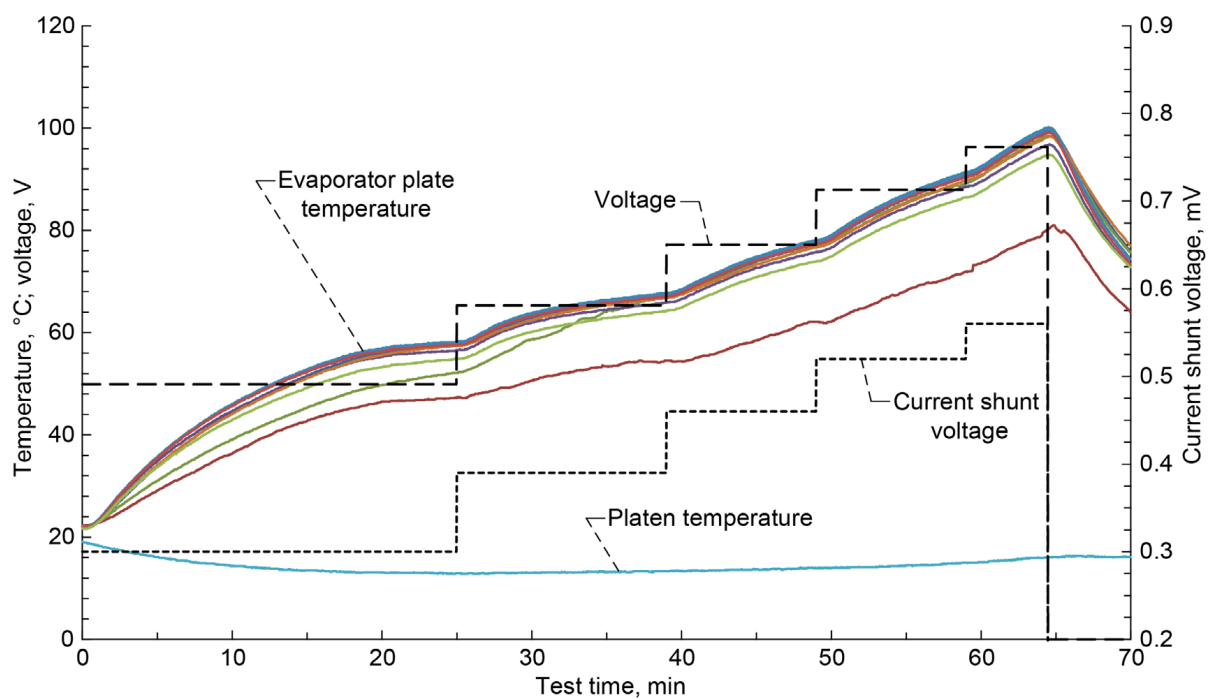


Figure A.54.—Heat pipe E, test run 3 on August 19, 2013, with Arctic Silver<sup>®</sup> paste, full condenser length, 100-lb platen force, 10 °C chiller setpoint, and horizontal operation.

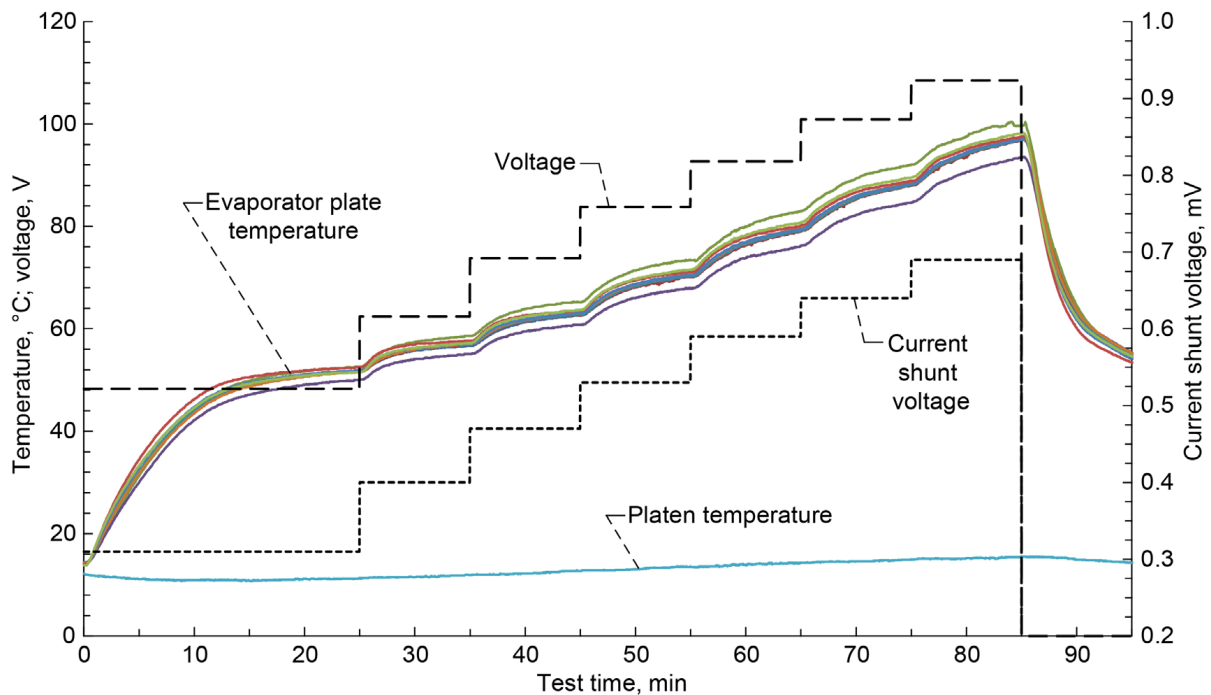


Figure A.55.—Heat pipe F, test run 1 on August 12, 2013, with Arctic Silver® paste, full condenser length, 100-lb platen force, 10 °C chiller setpoint, and horizontal operation.

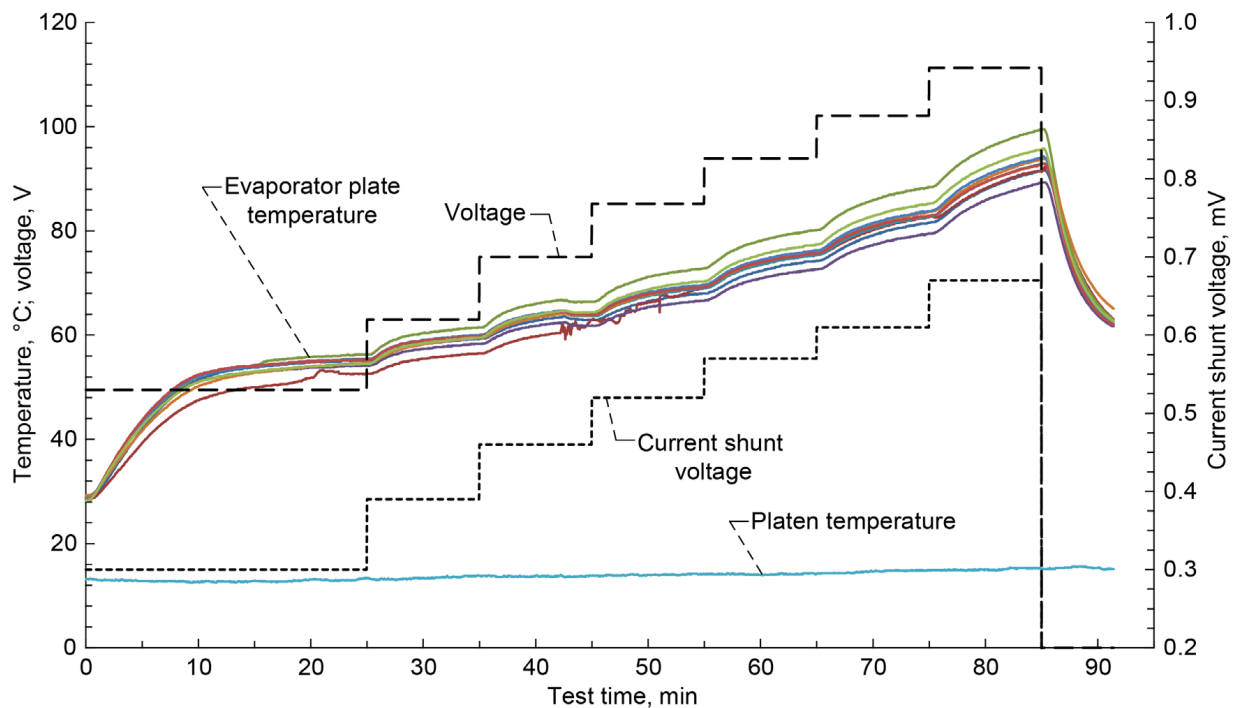


Figure A.56.—Heat pipe F, test run 2 on August 14, 2013, with Arctic Silver® paste, full condenser length, 100-lb platen force, 10 °C chiller setpoint, and horizontal operation.



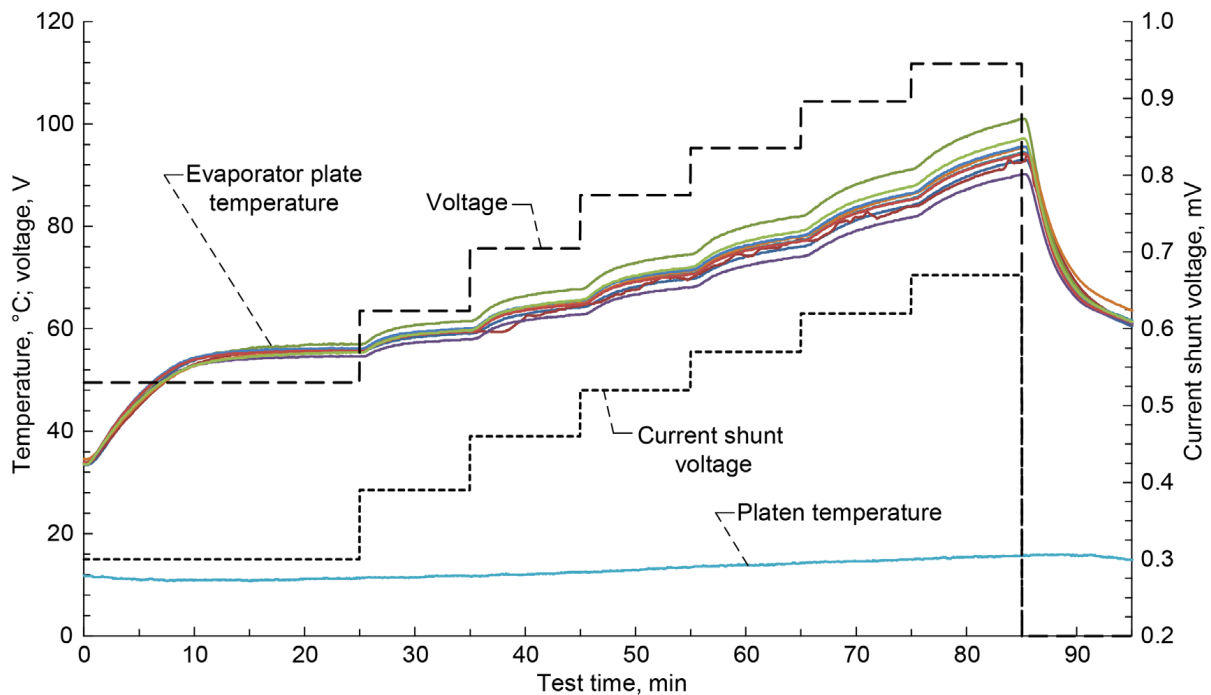


Figure A.57.—Heat pipe F, test run 3 on August 14, 2013, with Arctic Silver<sup>®</sup> paste, full condenser length, 100-lb platen force, 10 °C chiller setpoint, and horizontal operation.

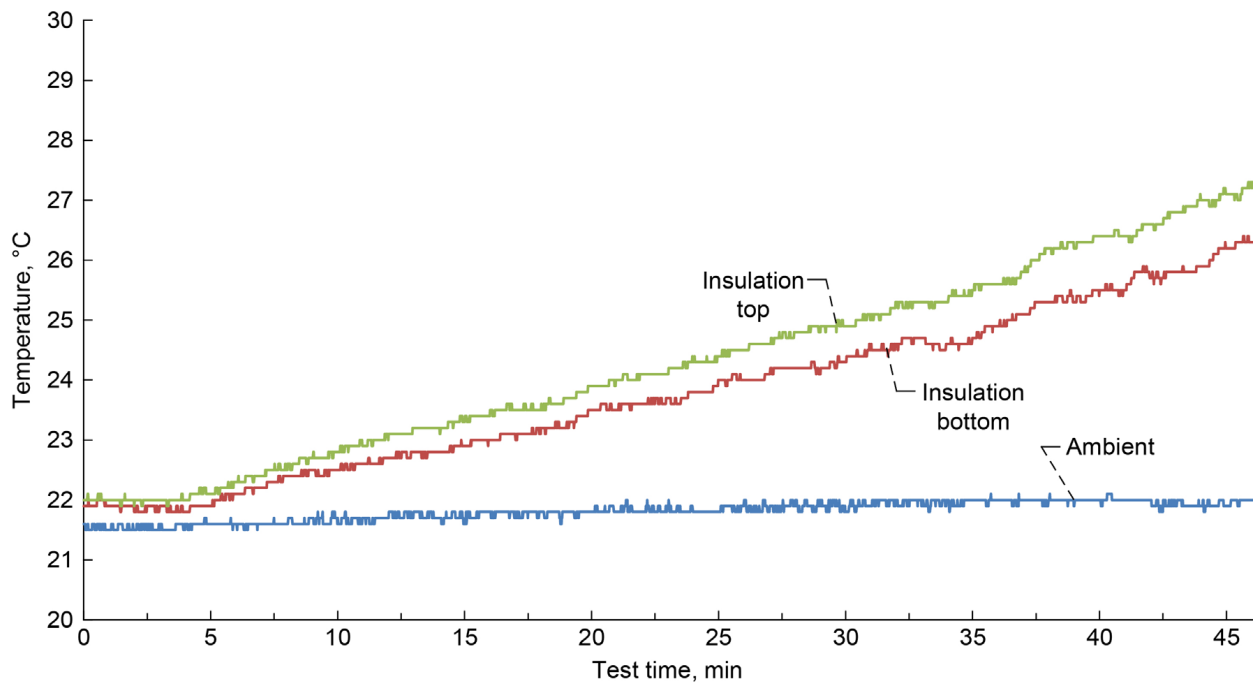


Figure A.58.—Heat-loss-related temperature measurement. Heat pipe 2 on August 13, 2012, with Arctic Silver<sup>®</sup> paste, full condenser length, 100-lb platen force, 8 °C chiller setpoint, and horizontal operation. Refer to Figure 13, Figure 17, and Figure 18 for thermocouple placement details.

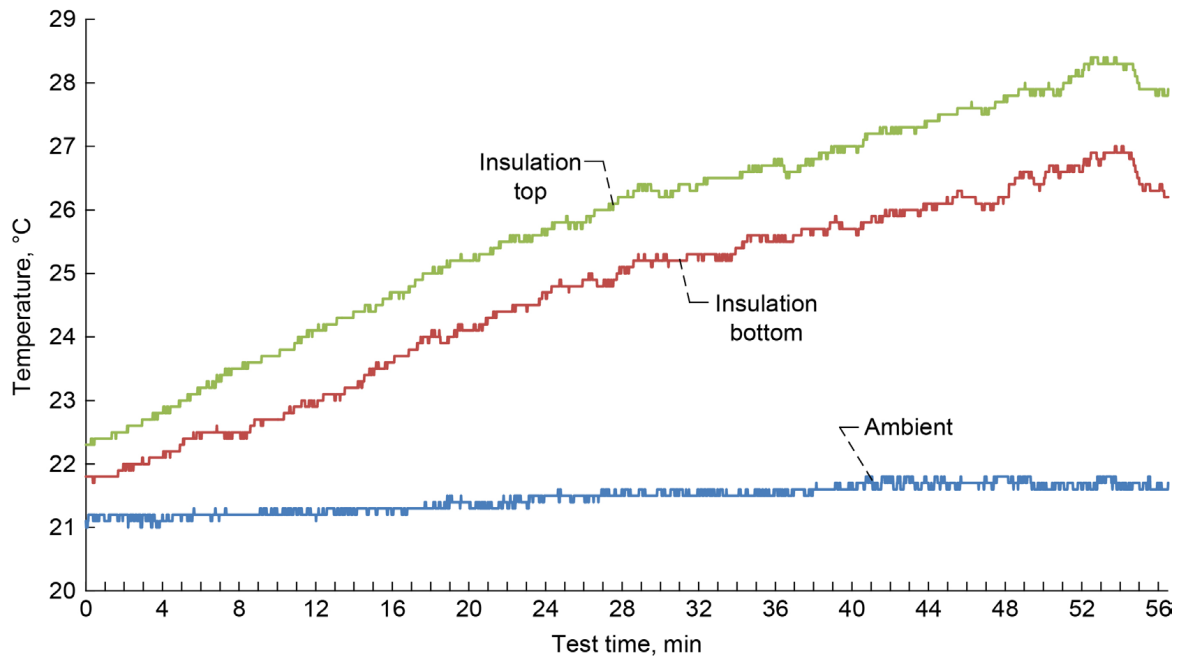


Figure A.59.—Heat-loss-related temperature measurement. Heat pipe 2 on August 17, 2012, with Arctic Silver® paste, 66-mm condenser length, 100-lb platen force, 8 °C chiller setpoint, and horizontal operation.

## Appendix B.—Experimental Procedure and Check Sheet

### Preliminary:

- (1) Check all electrical connections.
- (2) Verify the water level in chiller.
- (3) Attach the top connector and flash drive to data logger.
- (4) Put thermal grease on the heat pipe (HP) condenser if necessary.
- (5) Place the HP condenser in the press to the desired depth and orientation.
- (6) Apply 60 to 100 lb of pressure from the platens to hold the HP in place.

### Startup:

- (1) Plug in the chiller, press, power supply, and data logger.
- (2) Turn on the chiller and set the temperature to 4 °C or other desired temperature.
- (3) Turn on the press temperature readout by rotating the red knob and then flipping the orange switch.
- (4) Power on the data logger.
- (5) Set up the desired screen orientation (0 to 100 °C).
- (6) Ensure functionality of all sensor channels.
- (7) Set the data logger to record data to the flash drive in the proper format.
- (8) Wait for the platens to cool to equilibrium temperature.
- (9) Begin data logger recording.
- (10) Turn on the power supply.

### Operation:

- (1) Set the desired power level on the power supply by turning the current knob completely on and then adjust voltage knob.
- (2) Begin at 15 W (48.2 V and 0.31 A) and wait for the temperature of the HP to reach equilibrium.
- (3) Wait at least 5 min before adjusting the voltage to increase the power to 25 W.
- (4) Repeat the process of adjusting the voltage, reaching equilibrium, and waiting 5 min so that data is collected at all of the power levels listed in Table I.

TABLE I.—LIST OF VOLTAGE SETPOINTS AND  
CORRESPONDING CURRENTS FOR POWER SUPPLY

Power supplied, W	Voltage, V	Current, A	Time, min
15	48.3	0.311	5
25	62.4	.402	5
35	73.8	.475	8
45	83.8	.539	8
55	92.3	.596	10
65	100.9	.648	12
75	108.5	.696	15
85	114.8	.741	15

- (5) Adjust the waiting time to 8 min at 35- and 45-W power levels. Wait 10 min at 55 W. Wait 12 min at 65 W and 15 min at 75 W.

Shutdown:

- (1) If at any time the temperature of the HP reaches 100 °C, shut down the test by turning off the power supply.
- (2) Once heating is completed, turn off the power supply by moving the voltage and current knobs counterclockwise until zero appears on the monitor.
- (3) Flip the power switch to off on the supply and unplug the device.
- (4) Continue recording data until the HP temperature falls below 40 °C.
- (5) At this point, stop recording data. Ensure that “writing disk” appears on the screen.
- (6) Power off the data logger, chiller, and press.
- (7) Remove the HP from between the platens.
- (8) Unplug the data logger, chiller, and press.

## Appendix C.—Calibration Curve for Vise

The pound-force,  $F$ , value in lb is given by the second order polynomial best fit line

$$F = 0.003014\Theta^2 - 0.1502\Theta + 0.1892 \quad (6)$$

where  $\Theta$  represents degrees of vise handle rotation clockwise from initial contact and 0.0 lb of force.

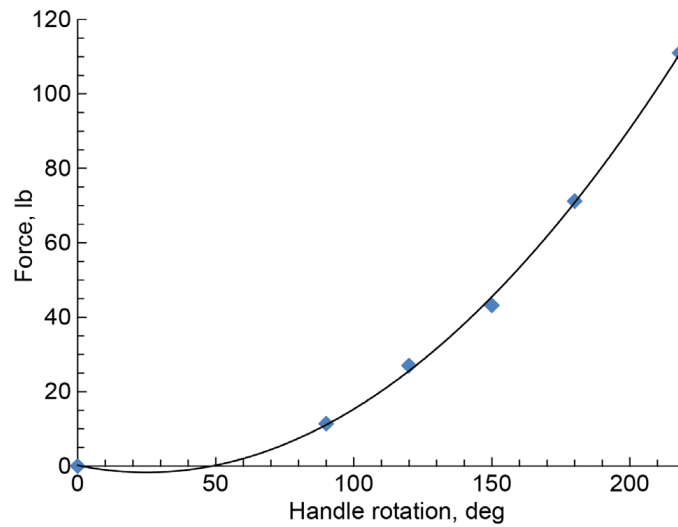


Figure C.1.—Measured levels of clamping force versus handle rotation.

## References

- Bejan, Adrian; and Kraus, Allan D.: Heat Transfer Handbook. John Wiley & Sons Publisher, New York, NY, 2003.
- Colozza, Anthony, et al.: Development and Experimental Evaluation of Passive Fuel Cell Thermal Control. NASA/TM—2014-218395, 2014. <http://ntrs.nasa.gov>
- Mills, A.: Basic Heat and Mass Transfer. Irwin Professional Publishing, Chicago, IL, 1994.
- Tilioua, A., et al.: Determination of Physical Properties of Fibrous Thermal Insulation. EPJ Web of Conferences, vol. 33, 2012.





